THE UNIVERSITY OF CHICAGO

TRAIT ASYMMETRY AND DEVELOPMENT IN THE MIDDLE DEVONIAN TRILOBITE GENUS *ELDREDGEOPS* STRUVE 1992

A DISSERTATION SUBMITTED TO

THE FACULTY OF THE DIVISION OF THE PHYSICAL SCIENCES

IN CANDIDACY FOR THE DEGREE OF

DOCTOR OF PHILOSOPHY

DEPARTMENT OF THE GEOPHYSICAL SCIENCES

BY

MATTHEW KENNETH WITTE

CHICAGO, ILLINOIS

JUNE 2021

TABLE OF CONTENTS

LIST OF TABLES

LIST OF FIGURES

ACKNOWLEDGEMENTS

A dissertation is not completed in isolation, it is the culmination of a vast network of dedication and support from many individuals, without whom I would not have been successful in this endeavor. The names that appear in this section represent a mere fraction of those who have had a profound impact on me over the years—this list is far from exhaustive. First and foremost, I would like to express my deepest gratitude to my dissertation advisor, Mark Webster. This journey has not always been easy nor straight forward and the completion of this dissertation reflects the guidance, patience, compassion, and enthusiasm that Mark has shown as an advisor throughout this project. I would also like to extend thanks to the rest my committee: Michael Foote, David Jablonski, and Graham Slater. Your advice and teachings have prepared me for a career characterized by high quality work and critical inquiry. Additionally, I would like to thank Susan Kidwell who, to me, is an honorary committee member for helping advise and guide my early thought processes with the rest of my committee while my nascent dissertation prospectus took shape. I would be remiss if I didn't extend my deep appreciation to my lab mate, Rhiannon LaVine, for being my "trilobite" twin, accountabili-buddy, and for the endless conversations we had to discuss research ideas, methods, and results. Thank you to all those within the halls of Hinds, past and present, who made these years in graduate school a truly remarkable experience, I am humbled to have been part of the ongoing legacy and considered one amongst the ranks of many great minds.

I also owe much of my success as a paleontologist to the mentorship provided by undergraduate advisor, Margaret (Peg) Yacobucci, who saw potential in me my first year at Bowling Green State University by allowing me to begin conducting my own independent research in the lab. Without Peg, I may have never discovered my profound love of trilobites, in particular the genus *Eldredgeops*, which became the subject of both my undergraduate and graduate work. In addition, I would like to thank Ina Terry for also providing an additional outlet to geek out about paleontology while at BGSU.

To my family, you have never shied away from letting me know how proud you are of me and my research—even if you at times had no idea what I was talking about. Your support and compassion have proven invaluable throughout my journey as both a first-generation university student and this PhD. In particular, I want to thank my cousins Denise Smith and Eric Wallack, you have always been and will always be my rocks against the tide. I am endlessly inspired by your compassion and creativity and owe much of who I am as a person to the two of you. Additionally, I would like to thank my sister for being one of the best siblings that a person could ask for, as well as, providing a place to finish this dissertation while the COVID 2019-2021 pandemic droned on.

Lastly, to my friends Jayme (Ace) Jones and Christopher Neal, this crazy journey called life has been so enriched by our years of friendship, I love you both so very much. To Maureen (Mo) Haley, I, Ranger Matt, do solemnly swear to always be your seeing-eye Matt when needed. To Sarah Tulga, thank you for providing an escape from the academy where we could catch up over some wonderful board games. To my fellow Dungeons and Dragons group, the weekly escape to a fantasy world has been remarkable. Doctor Kyras Elgwyn, Slayer of Demons and Kings, rolled for imitative and won! To Jacob Davidson, thank you for always believing in me, even when I didn't believe in myself. To the many others, thank you.

This dissertation is dedicated to the spirit and memory of Betty Kay Roland. Gone too soon but without whom none of this would have been possible. May your passion, support, and love live on in every page of this dissertation.

INTRODUCTION

Developmental systems regulate the expression of phenotypic variation (Laland et al., 2015) through various types of morphological homeostasis or canalization (per Canon, 1932; Waddington, 1957). This variation is one of the main drivers of evolution by means of natural selection (Darwin, 1859). The processes of environmental and/or genetic canalization—which control the expression of symmetric phenotypic variation among individuals in a population—are known to serve as a constraint on evolution (see revies by see reviews by Møller and Swaddle, 1997; Polak, 2003; Graham et al., 2010; Klingenberg, 2015; Webster, 2019 and references therein), whether and how homeorhesis—the process regulating within individual left-ride symmetry of individual traits—relates to phenotypic evolution is not well known; nor is the degree to which genetic and environmental canalization relate to homeorhesis. Empirical studies of homeorhesis have almost exclusively been conducted by neontologists. However, to understand the macroevolutionary consequences of morphological homeostasis, and to determine the timescale over which morphological homeostasis limits the expression of phenotypic variation—both within a species and across clades—it is necessary to study homeostasis within the fossil record (see discussion by Webster, 2019).

In order to answer these developmental questions, great care must be taken. Homeorhesis is measured as fluctuating asymmetry (FA; random deviations from symmetry in an otherwise symmetric structure) and is often a small component of overall variation (<1-5%) (Palmer, 1994; Palmer and Strobeck, 2003). Such analysis must be conducted on well-preserved traits. The use of traditional continuous traits, such as length measurements, are not often preserved to such an extent in the fossil record, however, meristic traits (i.e. simple counts) may be a reliable means of

assessing fluctuating asymmetry in the fossil record, and thus investigate the relationship between the components of phenotypic variation.

The Middle Devonian trilobite genus *Eldredgeops* Struve 1992 would be an ideal system to begin to try and understand the relationship between symmetric phenotypic variation and fluctuating asymmetry. The genus is well sampled by professional and amateur paleontologists and consists of several well constrained species distributed across the paleo-Great Lakes region (see Eldredge, 1972). The eyes of this genus would be an ideal meristic trait as they are well preserved with lenses organized into a series of dorso-ventral files (vertical columns of lenses) allowing for multi-trait comparisons.

The following studies build upon the central idea of understanding the components of variation within *Eldredgeops*. Chapter 1 presents a phylogenetic framework for the clade of interest, focusing on the taxonomic relationships of *Eldredgeops* within the larger context of the family Phacopidae. Using Bayesian inference and parsimony-based methods, trees were recovered that largely converged on similar topologies suggesting a greater degree of phylogenetic signal than previous phylogenetic studies examining the Phacopidae. Chapter 2 explores the relationship between the components of variation in related to eye-lens distributions in the eyes of two species of *Eldredgeops*. This study is the first to use a maximum likelihood method proposed by Young (2007) to estimate the symmetric and asymmetric components of variation. The final chapter, Chapter 3, further explores developmental asymmetries in the eye, as well as the relative addition of eye-lenses through ontogeny, to propose a model of eye development that can be applied to all trilobites.

These studies represent the first steps in testing developmental hypotheses in deep time ultimately aimed at understanding what role developmental asymmetries may have on the evolutionary trajectory of traits.

CHAPTER ONE:
A BACKBONE PHYLOGENETIC TREE FOR THE TRILOBITE FAMILY PHACOPIDAE BASED ON BAYESIAN INFERENCE METHODS

ABSTRACT— Arguments over the degree of taxonomic splitting, genera plagued by wastebasket taxa, and a relatively conserved morphology have left the systematics of the trilobite family Phacopidae in a state of disarray. Few published phylogenetic frameworks encompass the diversity of the group. Herein, 65 species, representing four of the five major tribes of the family Phacopidae, were coded for 69 characters and subjected to phylogenetic analysis using Bayesian inference and parsimony-based methods. A maximum clade credibility tree (MCCT) is proposed that shows strong posterior support for recovered genera. The data were reanalyzed using a degraded dataset where some characters were removed due to concerns about overweighting sculptural elements in the character-taxon matrix. Even after degradation of the dataset, recovered relationships remain stable, suggesting a greater degree of phylogenetic signal compared to previous studies. The proposed tree offers a framework upon which future phylogenetic studies may build and macroevolutionary studies may be conducted.

INTRODUCTION—Trilobites belonging to the enigmatic order Phacopida Salter 1864 have long been the focus of collectors and researchers due to their unique schizochroal eyes, and the family Phacopidae Hawle & Corda 1847 is a prominent exemplar of the group. This diverse family (see Moore, 1959; Jell & Adrain, 2003 for genera within Phacopidae) was long lived (late Ordovician [see discussion below] or Silurian–latest Devonian) and spread across all paleocontinents. Fine-scale stratigraphic analyses of phacopid trilobites have aided our understanding of trait evolution on relatively short geologic time-scales (~1 million years;

Crônier et al., 2004; Crônier et al., 2015) and served as case studies for stasis in the fossil record and evolution by means of punctuated equilibrium (Eldredge, 1972, 2011, 2015; Eldredge and Gould 1972; Koch II, 1990). Future fine-scale stratigraphic studies and work on phacopids (and other trilobites) may help bridge the gap between micro- and macroevolutionary patterns (Webster, 2019). To understand how such transitions within single species scale to clade-level dynamics, it is essential to have a hypothesis of evolutionary relationship among clade members.

Several concerns become apparent when working on the phylogeny of the Phacopidae. Until recently the existing taxonomy largely reflected a grade-based approach to systematics, as noted by McKellar and Chatterton (2009). Eldredge (1973) argued that taxa above the genus level were founded more on the basis of their geographic distribution rather than their phylogeny. Further complicating matters, convergence of similar character states is common and there are few unequivocal synapomorphies uniting phacopid clades. Morphological similarity between subgenera, genera, and tribes make phylogenetic analysis of the group as a whole subject to polytomies, homoplasy, and paraphyly depending on choice of characters and phylogenetic method. Many species within the Phacopidae have been volatile in their systematic position. These factors have left the group with highly unstable higher-level taxa and a situation in which many aspects of phacopid systematics are disputed (McKellar and Chatterton, 2009).

Phylogenies for the Phacopidae have been constructed using parsimony analyses (see discussion below as well as Ramsköld & Werdelin, 1991; McKellar & Chatterton, 2009; Oudot et al., 2019). The last decade has seen a revolution in phylogenetic methods with the use of probabilistic methods in phylogenetic analyses of morphological characters becoming more common place (Lewis, 2001; Nylander et al., 2004; Lee & Palci, 2015; Cau, 2017), though this is still a relatively novel approach in paleontology (Pyron, 2011; Wright & Hills, 2014; O'Reilly et

al., 2016; Cau, 2017). The co-estimation of topology and divergence times using morphological characters and tip-dating methods (Ronquist et al., 2012) allows for an integration of two of the main foci of paleontology: biostratigraphy and systematics. Use of a single macroevolutionary model, the Fossilized Birth-Death (FBD) process (Stadler, 2010; Heath et al., 2014), has allowed for fossil calibration in phylogenetic analyses integrating extant and extinct species. Initially developed to calibrate molecular clocks by incorporating a more realistic treatment of fossils, Gavryushkina et al.'s (2014, 2017) Bayesian phylogenetic model allows a sampled member of the analyzed in-group to be inferred as a direct ancestor of another sampled taxon. Together, the FBD process and sampled ancestors (SA) methods have largely been applied to datasets comprising both extinct and extant taxa (Heath 2015; Gavyruskina et al., 2017). Jointly inferring both topology and branch length using the fossilized birth-death process as a tree prior while also accounting for the possibility of ancestor-descendant relationships among sampled taxa is a promising field of study, particularly for entirely extinct clades. Studies of simulated datasets have shown that Bayesian inference methods may outperform parsimony analysis in the estimation of phylogenies from discrete morphological data, particularly in datasets prone to homoplasy (Wright & Hillis, 2014; O'Reilly et al., 2016; Puttnick et al., 2018; [see Goloboff, Torres & Arias, 2017 for rebuttal]).

Here, Bayesian inference methods, including use of the Fossilized Birth Death process and sampled ancestors as tree priors, are used to infer a backbone phylogeny for four of the five major tribes within the family Phacopidae. Parsimony methods are used as a means of further testing support for recovered clades across all phylogenetic analyses. Recent systematic work (see below; Basse, 2006; Basse, 2012) and phylogenetic work (McKellar & Chatterton, 2009; Oudot et al., 2019) on the Phacopidae have focused on taxa belonging to the Rhenish-Bohemian

and Anti-Atlas provinces of Gondwana. This study expands the focus to include enigmatic Laurentian/Euramerican taxa, allowing for a more comprehensive and global understanding of the Phacopidae. The results have profound implications for our understanding of the systematics and evolution of Phacopidae, some of which are discussed below.

CURRENT STATE OF PHACOPID SYSTEMATICS—After nearly two centuries of systematic description and research, phacopid systematics are currently in a state of disarray (Haas, 1998; McKellar & Chatterton, 2009; Eldredge personal communication 2016). Early work in the nineteenth century was largely concentrated on the German and Czech regions of the Rhenish-Bohemian subfaunal province (Emmrich, 1839; Barrande, 1846, 1872; Hawle & Corda, 1847; Barrande et al., 1852). Work expanded during the early twentieth century to include a broader geographic reach extending into North America, see for example Stewart (1927), Richter and Richter (1933, 1939, 1943), Delo (1935, 1940), Pribyl & Erben (1952), Kielan (1954), and Stumm (1953).

These research efforts were instrumental in establishing the systematic framework presented in the *Treatise on Invertebrate Paleontology: Part O* (Moore, 1959). In that work, the Phacopidae were split into two subfamilies: the Phacopidellinae Delo, 1935 and the Phacopinae Hawle & Corda, 1847. The subfamily Phacopidellinae, with members such as *Phacopidella* Reed 1905, were united in their more 'primitive' forms sharing a less vaulted exoskeleton, similar to the condition found in the sister family Dalmanitidae Vogdes 1890 (Moore, 1959). The Phacopinae generally consisted of what were considered more 'derived' forms including genera such as *Eophacops* Delo 1935*, Phacops* Emmrich 1839*,* and *Reedops* Richter & Richter 1925.

The decades following the publication of the *Treatise* saw renewed interest in phacopid systematics and description. Large works were undertaken on North American material (Campbell, 1967, 1977; Eldredge, 1971, 1972, 1973), Bohemian material (Chlupáč, 1971, 1977), and in the Anti-Atlas region of Morocco (Alberti, 1969, 1970a, 1981, 1983; Struve, 1970, 1972, 1982, 1989, 1990, 1992, 1995). During this period, taxonomic opinion began to depart from the organization found in the *Treatise* and arguments emerged regarding the hierarchical levels to which divisions within Phacopidae should be assigned. Early arguments treated large-scale divisions within Phacopidae as subgeneric in nature, so that a few taxa such as *Phacops* contained numerous assigned subgenera and species (see Campbell, 1967, 1977; Chlupác, 1971, 1977). Spearheaded largely by Struve (see Struve, 1970, 1972, 1982, 1989, 1990, 1992, 1995), others favored a greater degree of taxonomic splitting, recognizing several new genera and raising several subgenera to the generic level. Over the last few decades, workers have tended to favor the latter interpretation, though taxonomic opinions vary among authors (Schraut 2000; Basse, 2006, 2012; McKellar & Chatterton, 2009; Khaldi et al., 2016; Van Viersen et al., 2017; Oudot et al., 2019; and others).

Work throughout the 1980s and 1990s began to divide the Phacopidae into a series of proposed tribes: Ananaspini (informal grouping of Haas, 1998), Cordapeltini Struve 1989, Cryphopini Struve 1989, Geesopini Flick & Struve 1984, Phacopini Flick & Struve 1984, and the Reedopini Struve, 1989. A proposed classification scheme for the Phacopidae denoted by tribe can be found in Table 1.1 (adapted from McKellar & Chatterton 2009). However, the phylogenetic analysis of McKellar & Chatterton (2009) found the proposed tribal classification to be problematic, with all analyzed tribes being recovered as paraphyletic or gradational. This phylogenetic result necessitated either restructuring proposed tribal relationships or abandoning

them all together. McKellar & Chatterton (2009) favored a subfamily-genus structure found in the *Treatise on Invertebrate Paleontology* (1959) with many of the analyzed taxa classified within the subfamily Phacopinae.

There has recently been renewed interest in understanding phylogeny of the Phacopidae (see Ramsköld and Werdelin, 1991; McKellar and Chatterton, 2009; Oudot et al., 2019) as well as a number of recent studies investigating phacopid anatomy (Haas 1998, Bruton and Haas, 1999), musculature (Eldredge, 1971) and eye structure (Horváth et al., 1997, Schoenemann and Clarkson, 2011). Further, fine-scale stratigraphic analysis (Crônier et al., 2004, 2015) and study of ontogeny (Crônier and Feist, 1997; Abe and Lieberman 2012) have helped to inform our understanding of trait evolution on macroevolutionary timescales. It would be beneficial to have a robust systematic framework for the family Phacopidae within which relationships between proposed genera can be contextualized. Such a framework would provide a basis for future studies of less inclusive phacopid subclades as proposed by McKellar and Chatterton (2009) and Oudot et al. (2019).

The present study has two primary goals: (1) to unite and expand upon previous phylogenetic studies of the Phacopidae in an effort to establish a robust working hypothesis of a backbone phylogeny for the family; and (2) to expand knowledge of North American taxa such as *Eldredgeops* (Green 1832), *Paciphacops* Maximova 1971, *Viaphacops* Maximova 1972, and *Phacops iowensis* Delo 1935 and to understand the ambiguous relationships among these genera (see arguments by Eldredge 1972, 1973).

Tribe: Phacopini; Flick and Struve, 1984 (Hawle and Corda, 1847 *nom. transl.*)	*Phacops* (*Phacops*) Emmrich, 1839* *Phacops* (*Cultrops*) Struve, 1995
Tribe: Ananaspini (informal grouping of Haas, 1998)	*Ananaspis* Campbell, 1967* *Denckmannites* Wedekind, 1914 *Echidnops* Sandford, 2002 *Kainops* Ramsköld and Werdelin, 1991* *Lochkovella* Chulpáč, 1972 *Paciphacops* Maksimova, 1972* *Viaphacops* Maksimova, 1972*
Tribe: Geesopini Flick and Struve, 1984	*Geesops* Struve, 1972* *Arduennops* Struve, 1972 *Burtonops* Struve, 1990 *Drotops* Struve, 1990 *Eldredgeops* Struve, 1990* *Morocops* Basse, 2006* *Nyterops* Struve, 1972 *Omegops* Struve, 1976 *Pedinopariops* (*Hypsipariops*) Struve, 1982* *Pedinopariops* (*Pedinopariops*) Struve, 1972* *Teichertops* Struve, 1992
Tribe: Reedopini Struve, 1989	*Reedops* R. and E. Richter, 1925*
Tribe: Cordapeltini Struve, 1989	*Cordapeltis* Přibyl and Vaněk, 1971 ?*Boeckops* Chulpáč, 1971* *Chotecops* Chulpáč, 1971 *Liolophops* Struve, 1972 *Rabienops* Struve, 1989 ?*Signatops* Přibyl and Vaněk, 1971
Tribe: Cryphopini Struve, 1989	*Acuticryphops* Crônier and Feist, 2000 *Cryphops* R. and E. Richter, 1926 *Dianops* R. and E. Richter, 1923 *Eocryphops* R. and E. Richter, 1931 ?*Nephranops* R. and E. Richter, 1926 *Plagiolaria* Kegel, 1952 ?*Prokops* Chulpáč, 1971 *Trimerocephalus* M'Coy, 1849
Incertae credis:	*Acernaspis* Campbell, 1967 *Eophacops* Delo, 1935* *Phacopidella* Reed, 1905 *Rhinoreedops* Maksimova, 1978 Other unmentioned genera; see Jell and Adrain, 2003

Table 1.1 Current (1998) systematics of the family Phacopidae (largely according to Strüve, 1970; 1972; 1976; 1982; 1989; 1990; 1992; 1995; Flick and Strüve, 1984; and Haas, 1998) modified from McKellar and Chatterton (2009). This interpretation is at odds with that found in the *Treatise on Invertebrate Paleontology: Part O* (in Moore, 1959) on phacopids because it ignores the subfamily divisions used therein, and assigns members of the Phacopidellinae to the same tribe as members of the Phacopinae. This table does not include all of the available genera listed by Jell and Adrain (2003), because many have not been considered in the scope of this study and would simply be listed as additional *incertae credis*.
* Denotes taxa that a pertinent to this work, due to similarity in morphology and temporal distribution.
? Denotes uncertain placement in the classification scheme of Strüve.

METHODS—

Selection of Ingroup Taxa—Previous studies of the Phacopidae had different taxonomic emphases. The early effort by Ramsköld and Werdelin (1991) largely focused on stratigraphically older genera such as *Acernaspis* Campbell 1967 and *Ananaspis* Campbell 1967, while efforts by McKellar and Chatterton (2009) and Oudot et al. (2019) focused on recently described Devonian phacopids from the Anti-Atlas region of Gondwana.

To form a foundation for future phylogenetic studies may build, emphasis is herein placed on taxa ranging from the Silurian (Llandovery) to the Middle Devonian (Givetian). Species chosen for ingroup analysis were selected from all purported tribes with the exception of the Cryphopini. Representatives of the Cryphopini are generally confined to the Upper Devonian, with the early members such as *Prokops* Chlupáč 1971 only tentatively assigned to the Cryphopini or well-illustrated genera such as *Plagiolaria* Kegel 1952 or *Eocryphops* Richter & Richter 1931 first occurrencing in the Middle Devonian, well after the initial radiation of the Phacopidae (Chlupáč 1977; Holloway 2005; McKellar & Chatterton 2009; Crônier et al. 2011).

To resolve early character evolution within the tree, representatives are selected from several Lower Silurian genera. Previous studies have selected representatives of *Acernaspis* and *Ananaspis* for outgroup taxa (see Ramsköld & Werdelin 1991; McKellar & Chatterton 2009; Oudot et al. 2019), which are herein included as members of the ingroup taxa. Three representatives of the widespread and putatively diverse genus *Acernaspis* were coded from Chatterton and Ludvigsen (2004): *Acernaspis becsciensis* Lespérance & Letendre 1982, *A. cooperi* Chatterton & Ludvigsen 2004; and *A. orestes* (Billings 1860). Two members of the genus *Ananaspis* were selected: *Ananaspis fecunda fecunda* (Barrande 1846) and *Ananaspis fecunda aspera* (Hawle & Corda 1847).

Eophacops was assigned to the Phacopinae within the *Treatise*, but has subsequently treated as *incertae sedis* (see McKellar & Chatterton 2009; Crônier et al. 2011). Haas (1998) suggested that *Eophacops* might represent an early stem-lineage within the Phacopidae that diverged prior to the origination of *Acernaspis*, though this hypothesis has not been phylogenetically tested. Two species of *Eophacops* are included herein: *E. trapeziceps* (Barrande 1846) and *E. bulliceps* (Barrande 1846). Similarly, *Phacopidella,* while assigned to the Phacopidellinae in the *Treatise,* has subsequently been placed as *incertae sedis* and argued by Haas (1998) to represent the earliest stem-branch of an evolutionary tree of Phacopidae. One species of *Phacopidella*, *P. glockeri* (Barrande 1846) is included here, along with two species of its putative sister genus *Struveaspis* Alberti 1966: *Struveaspis fugitiva* (Barrande 1872) and *S. micromma* (Roemer 1852).

Trilobites belonging to the genus *Reedops* have often had a variable position within evolutionary hypotheses of the Phacopidae (compare fig. 4 Campbell 1977; fig. 26 Chlupáč 1977; fig. 1 Haas 1998; fig. 6 McKellar & Chatterton 2009). To test phylogenetic placement of this genus, four stratigraphically separate species were considered: *Reedops bronni* (Barrande 1846), *R. decorus* (Hawle & Corda 1847), *R. modestus* (Barrande 1872), and *R. cephalotes hamlagdadianus* Alberti 1983. Also considered are *Reedops*-like forms including one species of the genus *Lochkovella* Chlupáč 1972 (see fig. 26 in Chlupáč 1977) *L. misera* (Barrande 1852) and two species of *Boeckops* Chlupáč 1972 (see fig. 6 in McKellar & Chatterton 2009): *B. boecki* (Hawle & Corda 1847) and *B. stelcki* McKellar & Chatterton 2009.

Eldredge (1973) proposed that species belonging to *Paciphacops* and *Viaphacops* (then *Phacops logani*-complex and *Phacops cristatus*-complex, respectively) were phylogenetically close to each other and to *Phacops iowensis*. Under the systematic arrangement of Phacopidae at

the time, Eldredge could not separate these species from a definition of the genus *Phacops.* This phylogenetic relationship has been tested in previous phylogenetic studies, which has only raised more questions due to the placement of *Kainops* as a potential sub-genus of *Paciphacops* (see Ramsköld & Werdelin, 1991; McKellar & Chatterton, 2009). To understand the placement of *Phacops* Emmrich 1839 within the broader family the following species have been included: *Phacops araw* McKellar & Chatterton 2009, *P. latifrons* (Bronn 1825), *P. major* (Barrande 1852), *P. regius* Chlupáč 1971, and *P. iowensis* Delo 1935 including all three subspecies of *P. iowensis*; *P. iowensis iowensis* Delo 1935, *P. iowensis alpenensis* Stumm, 1953, and *P. iowensis southwerthi* Stumm 1953.

A total of four North American representatives of *Paciphacops* have been included in the present analysis: *Paciphacops birdsongensis* (Delo 1940); *P. campbelli* Ramsköld & Werdelin 1991; *P. eldredgei* Ramsköld & Werdelin 1991; and *P. logani* (Hall 1861). Ramsköld & Werdelin (1991) erected the genus *Kainops* to accommodate several species that formerly belonged to *Paciphacops*. Three species of *Kainops* have been included herein: *K. raymondi* (Delo, 1935), *K. invius* (Campbell 1977), and *Paciphacops* (*Kainops?*) *invius* small-eyed form of Ramsköld and Werdelin (1991) who argue that *Paciphacops invius* represents a two-species complex, reassigning the large-eyed form to *Kainops invius*. However, the small-eyed variant was never reclassified within the text and is presumed to belong to *Kainops* prior to analysis. Two species of the genus *Viaphacops* are considered here: *V. stummi* (Eldredge 1973) and *V. bombifrons* (Hall 1861).

Taxonomic assignment of the genus *Eldredgeops* Struve 1992—originally designated as a *nomen nudum* (Struve, 1990) and subsequently diagnosed within Struve (1992)—has been particularly problematic. This genus comprises subspecies formerly assigned to the species

Phacops rana (Green, 1832); whether these subspecies should be raised to species-rank or remain as subspecies-rank has not been clear in the literature (see *Eldredgeops rana rana* McKellar & Chatterton, 2009; *E. crassituberculata* Schoenemann & Clarkson, 2011; *E. rana milleri* and *E. rana crassituberculata* Levi-Setti, 2014). This is complicated by statements of Struve (1995) which argued that *Eldredgeops* consists of a five species complex but did not state which 'species' belong to that complex. Prior to analysis herein it is tentatively assumed that *Eldredgeops* is a valid genus and all eight possible 'species' of *Eldredgeops* are included to test the monophyly of the genus: *Eldredgeops africanus* (Burton & Eldredge 1974), *E. arkonensis* (Stumm 1953), *E. crassituberculata* (Stumm 1953), *E. milleri* (Stewart 1927), *E. norwoodensis* (Stumm 1953), *E. paucituberculata* (Eldredge 1972), *E. rana* (Green 1832), and *E. tindoufensis* (Burton & Eldredge 1974). However, arguments by Basse (2012) suggest that *E. africanus* may questionably belong within *Hypsipariops* [=*Hypsipariops? overwegi*].

Eldredge (1972) suggested that the sister genus to *Eldredgeops* is the genus *Geesops* (then *P. rana* and *P. schlotheimi* respectively). To test this hypothesis, three species of *Geesops* have been included herein: *Geesops fabrei* Khaldi et al. 2016, *G. schlotheimi* (Bronn 1825), and *G. sparsinodosus* (Struve 1970). Another putative sister clade to *Geesops* selected for inclusion in this analysis is the genus *Nyterops* Struve 1972 with two included species: *Nyterops nyter* (Struve 1970) and *Nyterops yeteifliensis* Basse 2006.

The genus *Hypsipariops* Struve 1982 has gone through periodic revisions, where some authors treat this genus as subgeneric in status [=*Pedinopariops Hypsipariops*](see Struve, 1982; McKellar & Chatterton 2009; Oudot et al., 2019), while other authors have treated *Hypsipariops* as its own distinct genus (see Basse, 2006; van Viersen, 2007; Basse, 2012, this paper). The following members of *Hypsipariops* have been included in this analysis to further clarify the

phylogenetic standing of this genus (see arguments in Basse 2006; van Viersen 2007): *Hypsipariops kowalskii* Struve 1992, *Hypsipariops lyncops* Struve 1982, and *Hypsipariops* [=*Pedinopariops* (*Hypsipariops*)] *vagabundus* Struve 1990. Further, Basse (2006) argued that the type species of *Liolophops* is exceedingly similar to *Hypsipariops* but treated the two as separate genera. To understand the relationship among *Pedinopariops, Hypsipariops*, and *Liolophops*, the type species *Liolophops sublevatus* Struve 1970 has been included.

Additionally, several representatives from the genus *Morocops* Basse 2006 have been selected for inclusion. The type species of *Morocops* was originally designated as *Geesops sparsinodosus struvei* Schraut 2000. In the following two decades, McKellar & Chatterton (2009) argued that the type species *M. struvei* was separate from their newly erect genus *Barrandeops*, however, subsequent arguments by van Viersen et al. (2017) considered *Barrandeops* to be synonymous with *Morocops*, though this argument has not been phylogenetically tested. To test this hypothesis the following members of *Morocops* are included: *Morocops* (=*Barrandeops*) *forteyi* McKellar & Chatterton 2009, *M.* (=*Barrandeops*) *lebesus* Chatterton et al. 2006, *M.* (=*Barrandeops*) *granulops* Chatterton et al. 2006, *M.* (=*Barrandeops*) *ovatus* McKellar & Chatterton 2009, *M. spinifer* van Viersen et al. 2017, *M.struvei* Schraut 2000, and *M. torkozensis* van Viersen et al. 2017.

To compare results with the recent phylogenetic analysis of Oudot et al. 2019, two final genera are selected within the ingroup, *Austerops* McKellar & Chatterton 2009 (using *Austerops kermiti* McKellar & Chatterton 2009 and *Austerops salamandar* McKellar & Chatterton 2009) and *Chotecops* Chlupáč 1971 (using *Chotecops auspex* Chlupáč 1971).

Selection of Characters—Many of the characters and character states used within this study have been adapted from previous phylogenetic studies of phacopids, including those of Ramsköld and

Werdelin (1991), McKellar and Chatterton (2009), and Oudot et al. (2019). In some cases, character states were modified following the recommendation of authors (see McKellar & Chatterton 2009) or to better fit the morphological range of the taxa selected for this study. A total of 69 characters were used (Appendix A), 20 of which are binary and 49 are multistate in nature. Multistate characters are treated as unordered. Analyses using Bayesian inference removed character 21, due to it being invariant within the ingroup and only used to separate the outgroup from the ingroup in the parsimony analysis.

Characters represent all parts of the trilobite exoskeleton but as with previous studies of phacopids there is an emphasis on the cephalon, ornamentation, and characteristics of the eyes. Characters describing the thorax and the pygidium were included but could not be coded in several species due to poor preservation or lack of representation in the literature.

Bayesian Inference methods—Bayesian phylogenetic methods are becoming increasingly used to sample tree topologies for datasets composed of morphological and fossil data. These methods combine a probabilistic model of character evolution with a set of prior probabilities for model parameters to generate a sample from a posterior probability distribution of phylogenetic trees. These probabalistic models and associated priors have been well described in the literature (see Mau 1999; Lewis, 2001; Drummond & Rambaut, 2007; Stadler 2010; Heath et al., 2014; Gavryushkina et al., 2014, among others). The Bayesian framework used herein has been adapted and modified from previous authors (see Gavryushkina et al., 2014; Heath 2015; Wright 2017).

A fully discretized matrix of taxa and character states was loaded into BEAUti 2.5.2 (Bouckaert et al., 2019) for parameterization. Morphological characters were allowed to evolve

under the Lewis Mk model of trait evolution. Under this model, discrete morphological characters are allowed to take *k* unordered states. Following a Markov process, characters are allowed to change between *k* states along a single branch with character change assumed to be symmetrical (Lewis, 2001). Data were treated under the default partitioning scheme based on the number of character states.

Several tree prior models have been discussed in the literature which can be implemented within the program BEAST2. The fossilized birth-death (FBD) process (Stadler, 2010; Didier et al., 2012; Heath et al., 2014) treats fossil observations as part of the branching process, an extension to previous constant rate birth-death models commonly used in paleontology (e.g. Raup et al., 1973; Raup 1985). The FBD process is a stochastic branching process describing macroevolutionary dynamics, fossil preservation, and sampling such that:

$$f\left[\tau \middle| \lambda, \mu, \rho, \Psi, x_c\right] \quad (1)$$

For a phylogeny with a possible given topology (τ), the FBD process will begin at some time x_c >0 in the past and ends when x=0. At any point within the model, each lineage may probabilistically undergo one of three process-based events, each according to their own constant rate Poisson process: branching (i.e. speciation) with rate λ, extinction with rate μ, or fossil preservation and sampling with rate Ψ (Stadler, 2010; Heath et al., 2014; Wright 2017). Previous studies using fossil taxa have conditioned the analysis on the rho (ρ) parameter, which represents the probability of sampling a tip in the present (Gavyrushkina et al. 2014, 2017). Datasets that incorporate fossil-only data lack extant representatives and have set ρ=0 (e.g. Cau, 2017). Herein ρ has been omitted and the analysis is conditioned on the origin of the clade.

The trilobite *Sambremeusaspis fossesensis* Lespérance, 1988 from the Ashgill of the Upper Ordovician was assigned to the family Phacopidae, placing it as the only member of the family

within the Ordovician. However, Lespérance and Sheehan (1988) discussed the problematic nature of the eyes found in *S. fossesensis,* which are unique among the family and only shared with the genus *Ormathops* Delo 1935, raising questions about its affinity within the Phacopidae, though it clearly belongs to the Phacopina. The earliest definitive representatives of Phacopidae first appear at or near the Ordovician-Silurian boundary (Chlupáč, 1975) and are best represented by species belonging to the genus *Acernaspis*. Haas (1998) suggested that the primitive condition found within the Phacopidae would be represented by *Phacopidella*. The morphological differentiation between the Phacopidellinae (*Phacopidella*) and the Phacopinae (*Acernaspis*) as well as the possible affinity of *S. fossesensis* suggests that the origin of the Phacopidae must occur before the Ordovician-Silurian boundary. To structure the analysis, the origin prior was modeled using an offset log-normal distribution with offset 443, mean (M) 1.7 and standard deviation (S) 1.0. These parameters result in a mean value of 453 Ma (on the Sandbian-Katian boundary), and with 95% CIs between 445-483 Ma. Such a distribution favors somewhat uniform probabilities for the origin of the Phacopidae across much of the Middle to Upper Ordovician, with diminishing probabilities approaching the Cambrian-Ordovician boundary.

Recently, Gavyruskina et al. (2014; 2017) extended the FBD model with a package called SA ("Sampled Ancestors") modifying the conditioning parameters and allowing for fossils to be sampled along lineage branches. Under this implementation of the FBD model the following parameters are considered: net diversification with rate *d*, "turnover" described by *r* (note that this is not turnover in the paleontological sense and is better envisioned as the 'extinction fraction'), and the probability of a fossil observation prior to species extinction described by *s*; such that:

$$d = \lambda - \mu \quad (2)$$

$$r = \frac{\mu}{\lambda} \quad (3)$$

$$s = \Psi / (\mu + \Psi) \quad (4)$$

Net diversification rate is expected to be small (≤ 1) and was modeled using an exponential distribution with mean of 1.0. Such a distribution places a higher probability on lower values of net diversification. Sampling probability was modeled using a beta distribution with α=2.0 and β=2.0 such that probabilities are symmetric about a probability of 0.5. A starting seed value of 0.39 was chosen for the sampling proportion following suggestions by Bapst and Hopkins (2017).

A beta prior with α=2.0 and β=1.0 was used for turnover. Marshall's (2017) third law of paleobiology states that average extinction rate is approximately equal to the average rate of speciation (also described in Stanley 1979, 1990; Valentine 1969, 1990; Sepkoski, 1998 among others). Turnover is equal to extinction rate (μ) divided by speciation rate (λ) (equation 3), and where rates are expected to be similar, turnover values should be expected to approach 1.0. Further, low turnover rates would suggest exponential speciation within phacopids—an unrealistic scenario given limited resource availability and realized by the complete extinction of the clade. Higher turnover rates would yield relatively shorter species durations compared to the to the total age of the clade, which is observed within the fossil record (Marshall, 2017).

Bayesian tree search analyses were conducted using BEAST 2.5.2 (Bouckaert et al., 2014) with plugin SA v.2.0.1. The MCMC chain length was set to 50 million iterations, sampling every 2500 generations. Five independent chains were run and *post hoc* analysis performe in Tracer v. 1.7.1 (Rambaut et al. 2019) to ensure that chains converged on the same posterior distribution. Runs were then combined using Log Combiner v.2.5.2 (Rambaut et al. 2019), where 15% of each run was treated as burn-in and discarded from the analysis. Tree annotator v. 2.5.2 (Drummond & Rambaut, 2007) was used to recover the Maximum Clade Credibility Tree (MCC Tree or MCCT), that is the tree whose topology results in the highest product of posterior clade probabilities.

One of the benefits of probabalistic analytical methods in phylogenetic studies is that they allow for the integration of both phenotypic and stratigraphic data, permitting the co-estimation of topologies, divergence dates, and evolutionary rates using tip-dating methods (Ronquist et al., 2012; Cau, 2017; Paterson et al., 2019). Species FADs were constrained to the nearest lower stage boundary, dated event horizon, or base of the nearest conodont zone (Appendix A, Table A.1). All dates, events, and conodont zones were calibrated against the 2012 Geological Time Scale (Gradstein et al., 2012).

Taxa included in this analysis are temporally distributed from the base of the Silurian to the end of the Middle Devonian. For species origintating the Silurian, tip-dates could be constrained to the nearest lower stage boundary. Devonian species could be assigned to the nearest conodont or dated event horizon. Dates for conodont zones were adapted following the GTS2012 spline age (Kaufman, 2006; Gradstein et al., 2012). The Daleje Event horizon, a transgressive pulse, is recognized across Europe and North Africa and represents strata separating the Zlichovian and the Dalejan. A formal Lower/Upper Emsian substage boundary has been proposed to be placed near the Czech Zlichovian-Dalejan boundary (Chlupáč and Lukes, 1999; Gradstein et al., 2012). The base of the Daleje Event, dated to 399.5 Mya, is used herein to define the separation of the Lower/Upper Emsian and has been used to date species that could only be age-constrained to near the base of the Upper Emsian.

Model Comparison—Path sampling analysis was conducted on four different clock models: random local, strict, relaxed exponential, and relaxed log-normal. Each clock model was run for a total of 50 steps, comprising 1,000,000 chain iterations, with marginal likelihood estimates computed for each following their run. Bayes Factors (Kass and Raftery, 1995) were calculated comparing each of the models against the others (Table 1.2). In this case, a relaxed log-normal

clock was found to have the highest marginal likelihood. Under this model, the rate on any one branch does not depend on the rate of a neighboring branch, and rates are pulled from a log-normal distribution whose parameters are also sampled by the MCMC (Li and Drummond, 2012). A strict clock, where a uniform evolutionary rate is applied to every branch, was separated from the relaxed log-normal clock by a Bayes Factor of 1.38 (< 2) which suggests that neither model can be explicitly favored. Analysis using both clock models produced similar MCC trees that shared topology and only differed in some branch lengths. Differences in branch lengths between clock models may impact future analysis that focus on rates. However, the present study is concerned with the topologic relationships across the Phacopidae, and subsequent presentation of Bayesian results will be discussed relative to trees produced using the relaxed log-normal clock model.

	Relaxed Ln	Relaxed Exp.	Random Local	Strict
Relaxed Ln	-3638.0	-	-	-
Relaxed Exp.	5.36	-3652.65	-	-
Random Local	3.14	3.04	-3642.81	-
Strict	1.38	5.29	2.92	-3638.5

Table 1.2: Comparison of clock models using Bayes Factors (Kass and Raferty, 1995). Diagonal contains marginal likelihoods. Values >2 indicate the row model is favored over the column model.

Parsimony analyses—Previous phylogenies of phacopids have been constructed using parsimony-based methods (see Ramsköld & Werdelin, 1991; McKellar & Chatterton, 2009; Oudot et al. 2019). For methodological comparison and to further test clade support, data were subjected to parsimony analysis using PAUP*4.0a build 165 (Swafford, 2002). Due to the total number of taxa considered an exhaustive search of tree space was not possible. To find the most parsimonious tree, data were subjected to a heuristic search where taxa were added by random stepwise addition using a total of 100 replicates and branch swapping performed using the tree bisection

reconnection (TBR) algorithm. All characters were treated with equal weight and as unordered. A strict consensus tree was recovered for the analysis and consistency indices were computed.

To determine cladogram polarity, care must be taken when selecting an outgroup. Though opinions have differed which group or groups are sister to the Phacopidae, it is generally accepted that the Pterygometopidae are the sister clade to the Phacopidae (Eldredge, 1971; Ludvigsen & Chatterton, 1982; Ramsköld, 1988; Ramsköld & Werdelin, 1991). The Eomonorachinae (*sensu* Ludvigsen & Chatterton, 1982) within the Pterygometopidae include genera such as *Calyptaulax* Schuchert & Cooper 1930 and *Podowrinella* Clarkson et al. 1977 that share possible synapomorphies with early members of the Phacopidae such as the loss of the genal spines, a shallow or effaced lateral border furrow, deepening of the vincular furrow, and a widening of the pygidium such that it better fits within the cephalon during enrollment (Ramsköld & Werdelin, 1991). Previous cladistic studies on phacopids have focused on Lower and Middle Devonian genera (McKellar & Chatterton, 2009; Oudot et al., 2019) and have used the pterygometopid *Calyptaulax glabella* Schuchert & Cooper 1930, in addition to the early phacopids *Acernaspis* and *Ananaspis,* as designated outgroups to determine polarity. As *Acernaspis* and *Ananaspis* are considered ingroup members herein, designation of these taxa for the outgroup would be inappropriate. Reliance on *C. glabella* as the sole species for cladogram polarization is problematic for the following reasons: (1) if *C. glabella* is sister to the Phacopidae, it is separated by 10 million years of independent evolution from the first members of *Acernaspis*, if the genus as a whole is sister to the Phacopidae then there is greater than 20 million years of independent evolution separating *Calyptaulax* from the most earliest members of *Acernaspis* raising possible concerns about long branch attraction (*sensu* Sanderson et al., 2000; Bergsten, 2005); (2) Ramsköld and Werdelin (1991, p. 31) stated that "*C. glabella* [Schuchert &]Cooper 1930 (redescribed by

Ludvigsen & Chatterton, 1982) shows many derived (autapomorphic) characters with respect to other *Calyptaulax*" and suggested the use of other members of the genus. It is possible that the genus *Calyptaulax* is a complex represented by two subgenera *C.* (*Calyptaulax*) and *C.* (*Calliops*) (see McCormick, 1995), where outgroups recommended by Ramsköld and Werdelin (1991) belong to the *C.* (*Calliops*) complex. For this study, a broad sample of taxa were chosen for outgroup character polarization including the following: *Eomonorachus intermedius* (Walcott, 1877), *Calyptaulax* (*Calliops*) *callicephala* (Hall, 1847), *Calyptaulax* (*Calyptaulax*) *glabella*, and two members of the Silurian pterygometopid genus *Podowrinella* (*P. straitonensis* (Lamont, 1965) and *P. christiei* Lane, 1988). Henry (1980, 1984) argued that the genus *Morgatia* Hammann, 1972 is the earliest member of Phacopidae; however shared characters of vincular pits are the result of convergent evolution and the genus belongs to the Dalmanitidae (Lespérence & Letendre, 1982; Lespérence, 1988; Ramsköld & Werdelin, 1991). Due to the presence of convergent trait evolution and concerns of long branch attraction, *Morgatia* was excluded from outgroup selection.

RESULTS—

Bayesian Inference—Following the removal of burn-in, a total of 85,005 tress were sampled with a total of 6403 unique clades recovered across all trees, represented by a majority rule consensus tree (Figure 1.1). At this scale, the species assignments within genera are generally stable, either recovered entirely monophyletically (e.g. *Smithops* [formerly *Phacops iowensis*], *Eophacops, Nyterops*) or are united at a nodal polytomy (e.g. *Phacops*, *Kainops*).

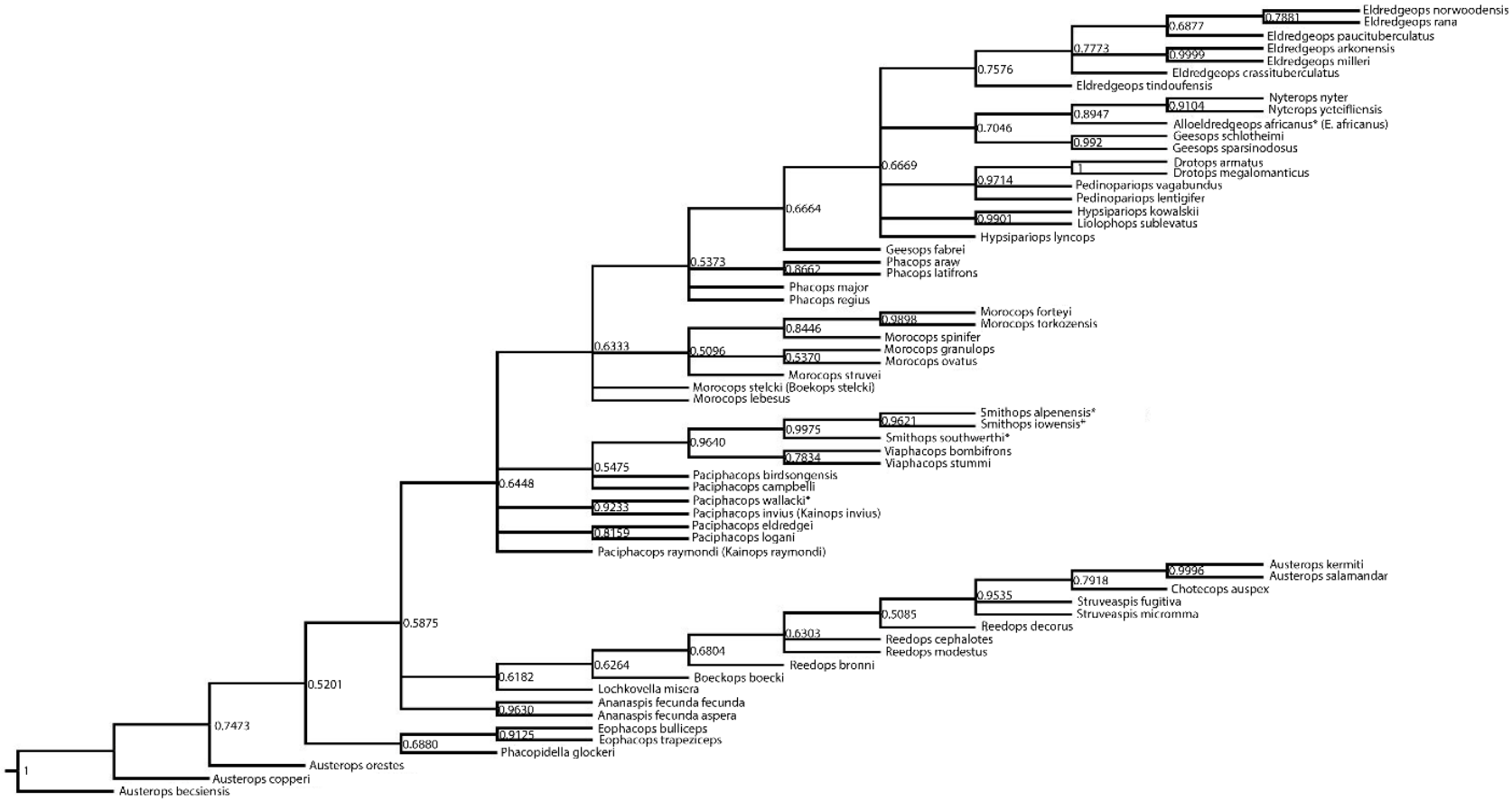

Figure 1.1—Majority rule consensus (50%) tree for all trees recovered via Bayesian inference of the full dataset. Numbers at nodes indicate consensus support for recovered clades. Taxa names used reflect the systematics argued as a result of the analyses presented in this study. New taxa assigned are indicated with an asterisks (*), taxa names in parentheses indicate previous taxonomic assignment.

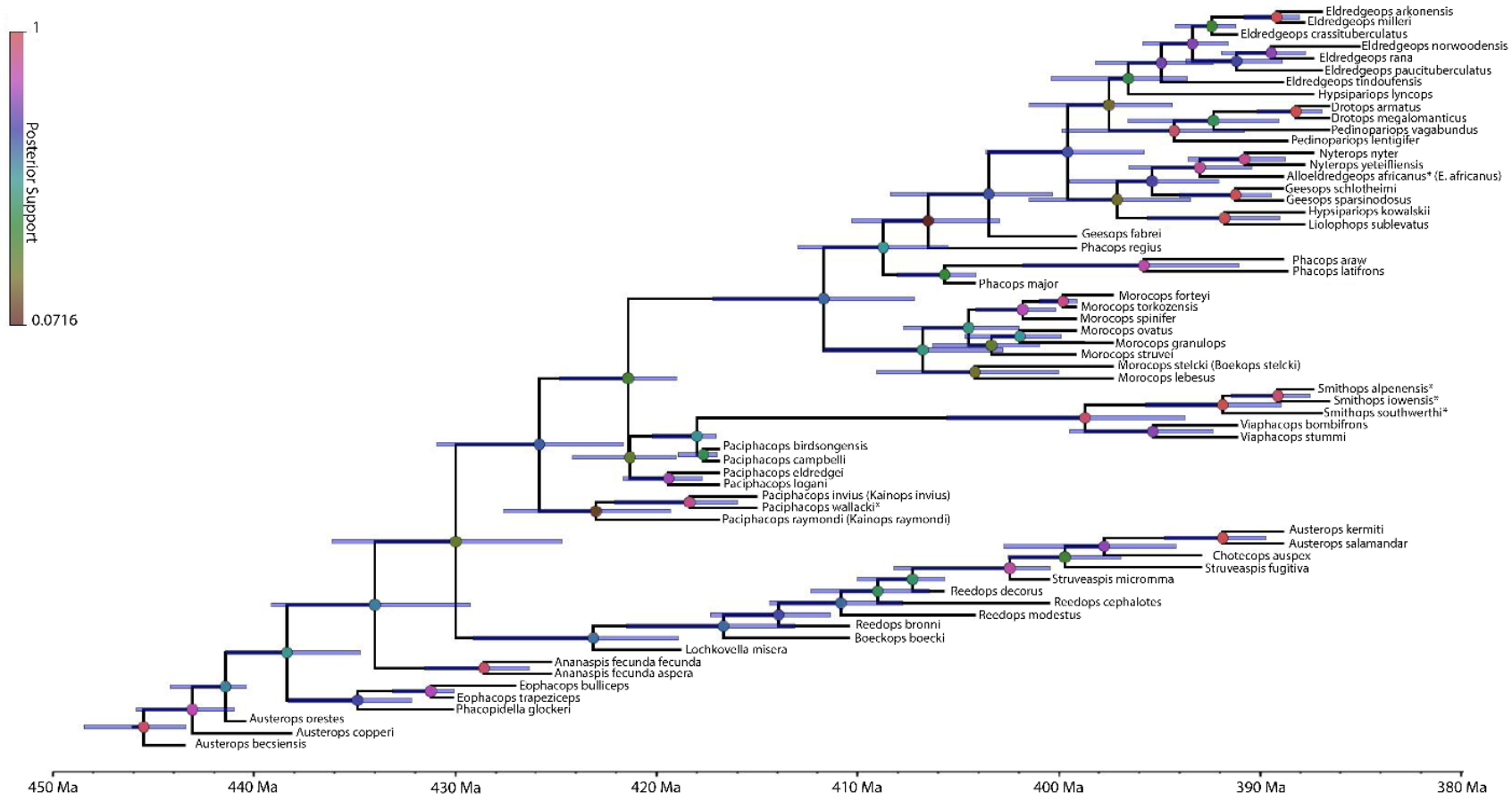

Figure 1.2—Timescaled Bayesian maximum clade credibility (MCC) tree recovered for the full dataset. Node symbols indicate posterior support values. Bars at nodes indicate 95% CI for the timing of the recovered branching event. Taxa names used reflect the systematics argued as a result of the analyses presented in this study. New taxa assigned are indicated with an asterisks (*), taxa names in parentheses indicate previous taxonomic assignment.

The maximum clade credibility tree (MCCT)(Figure 1.2) results in a fully resolved time-scaled phylogeny among members of the Phacopidae. Within this tree, the origin of the clade is recovered at ~445.8 million years ago (95% CI: 443.7-448.8 Ma), just prior to the Katian-Hirnantian boundary in the Upper Ordovician. Neither the consensus tree nor the MCCT recovered any of the previously recognized tribes as monophyletic, with all being paraphyletic or polyphyletic.

As recovered by the consensus Bayesian tree (Figure 1.1), genera that had been assigned to the tribe 'Ananaspini' can be recovered as grades, though this is true only of the North American genera (*Kainops*+*Paciphacops*+*Viaphacops*) within the MCCT (Figure 2). A clade representing *Phacops iowensis* (henceforth designated *Smithops* n.g.) and *Viaphacops* is recovered with a high degree of support (0.964). The interrelationships between species that have been assigned to *Kainops* and *Paciphacops* remain more difficult to parse. While *Kainops invius*+*Paciphacops wallacki* n.s. (originally *Paciphacops invius* small-eyed variant) are recovered with strong support (0.923), the monophyletic *Kainops* recovered in the MCCT is not very well supported (0.126).

Species that are here treated as *Morocops* are recovered in a monophyletic group that also includes *Boeckops stelcki*. Among other genera that have previously been assigned to the 'Geesopini', monophyly of the genus *Hypsipariops* is not supported, with neither *H. kowalskii* nor *H.* (=*Pedinopariops*) *vagabundus* recovered as sister to the type species *H. lyncops*. All members of *Eldredgeops* form a monophyletic group except for *E. africanus* (henceforth considered *Alloeldredgeops africanus* n.g.).

Modified Bayesian Inference—Following the initial runs of the full dataset, the dataset was degraded, removing a total of 8 characters (characters 4, 5, 21, 33, 34, 35, 39, 42). These characters relate to sculpture across the cephalon and eyes of the trilobite and were removed due to concerns of non-independence among those characters which would overweight the relative importance of sculpture in trait evolution across the Phacopidae.

As with the runs that used the entire dataset (above), the degraded dataset was subjected to five separate MCMC chains that were run and combined. Following the removal of burn-in, a total of 80,005 trees were recovered representing a total of 9,754 unique clades sampled across all trees. A consensus tree (Figure 1.3) was recovered that shows less resolution but similar within-genus sister relationships to the Bayesian analysis of the full dataset. The time-scaled topology of the MCCT of the degraded data set (Figure 1.4) recovers a nearly identical origin for the Phacopidae within the Upper Ordovician ~445.7 Ma (95% CI: 443.7-448.7 Ma).

Towards the root of the tree, the MCCT recovered from the full and degraded datasets show similar branching topologies. However, the consensus tree is largely unable to resolve the early branching relationships, with a large polytomy recovered for [*Lochkovella*+*Austerops*]+[*Viaphacops*+*Smithops*]+*Ananaspis*+*Paciphacops*+*Kainops.* All purported tribes (Table 1.1) are again recovered as either polyphyletic or paraphyletic in nature, with no support for the established tribe Cordapeltini.

As found in the MCC tree of the full Bayesian dataset, the North American members of the ‘Ananaspini’ are recovered paraphyletically. While *K. invius* is still recovered as sister to *Paciphacops (Kainops?) wallacki* with strong support (0.888), the genus *Kainops* is paraphyletic. A clade representing *Viaphacops* as sister to *Smithops* (*P. iowensis*) is similarly recovered with strong support (0.953).

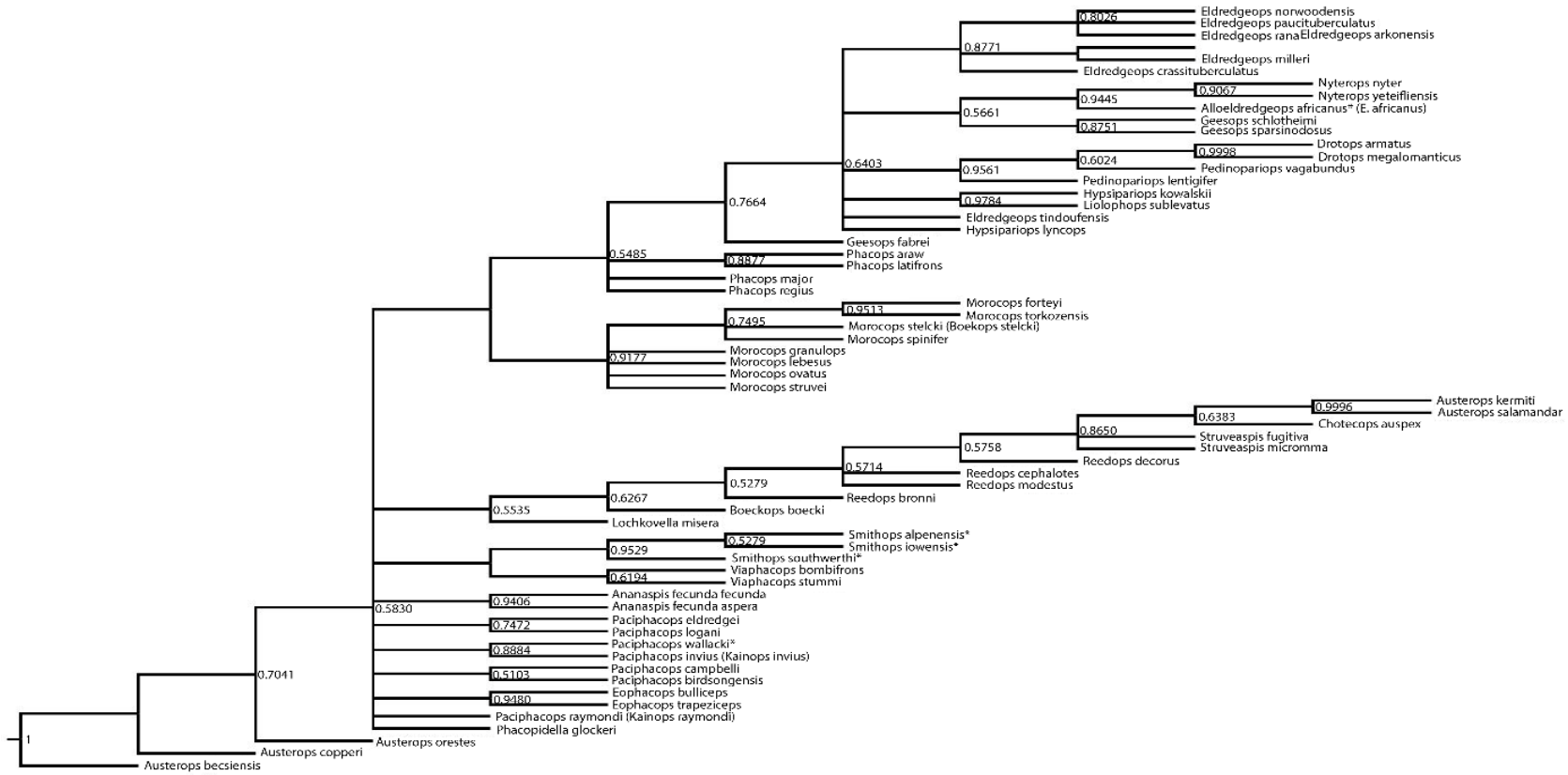

Figure 1.3— Majority rule consensus (50%) tree for all trees recovered via Bayesian inference of the degraded dataset (characters 4, 5, 21, 33, 34, 35, 39, 42 removed). Numbers at nodes indicate consensus support for recovered clades. Taxa names used reflect the systematics argued as a result of the analyses presented in this study. New taxa assigned are indicated with an asterisks (*), taxa names in parentheses indicate previous taxonomic assignment.

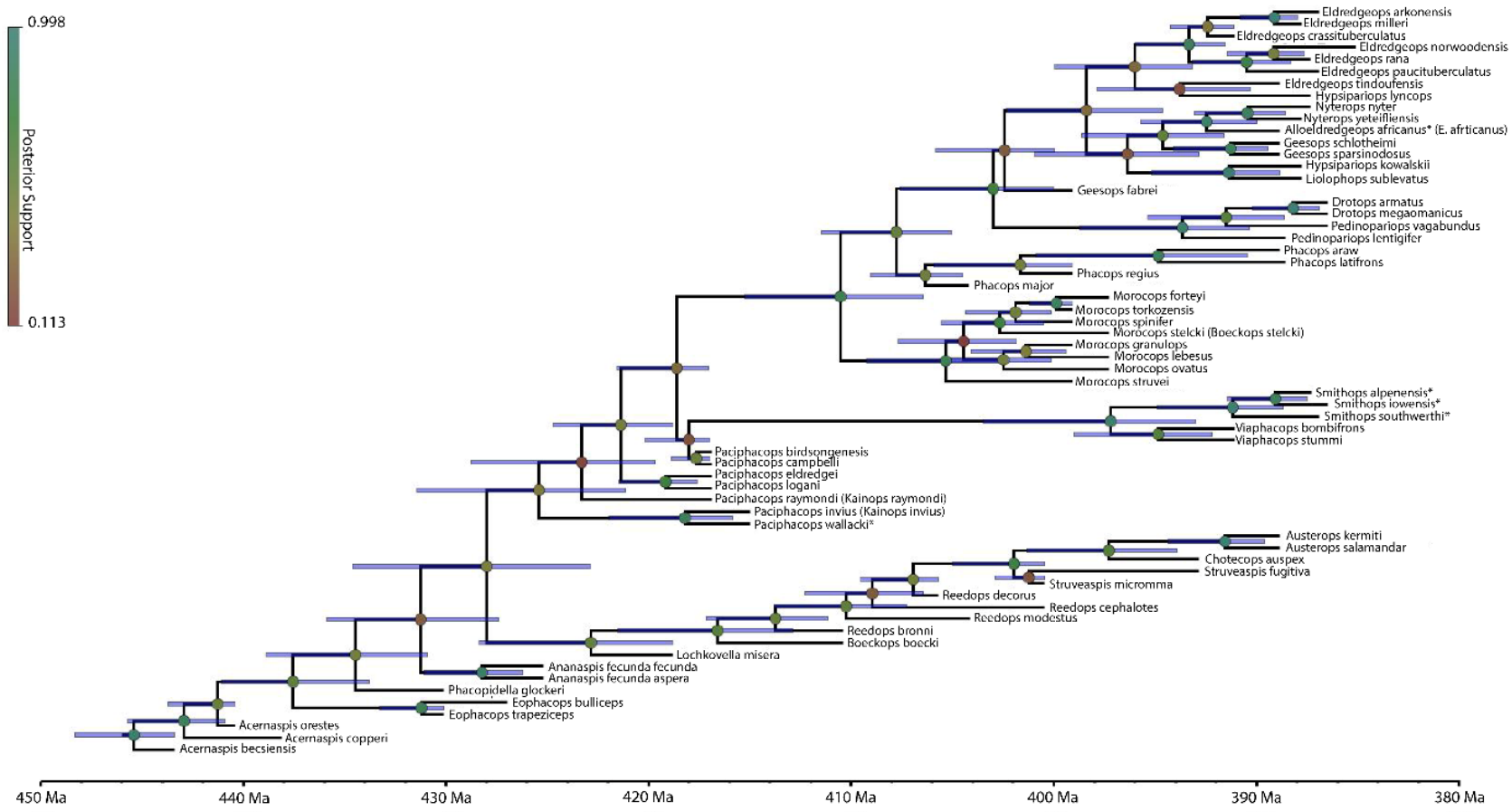

Figure 1.4—Timescaled Bayesian maximum clade credibility (MCC) tree recovered for the degraded dataset (characters 4, 5, 21, 33, 34, 35, 39, 42 removed). Node symbols indicate posterior support values. Bars at nodes indicate 95% CI for the timing of the recovered branching event. Taxa names used reflect the systematics argued as a result of the analyses presented in this study. New taxa assigned are indicated with an asterisks (*), taxa names in parentheses indicate previous taxonomic assignment.

All species that have been assigned to *Morocops* again form a monophyletic clade that also includes *B. stelcki*. This clade shows relatively strong posterior support (0.818), and is basal to the Eurafrican members of *Phacops* and all other species that were previously assigned to the 'Geesopini', similar to that of the full dataset. However, the Eurafrican members of *Phacops* are recovered as monophyletic, though with moderate support (0.494).

Alloeldredgeops n.g. (*E. africanus*) is again recovered as sister to the genus *Nyterops* with strong support (0.944). However, *Eldredgeops* (not *Alloeldredgeops*) is recovered paraphyletic with a clade uniting all North American members of the genus and a clade now representing *E. tindoufensis* and *H. lyncops*. The distribution of posterior clade support on these relationships are lower than recovered by the full data set (compare Figures 1.2, 1.4).

Parsimony Analysis —A heuristic search conducted using random stepwise addition with 1000 replicates yielded a total of 18 most parsimonious trees, each with a length of 995, a consistency index (CI) 0.15, retention index (RI) 0.56, and rescaled consistency index (RC) 0.085. While these metrics suggest some degree of homoplasy within the tree, the topology of the strict consensus tree (Figure 1.5) is well resolved and shows similar clade relationships as found in the Bayesian inference analyses. The most significant departure between the recovered parsimony topology with that of Bayesian, highlighted by an Adams consensus tree (Figure 1.6), is the recovery of *Struveaspis+Chotecops+ Austerops*. While recovered as sister to *Reedops* within the Bayesian analysis, under parsimony this clade was instead recovered sister to *Phacopidella+Eophacops*. No established tribes were recovered as monophyletic; instead, all were all recovered as gradational or polyphyletic in nature.

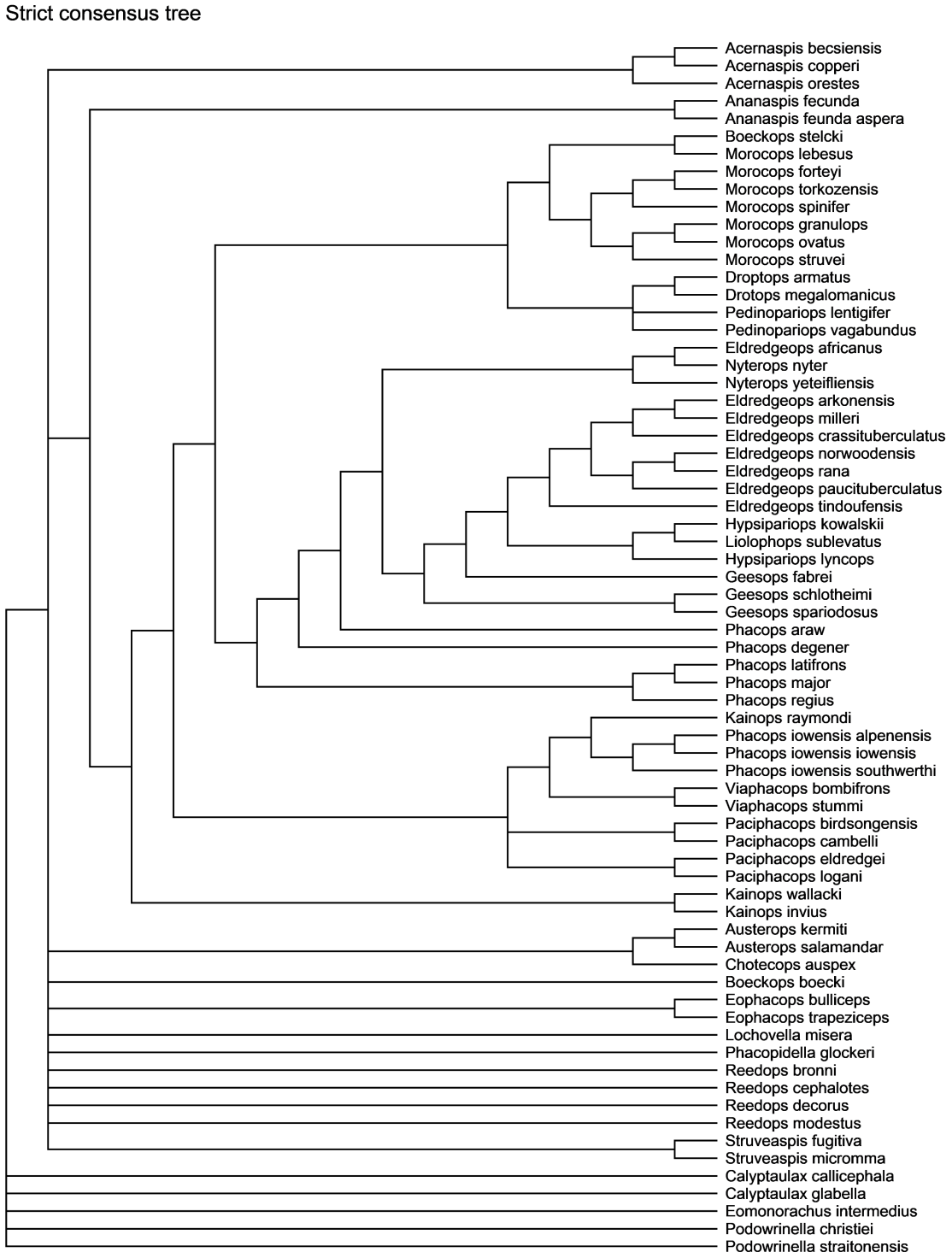

Figure 1.5—Strict consensus of 18 most parsimonious trees recovered in PAUP*.

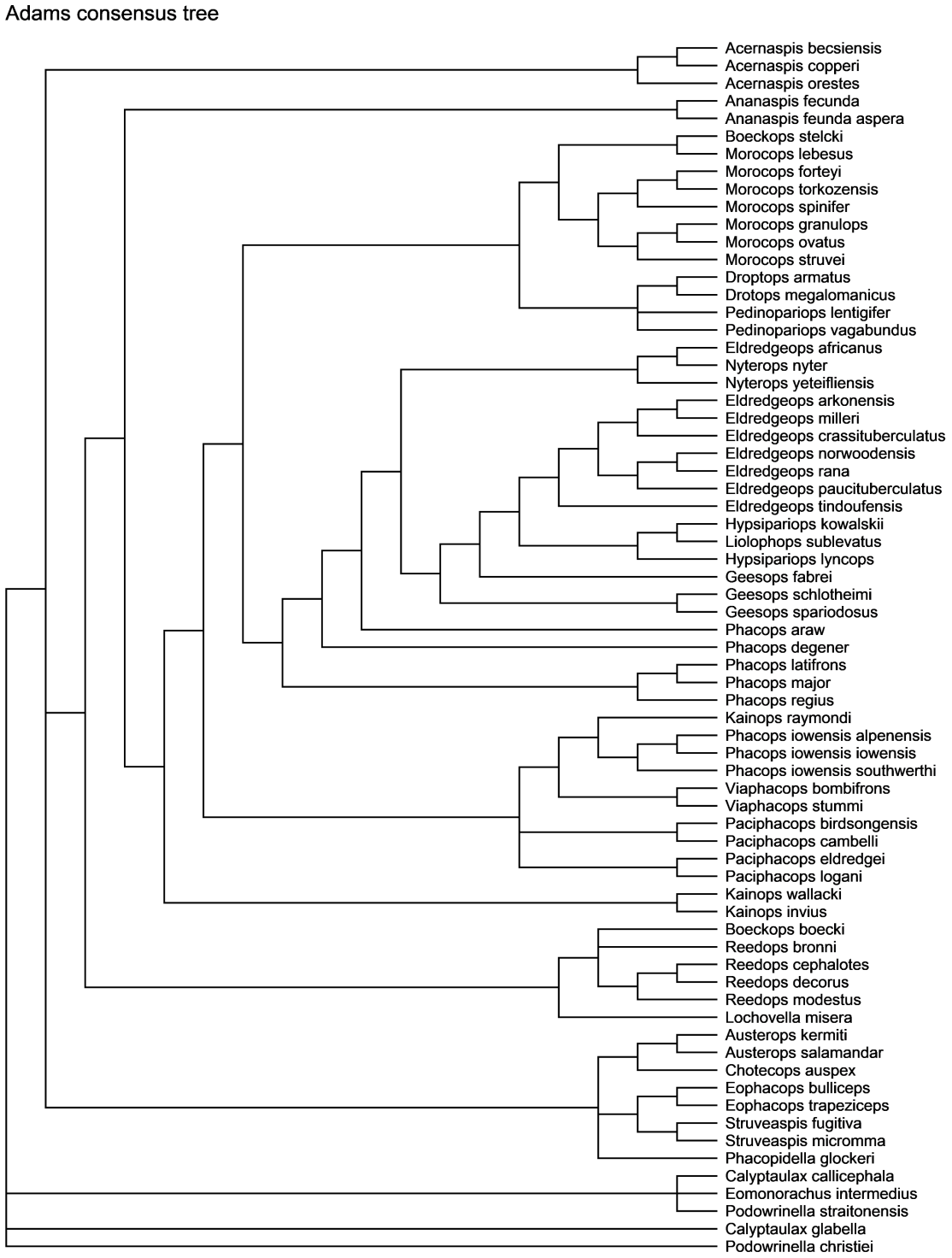

Figure 1.6: Adams consensus tree of 18 most parsimonious trees recovered in PAUP*.

A polytomy near the root of the tree was recovered, uniting a clade representing a monophyletic *Acernaspis*, a clade representing *Phacopidella-Eophacops-Struveaspis-Chotecops-Austerops*, and a branch uniting all other ingroup representatives of Phacopidae.

The tribe Ananaspini is recovered as polyphyletic, with a similar branching structure recovered via Bayesian inference, such that *Ananaspis* is sister to the rest of the clade. *Kainops invius* and *Paciphacops* (*Kainops?*) *wallacki* are recovered as a clade that is sister to *Paciphacops+Viaphacops+Smithops*. Sister relationships for these genera are similar to that recovered by the Bayesian inference analyses, the exception being *Kainops raymondi* recovered sister to *Smithops*.

As with all recovered topologies via Bayesian inference, the clade representing *Morocops* is sister to the clade representing *Phacops* and all other genera that have previously constituted the *'*Geesopini*'*. *Boeckops stelcki* is recovered sister to *M. lebesus*, the two species forming a sister-clade to all other species within the genus *Morocops* (see also Figure 1.2). However, the clade representing *Pedinopariops+Drotops* is recovered as sister to *Morocops* instead of its position closer to *Geesops* and *Hypsipariops lynncops+Eldredgeops* as found in previous analyses. A monophyletic *Eldredgeops* is recovered with exception of *Alloeldredgeops africanus* (= *E. africanus*) which was recovered as sister to *Nyterops nyter*, as found in trees recovered by Bayesian inference. Within this analysis, *Eldredgeops* (not *Alloeldredgeops*) is recovered as sister to *Hypsipariops lyncops*, as was recovered by Bayesian inference; however, *Hypsipariops lyncops* here forms a united clade with *Hypsipariops kowalskii* and *Liolophops sublevatus*. A monophyletic *Geesops* is not recovered within this analysis.

DISCUSSION—A consistent concern among phacopid workers regarding taxonomy/phylogenetics has been the recovery of trees that represent a small number of taxa with few characters that are often conserved across the clade leading to concerns of homoplasy and phylogenetic bouncing (see discussions by McKellar & Chatterton 2009). The analyses presented herein consist of the largest dataset thus far assembled for phylogenetic analysis of the trilobite family Phacopidae. Consensus trees recovered via Bayesian analyses suggest that the range of characters used herein sufficiently captures reliable phylogenetic signal within the data. This is further supported by generally close agreement between the trees that were recovered via probabilistic Bayesian inference methods and cladograms that were recovered using heuristic parsimony-based methods.

There are few unequivocal autapomorphies that define clades within the family Phacopidae, with several instances of reversals and convergent evolution. Although this situation is not ideal for delineating taxa, phylogenetic splitting over the last several decades seems to be largely beneficial to our understanding of the evolutionary history of the Phacopidae. There is a degree of agreement across the broad-scale branching patterns of shared genera included within this study and recent phylogenetic studies on phacopids (see McKellar & Chatterton, 2009; Oudot et al. 2019). However, some of the established genera are not supported as monophyletic or are unstable in phylogenetic position when subjected to large-scale phylogenetic analyses. The tip-dated MCCT presented in Figure 1.1 reflects the systematics argued within this paper. This allows for discussion of the macroevolutionary history of the Phacopidae, as well as the ability to understand rates of trait evolution through time.

Eldredgeops and Punctuated Equilibrium—The theory of punctuated equilibrium (Eldredge & Gould, 1971; Gould and Eldredge 1977, 1986, 1993) posits that while species may exhibit periods of change in a given direction, these trends are usually reversed and over their duration (sometimes over a period of millions of years) a species will exhibit little or no net morphological change, which has been termed "stasis". Though the biological underpinnings of how and why species may exhibit stasis are a source of much debate in the literature, punctuated equilibrium as a form of speciation and the tendency of morphological stasis are common observations of the fossil record. As such, phacopid trilobites play an integral part in the story of punctuated equilibrium, as they were one of the original two case studies discussed by Edlredge and Gould (1972).

As part of his PhD (1969) and early work as a curator at the American Museum of Natural History (1972), Eldredge made detailed observations and measurements of different populations of *Eldredgeops* (then *Phacops rana*) sampled from Middle Devonian strata across the Michigan and Appalachian basins. The data consisted of extensive measurements across the trilobite cephalon, as well as meristic counts, such as the total number of dorso-ventral files within the eye, which were then subjected to factor analysis to determine relative trends in variation for each of the various 'subspecies' of *Phacops rana*. Analysis revealed that while some subspecies would exhibit small amounts of change in their overall morphology, these trends would be reversed in stratigraphically younger populations. However, one trend he observed over all 'subspecies' was that the total number of dorso-ventral files remained constant within a lineage. Eldredge (1971, 1972) used cladistics to try and reconstruct a phylogeny for the group (Figure 1.7a-c).

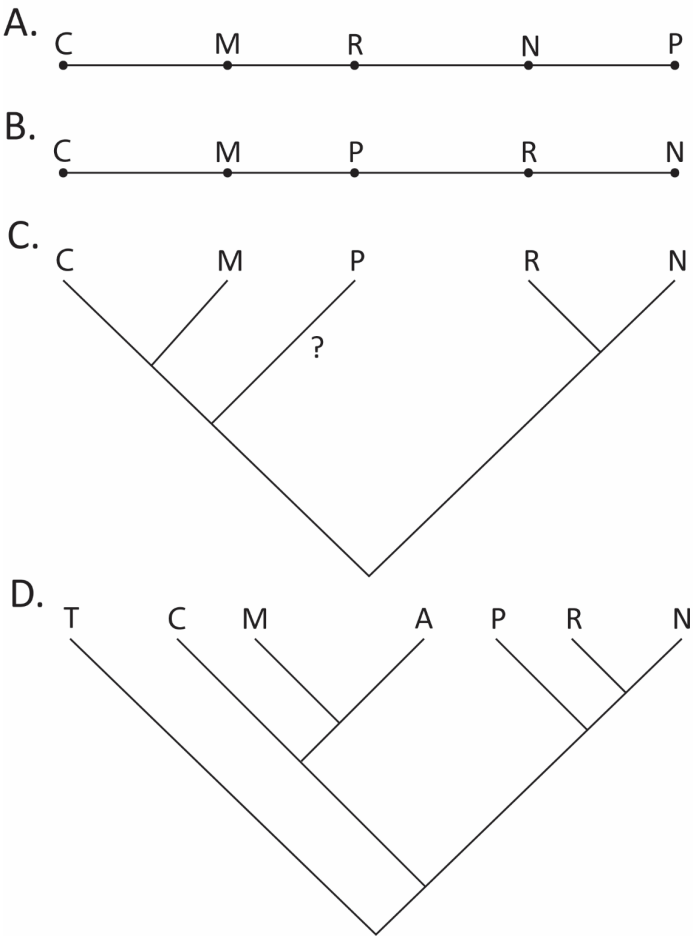

Figure 1.7: Simplified comparison of the results of Eldredge (1972) to the results recovered in this study. A-C are adapted from Eldredge (1972) A. simplified diagram of character gradients for species of *Eldredgeops* (then *Phacops rana*) where taxa are arranged solely on the number of dorso-ventral files. B. simplified character gradient where taxa are arranged based on all characters discussed within Eldredge (1972). C. simplified cladogram for the relationships of species of *Eldredgeops* (then *Phacops rana*). D. simplified cladogram of relationships recovered for *Eldredgeops* in the MCCT of the full dataset from Bayesian inference. Taxa symbols are as follows: A- *Eldredgeops arkonensis*; C- *E. crassituberculatus*; M- *E. milleri*; N- *E. norwoodensis*; P- *E. paucituberculatus*; R- *E. rana*; T- *E.tindoufensis*.

With the addition of the African members of '*Eldredgeops'* and testing for the validity of *Phacops rana arkonensis* within the group, the results of the present study confirm the results of Eldredge (1972) and recover a similar tree topology (Figure 1.8d). The recovered topology (Figure 1.1, Figure 1.2), confirms the hypothesis of Eldredge (1973) that *Phacops iowensis* (herein placed in *Smithops* n.g.) is more closely related to *Viaphacops* (then *Phacops cristatus*) than it is to the European *Phacops latifrons*. Further, as argued in Eldredge (2001), the 'subspecies' formerly assigned to *Phacops rana* should be considered separate species. It is herein argued that the designation of the genus *Eldredgeops*, honoring the many contributions of Dr. Niles Eldredge, be considered valid, but that it should exclude *Phacops rana africanus* which is herein designated as *Alloeldredgeops africanus*.

Phylogeography: The evolution of Phacopidae in North America—It has long been observed that North American members of *Eldredgeops* are more morphologically similar and, by extension, more closely related to phacopids originating from the Eurafrican region of Gondwana than they are to other Laurentian phacopids (Hall and Clarke, 1888 p.24; Eldredge 1972, p.59). Two competing hypotheses have been proposed as to which genus is likely sister to *Eldredgeops*. Original arguments made by Eldredge (1972) suggested that the sister genus to *Eldredgeops* is the European genus *Geesops* (then *P. rana* and *P. schlotheimi* respectively). The alternative hypothesis, presented by Struve (1990, 1992, 1995), argues the sister to *Eldredgeops* was the Eurafrican genus *Pedinopariops*. The arguments by both authors suggest an independent invasion of the Laurentian continent during the Middle Devonian of species from Gondwana. This Gondwana-to-Laurentia invasion has been reported for other trilobite groups during this time: four species of the genus *Greenops* Delo 1935 represent the single North American members of the trilobite subfamily Asteropyginae which is otherwise confined to the Gondwanan continent (Eldredge, 1972).

Previous phylogenetic hypotheses do not support the invasion of North America by *Eldredgeops* (see Ramsköld & Werdelin, 1991; McKellar & Chatterton, 2009). Both those studies recovered *Eldredgeops* as an intermediate between the other North American phacopids (such as *Kainops, Paciphacops,* and *Viaphacops*) and the European *Phacops*. Under such a phylogenetic arrangement, diversification is reversed such that *Eldredgeops* origintated within the Laurentian continent and subsequently invaded Gondwana.

All analyses presented herein support the original observations made by Hawle & Clarke (1888) and Eldredge (1972), whereby the North American members of *Eldredgeops* are more closely related to Eurafrican phacopids. All recovered phylogenetic hypotheses find marked

separation between the 'North American stock' (*Kainops?, Paciphacops, Viaphacops,* and *Smithops*) and *Eldredgeops*, suggesting that the *Eldredgeops* clade independently invaded the Laurentian continent during the Middle Devonian period, well after the origination of the North American phacopids that gave rise to *Paciophacops, Viaphacops,* and *Smithops*.

Lens Development and Rosa's Rule—"Rosa's rule" is a biological principle that argues there is a tendency for greater trait variation in early members of a group or clade which drives towards the point of trait fixation in later members (Rosa, 1899; Wagner, 1988; Sterns, 1993; Webster, 2019). Documentation of a higher degree and frequency of intraspecific variation in Cambrian relative to post-Cambrian trilobites—at least in some traits—offers empirical support for such a pattern (reviewed by Webster, 2019, pp. 100-101). Rosa's rule may suggest that developmental systems became progressively more tightly regulated through clade history, resulting in a declining degree of trait variation.

The present study offers an apparent example of Rosa's rule within the Phacopidae. Using the MCCT produced from the full Bayesian dataset, trait mapping of the total number of dorso-ventral files within an eye (Figure 1.8) reveals taxa branching from the earliest nodes (*Acernaspis* through *Lochkovella+Austerops*) show the greatest degree of intraspecific variation (and interspecific disparity) in number, ranging from 12 dorso-ventral files within *Struveaspis* to 26-29 within *Reedops.* Variation in the total number of dorso-ventral files is particularly accentuated in the genus *Reedops*, where *R. bronni* possesses 14-16 dorso-ventral files while its very close relative (one node crownward) *R. modestus* possesses 26-29 dorso-ventral files.

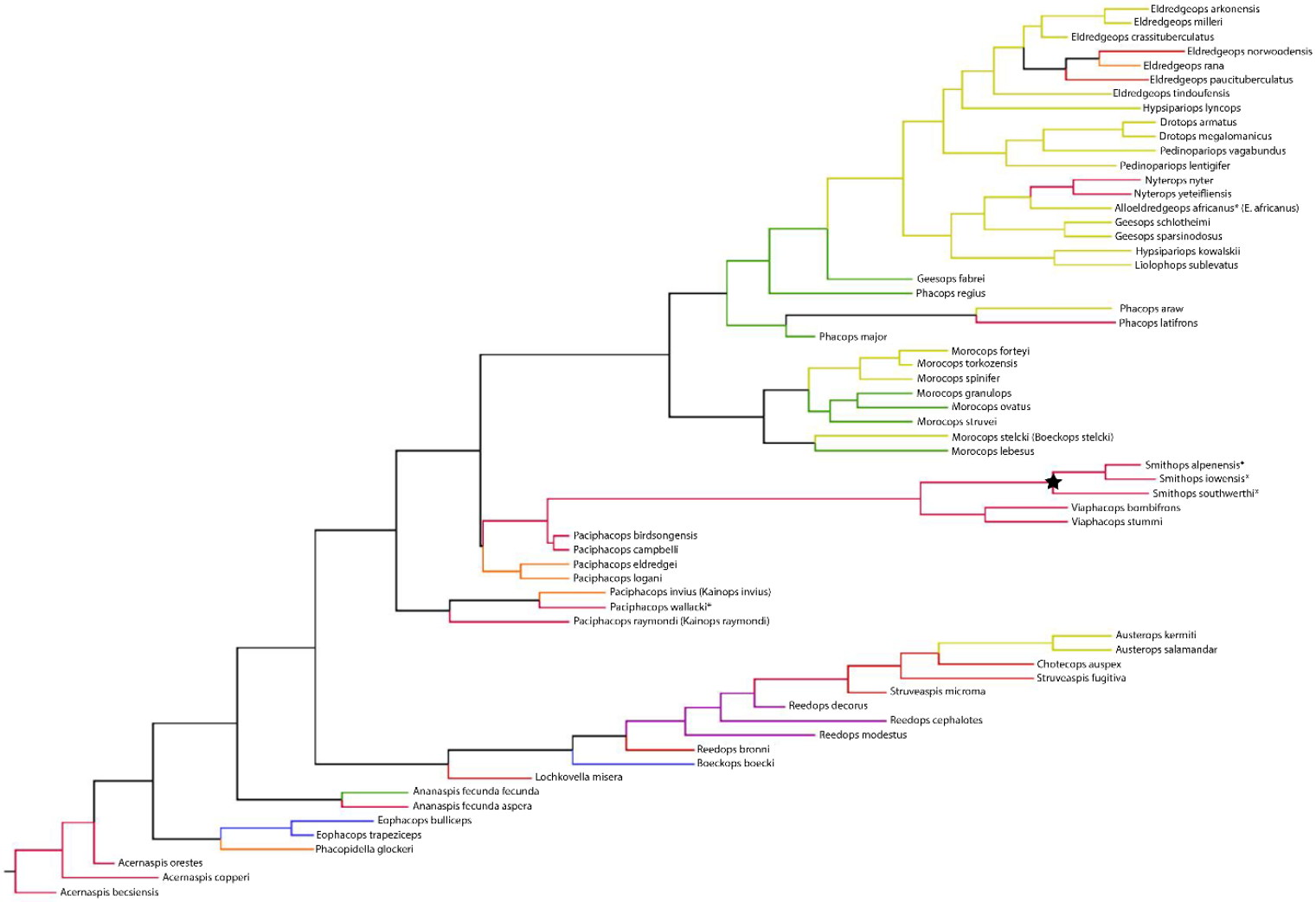

Figure 1.8—Maximum clade credibility tree recovered via Bayesian inference of the full dataset colored mapping the maximum number of dorso-ventral files for a given species. Taxa that have been reassigned are indicated with their previous taxonomic name in parentheses, new taxa are indicated with and asterisks (*) and star reflects the taxonomic change of species formerly assigned to *Phacops iowensis*. Colors indicate the total number of dorso-ventral files as follows: Red, 13-16; Orange, 17; Yellow, 18; Green, 19; Blue, 21-23; Purple, 24-26.

Through the subsequent diversification of the Phacopidae, the variation in number of dorso-ventral files lessened, with most species and genera crownward of the node connecting *Morocops* to the rest of the tree having a number of dorso-ventral files fixed at either 18 or 19 dorso-ventral files.

A similar pattern of decreasing variation is also observed among the initial North American stock of phacopids (*Paciphacops, Viaphacops,* and *Smithops*). The earliest members of this group belonging to the genus *Paciphacops*, show lability in the total number of ranging between 14 to 18 dorso-ventral files depending on the species. Later genera of the group are characterized by stability in the number of dorso-ventral files (14 in *Viaphacops,* 13 in *Smithops*).

It is noteworthy that this general pattern of decreasing intraspecific variation and interspecific disparity in the number of dorso-ventral files within the Phacopidae is broken to some extent within the genus *Eldredgeops*. Indeed, while the number of dorso-ventral files remains constant within each species of *Eldredgeops*, the total number of dorso-ventral files changed at least twice within that genus if the most recent common ancestor of *E. paucituberculatus* and *E. rana/E.norwoodensis* possessed 15 dorso-ventral files, or three times if the most recent common ancestor possessed 18 dorso-ventral files (Figure 1.8).

A pattern of decreasing variation consistent with Rosa's rule can arise through various means, including the partitioning geographically-structured variation within daughter species following allopatric speciation, the exhaustion of genetic variation, or from increased morphological homeostasis (Webster, 2019). Any long-term decrease in phenotypic variation, on

the order of 10^6 to 10^7 years, may have profound consequences for a clade in terms of evolutionary rate and survivorship (reviewed by Webster, 2019).

The Late Devonian was characterized by several major extinction pulses, one of which (the Hangenberg event) saw the ultimate extinction of the Phacopidae (Chlupáč, 1975;Crônier & Feist, 2000; Feist et al., 2009, McNamera & Feist, 2016, Feist, 2019) A large-scale trend observed above the species-level of members of the Phacopidae show both a progressive decrease in the number of lenses within a dorso-ventral file and a decrease in the number of dorso-ventral files, up to and including complete blindness (Chlupáč, 1975; Feist, 2019). Such atheloptic genera are not included in the present study, and their placement within the phylogenetic framework presented herein remains to be determined. It is therefore unknown whether these Late Devonian taxa represent a single clade, and whether the changes in lens and file number within any such clade(s) represents a retention of plesiomorphic lability or a de novo establishment of variation within previously fixed traits. Explorations of the mechanisms underlying phenotypic variation in traits such as eye lens number and arrangement, and of the extent to which such variation served as a constraint in phacopid disparification and survivorship through the Middle and Late Devonian, represent fruitful avenues for future research.

SYSTEMATIC PALEONTOLOGY—

Class Trilobita Walch 1771
Order Phacopida Salter 1864
Family Phacopidae Hawle and Corda 1847

Discussion—As predicted by previous studies (McKellar & Chatterton, 2009; Oudot et al., 2019), there is little support for many of the purported tribes within the family Phacopidae. Within the present analysis, the only tribe recovered as monophyletic was the monogeneric ‘Reedopini’, and

even that only via Bayesian inference. The 'Ananaspini,' 'Cordapeltini,' 'Geesopini,' and the 'Phacopini' were all recovered as either paraphyletic or polyphyletic. Genera are herein discussed in order from the phylogenetically most basal-branching to the phylogenetically most crownward, as determined by the present analysis.

Genus *Paciphacops* Maksimova 1972

Type species— *Phacops logani* (Hall 1861)

Discussion— Maksimova (1972) erected the genus *Paciphacops* and recognized two subgenera within it: *P.* (*Paciphacops*) with type species *Phacops logani* and *P.* (*Viaphacops*) with type species *P. pipa* Hall & Clarke 1847 (a junior synonym of *P. bombifrons*, see Eldredge, 1973). The original concept of *Paciphacops* (*Paciphacops*) included the North American *Phacops logani*-group, as well as several representatives from Russia and Australia (see Maksimova, 1972). Campbell (1977) reviewed both subgenera of *Paciphacops* and assigned new species of North American phacopids, including two morphs of *P. invius*, to the subgenus *Paciphacops* (*Paciphacops*).

Phylogenetic analysis by Ramsköld and Werdelin (1991) focused on early evolution within the family Phacopidae, comprising many representatives from genera such as *Acernaspis*, *Ananaspis*, *Paciphacops* (*Paciphacops*), *Paciphacops* (*Viaphacops*), and *Phacops* (taxonomic assignments per 1991). That analysis resulted in six species previously assigned to *Ananaspis* and *Paciphacops* (*Paciphacops*) being reassigned to the new genus *Kainops* with type species *Kainops micops*. *Kainops* shares many overlapping traits with *Paciphacops* but is most easily diagnosed by differences in the sclera of the eye.

McKellar and Chatterton (2009) expressed concern regarding the generic status of *Kainops* following their phylogenetic analysis, suggesting that *Kainops* may be a subgenus of *Paciphacops*. In the present analysis (above), a monophyletic *Kainops* was only recovered in the MCCT of the full dataset, though with low support (0.126). Neither of the Bayesian consensus trees, nor the MCCT of the degraded Bayesian dataset, nor strict consensus tree recovered in PAUP recovered a monophyletic *Kainops*, and that genus shows repeated polyphyly with respect to the genus *Paciphacops*. It is thus argued that at this time *Kainops* be suppressed as a genus and all species previously assigned to *Kainops* be treated as *Paciphacops* until subsequent phylogenetic analysis can better resolve the relationship between members of *Paciphacops* (*Paciphacops*) and *Paciphacops* (*Kainops?*).

Paciphacops wallacki new species

1977 *Paciphacops* (*Paciphacops*) *invius*, Campbell, p. 55-56, pl. 15 fig. 1-2.

Type material—OU 7212A, herein designated as the holotype. Material used to code phylogenetic analysis is figured in Campbell (1977) plate 15. Specimens were not examined first-hand by the author.

Etymology—Named in honor of Eric Wallack, professor of fine and performing arts at Owens Community College, for his dedication to his students, and his passion and appreciation for paleontology.

Diagnosis— Eye with 15 dorso-ventral files, maximum five lenses per file. Lenses reduced or flush with the scleral wall, sclera thick throughout the eye. Glabellar ornament with crowded depressed tubercles, otherwise few superimposed granules over the surface. Subocular librigenal

field shows posterior widening relative to *Paciphacops invius.* Lateral nodes of 1p globular, poorly defined medially, which is generally narrower than in other species.

Occurrence— Described from 3 specimens from the Fittstown member of the Bois d'Arc formation (Lochkovian) of Oklahoma.

Remarks—Campbell (1977) described the new species *Paciphacops* (*Paciphacops*) *invius* with two morphs based on the overall morphology of their eye (a "large-eye morph and a "small-eye" morph). Ramsköld and Werdelin (1991) argued that there is "no morphological or circumstantial evidence supporting [dimorphism], and regard *P. invius* and the 'small-eyed morph' as two species." Within Ramsköld and Werdelin (1991), *P. invius* was reassigned to their new genus *Kainops* as *Kainops invius*; however, the "small-eyed morph" was not subsequently reassigned as a new species to either *Paciphacops* or *Kainops*. Following the phylogenetic analysis presented above, the "small-eyed morph" is herein formally named *Paciphacops wallacki* n.s.

Genus *Viaphacops* (Maksimova 1972)

Type species—*Phacops bombifrons* (Hall 1861); Original type designation *Phacops pipa* Hall and Clarke 1888 (junior objective synonym of *Phacops bombifrons, =Phacops cristatus bombifrons* fide Eldredge 1973, p. 315).

Emended diagnosis—Glabella strongly inflated covered in coarse, low tubercles. Glabellar furrows 2s and 3s weakly developed, sometimes absent. Axial furrow shallows adjacent to 1p

lateral node. Occipital ring narrow relative to other members of Phacopidae. Palpebral furrow weakly developed along the median one-third of its course. Subocular librigenal field wide relative to other members of Phacopidae. Genal angle drawn out, with an acute tip or small spine. Eyes with 13-17 dorso-ventral files, lenses generally reduced or flush with scleral wall, sclera thickly developed.

Pygidium with six to nine axial rings plus terminal piece. Six to eight pleurae. Semicircular in outline, posterior nearly transverse medially. Interpleural furrows developed. Pygidium usually covered in low, round tubercles and granules.

Included species—*Viaphacops bombifrons*, *Viaphacops canadensis* (Stumm 1954), *Viaphacops cristatus* (Hall 1861), *Viaphacops gaspensis* (Clarke 1908), *Viaphacops nasutus* (Stumm 1954), *Viaphacops stummi* (Eldredge 1973), *Viaphacops variablis* (Eldredge 1973).

Discussion—Maksimova (1972) erected the subgenus *Paciphacops* (*Viaphacops*). Trilobites belonging to the North American *Phacops cristatus* and its associated species/subspecies were placed within. The genotype was originally designated as *Phacops pipa*, but Eldredge (1973) argued that *P. pipa* is a junior objective synonym of *Phacops bombifrons*. Eldredge (1973) regarded all species of *Viaphacops* as part of a subspecies complex belonging to *Phacops cristatus* and assigned all to the genus *Phacops*. Subsequent work viewed the transfer of the *cristatus*-complex to *Viaphacops* as valid but often treated *Viaphacops* as a subgenus of *Paciphacops* (see Campbell, 1977). Phylogenetic analysis by Ramsköld and Werdelin (1991) found separation between *Viaphacops* and *Paciphacops*, such that the authors argued the two be treated as separate genera. Further, Ramsköld and Werdelin (1991, Appendix 1) argued that the

individual subspecies of '*Viaphacops cristatus*' be treated as separate species, which has been adopted herein.

Struve (1990) erected the genus *Burtonops* as a wastebasket taxon to encompass the diversity of forms he argued were erroneously assigned to *Phacops rana africanus*. The type species of *Burtonops* was designated as *Viaphacops cristatus* [*Phacops cristatus* within the text] (Hall 1861). *Burtonops* appeared within Struve (1990, 1992) but neither publication specified the internal taxonomy of *Burtonops*. As such, Struve remains the only author to use *Burtonops*. It is here argued, as in McKellar and Chatterton (2009), that *Burtonops* be suppressed as a genus.

Genus *Smithops* new genus

Type Species— *Smithops iowensis* Delo, 1935, from the Middle Devonian Traverse Group of Michigan.

Etymology—The surname Smith is combined with the Latin suffix *-ops* (from *Phacops)* in reference to the phylogenetic affinities of the specimens described herein. The genus is named in honor of Denise Smith, Provost and Vice President of Academics at Owens Community College for her passionate support and dedication to first generation college students.

Diagnosis—Moderately large eyes bearing 13 dorso-ventral files. Lens surface generally flush with scleral wall, lenses separated by a relatively thick sclera. Tuberculation generally coarse across all regions, particularly across various regions of the cephalon, including the subocular platform and genae. Tubercles may be conical; generally uniform in size. Some overhang of the glabella over the frontal margin. Genal angle terminating at bluntly rounded angle. Glabellar

furrows 2p and 3p weakly developed to absent. L1 lateral node transverse to subquadrate, L1 lateral nodes not strongly separated from medial portion of L1.

Thorax generally covered with tubercles similar to those on the cephalon.

Pygidium with eight to 10 axial rings; six to eight pleurae. Pleurae highly arched, with deeply incised plural furrows. Generally semicircular in outline though nearly transverse medially. Tuberculation coarse across all regions of pygidium.

Included species—*Smithops iowensis* (Delo, 1935), *S. alpenensis* (Stumm, 1953), and *S. southwerthi* (Stumm, 1953).

Occurrence—All species of *Smithops* are confined to the Middle Devonian Traverse Group of Michigan (see Eldredge, 1972, Table 8).

Discussion—Eldredge (1972, 1973) proposed that the subspecies belonging to *Phacops iowensis* were taxonomically similar to the other North American phacopids *Viaphacops* (then *Phacops cristatus*-group) and *Paciphacops* (then *Phacops logani*-group), though those taxa all fell within the broad diagnosis of *Phacops* (sensu *Phacops latifrons*) at that time. All phylogenetic analyses within this present study recovered *Phacops iowensis* as sister to *Viaphacops* (with the exception of *Kainops raymondi* within the parsimony analysis), rather than closely related to *Phacops latifrons*. *Phacops iowensis* is therefore reassigned herein to *Smithops* n.g.. The three subspecies of *Phacops iowensis* recognized by previous workers are uniquely diagnosable and are herein raised to the species level.

Smithops iowensis (Delo 1935)

1935 *Phacops iowensis* Delo, p. 422-423, pl. 48.
1953 *Phacops iowensis iowensis* Stumm, p. 140-142, pl. 12
1972 *Phacops iowensis iowensis* Eldredge, p. 58-59, 92, fig. 3.

Type material—Holotype: No. 9-266, Department of Geology, State University of Iowa.

Hypotypes: No. 2257, 27055, 27061, 29229, and 29230, Museum of Paleontology, University of Michigan.

Diagnosis—See Eldredge (1972, p. 92).

Smithops alpenensis (Stumm 1953)

1953 *Phacops rana alpenensis* Stumm, p. 139-140, pl. 11.
1953 *Phacops rana bellensis* Stumm, p. 139, pl. 10.
1972 *Phacops iowensis alpenensis*, p. 91-92, fig. 22.

Type material—Holotype: UMMP 25516

Diagnosis—see Eldredge (1972, p. 92).

Smithops southwerthi (Stumm 1953)

1953 *Phacops iowensis southwerthi* Stumm, p. 141-142, pl. 12.
1972 *Phacops iowensis southwerthi* Eldredge, p. 92, fig. 23.

Type material—Holotype: UMMP 24313

Diagnosis—see Eldredge (1972, p. 92).

Genus *Morocops* Basse 2006

2006 *Morocops* n.g., Basse, p. 117–118, pl. 29, fig. 277–279.
2009 =*Barrandeops*, McKellar & Chatterton.
2016 *Barrandeops*, Khaldi et al., p. 360.
2017 *Morocops*, van Viersen, Holland & Koppka, p. 6–7.

Type species—*Phacops* (*Phacops*) *sparsinodosus struvei*, Schraut, 2000b

Included species— *Morocops chattertoni* (Khaldi, Crônier, Hainaut, Abbache & Ouali Mehadji, 2016); *Morocops forteyi* (McKellar & Chatterton, 2009); *Morocops granulops* (Chatterton, Fortey, Brett, Gibb & McKellar, 2006); *Morocops lebesus* (Chatterton, Fortey, Brett, Gibb & McKellar, 2006); *Morocops ovatus*, (McKellar and Chatterton, 2009); *Morocops torkozensis* (Schraut, 2000a); and *Morocops spinifer* (Van Viersen, Holland & Koppka, 2017).

Emended Diagnosis—See Van Viersen, Holland & Koppka (2017). Eye with 18 dorso-ventral files and a maximum of eight lenses per file.

Discussion— Schraut (2000b) erected the subspecies *Geesops sparsinodosus struvei* and figured the holotype and several paratypes. The holotype was refigured in Basse (2006) and reassigned to the new monospecific genus *Morocops*. McKellar and Chatterton (2009) included *Morocops struvei* within their phylogenetic analysis, having coded *Morocops* from figures in both Schraut (2000) and Basse (2006). McKellar and Chatterton (2009) also erected the genus *Barrandeops* to encompass the diversity of newly described, highly tuberculate phacopids from Morocco. van Viersen et al. (2017) argued that the specimens figured by Schraut (2000b) actually represent two separate species, raising questions about the phylogenetic placement of *Morocops* within McKellar and Chatterton (2009). Further, van Viersen et al. (2017) argued that *Barrandeops* is a junior subjective synonym to *Morocops*, though this hypothesis had not been phylogenetically tested until the present analysis.

To determine the relationship of *Morocops struvei* to species previously assigned to *Barrandeops*, only references to the type species figured in Basse (2006) have been used herein to code *M. struvei*. Within all analyses presented here, species of *Barrandeops* were recovered in a clade that also included the type species *M. struvei*, supporting the hypothesis by van Viersen

et al. (2017) that *Barrandeops* be regarded as a junior subjective synonym of *Morocops.* Further, *Boeckops stelcki* was consistently recovered within the *Morocops* clade, warranting the reassignment of that species to *Morocops*.

Morocops stelcki (McKellar and Chatterton, 2009)

2009 *Boeckops stelcki* McKellar and Chatterton, p.41-43, pl. 11.1-11.10, 12.1-12.6.

Diagnosis—See McKellar and Chatterton (2009, p. 41-43).

Discussion—As noted by McKellar and Chatterton (2009, p. 62) placement of *B. stelcki* within the genus *Boeckops* was questionable. *Boeckops stelcki* was intermediate between the branches representing *Boeckops boecki* and *Barrandeops* (see McKellar & Chatterton 2009, fig. 6). *Boeckops stelcki,* as described by McKellar and Chatterton (2009), is congruent with the emended diagnosis of *Morocops* by van Viersen et al. (2017); that finding is supported herein.

Pedinopariops Struve, 1972

Type species—*Phacops* (*Phacops*) *lentigifer* Struve 1970

Diagnosis—Relatively large eye with 18 dorso-ventral files, averaging six to 10 lenses per file. Cephalon subangular to angular. Glabella covered in coarse tubercles. Lateral node of 1p not strongly inflated; 1p increases in length such that its sagittal length is equal to or larger than the length of the occipital ring. Short row of small spines along posterior border.

Discussion—Thickened sclera with tubercles, shared synapomorphy with sister genus *Drotops.* Members of *Pedinopariops* show may be differentiated from *Drotops* based on their lack of exaggerated sculptural elements (spines or sharp conical tuberculation) and may be slightly

smaller. Morphologically mature specimens of *Pedinopariops* are still comparatively large to other members of the Phacopidae. Glabellar furrows 2p and 3p weakly developed and show a relative increasing in spacing compared to sister genera.

Pedinopariops vagabundus (Struve, 1990)

1990 *Pedinopariops (Hypsipariops) vagabundus*; Struve, p. 255, Abb. 5
1995 *Pedinopariops* (*Hypsipriops*) *vagabundus*; Struve, p. 95-96, Abb. 24.
2009 *Pedinopariops* (*Hypsipariops*) *vagabundus*; McKellar & Chatterton, p. 57–60, pl. 19.

Type Material—Holotype: SMF 49402 from Southeast Morocco, Eifelian limestone chalk (Middle Devonian).

Diagnosis—See McKellar & Chatterton (2009) for diagnosis and extensive description of material.

Discussion—All phylogenetic analyses conducted herein recover *Pedinopariops* (*Hypsipariops*) *vagabundus* as sister to the type species of *Pedinopariops* (*P. lentigifer*) and failed to recover it as sister to *Hypsipariops lyncops*. Therefore, the trilobite is hereby reassigned soley to the genus *Pedinopariops*.

Alloeldredgeops new genus

Type Species—*Phacops rana africanus* Burton & Eldredge, 1974.

Etymology—The prefix "*Allo–"* from the Latin *alius*, meaning different or other, is combined with the genus name *Eldredgeops*.

Diagnosis—Eye small, set high on gena, with 18 dorso-ventral files, maximum five to six lenses per file. Subocular pad well developed beneath eye, both in height and width. Lenses reduced or flush with scleral wall, thick sclera developed throughout. Glabella covered in coarse, pustular tubercles. Glabellar furrows 2p and 3p weakly developed or absent, commonly obscured by tuberculation otherwise cephalon generally free of ornamentation. Intercalating ring weakly developed, lateral nodes of occipital ring poorly developed. 1s furrow approximately subparallel to occipital ring. Anterolateral border of cephalon semicircular in outline.

Pygidium semicircular in profile. Pygidial axis almost reaches posterior of pygidium. Total of nine-11 axial rings with six to seven pleurae. Pleurae strongly developed and wide. Pygidium lacks ornament.

Occurrence—Tifariti area and Gor Lutund, Western Sahara (presently claimed by Morocco); Zagora, Tafilalet, Morocco.

Discussion—Burton and Eldredge (1974) described two new 'subspecies' of *Phacops rana* from western Africa: *Phacops rana africanus* and *Phacops rana tindoufensis*. *Phacops rana africanus* was compared to *P. rana crassituberculata*, and several differences were noted mostly regarding eye morphology. *Phacops rana africanus* was noted to have a relatively smaller eye, with a rather large subocular pad and *P. rana africanus* has comparatively less ornament compared to other members of *'Phacops rana*'.

Struve (1990) erected the new genus *Eldredgeops*, which included trilobites belonging to *Phacops rana* from both North America and North Africa; however, a formal generic description

was not given until Struve (1992). In neither case was it explicitly stated which species/subspecies should be assigned. The last statement by Struve on the status of *Eldredgeops* was: "*Eldredgeops* belongs to a five-species group in North America and North Africa…which includes *E. africanus* and *E. tindoufensis*" (Struve, 1995, p. 83). However, systematic placement of *E. africanus* has remained unsettled. Struve (1990) also erected the genus *Burtonops* to contain a diversity of forms he believed had been erroneously assigned to *E. africanus*, but could not be allocated within the genus *Droptops*. Taxonomic affinity of *Burtonops* has not been discussed and the genus should be suppressed as a junior subjective synonym of *Viaphacops* (see above). Basse (2012) argued that *E. africanus* questionably belongs to the genus *Hypsipariops* and is synonymized into *Hypsipariops? overwegi*. No analyses presented herein recovered *E. africanus* as sister to either *Eldredgeops* nor *Hypsipariops*; instead, all consistently recovered the species as sister to the genus *Nyterops*. "*Eldredgeops" africanus* differs in many regards from *Nyterops*, most significantly in a reduction in overall sculptural elements of the cephalon, thorax, and pygidium. Accordingly, the species is herein assigned to a new, monotypic genus *Alloeldredgeops* n.g.

Alloeldredgeops africanus (Burton & Eldredge, 1974)

1939 *Phacops latifrons* Bronn; Le Maître, p. 203.
1964 *Phacops schlotheimi* Bronn; Arden and Rehrig, p. 1522.
1974 *Phacops rana africanus* Burton & Eldredge, p. 353–355, pl. 47, fig. 8-9; pl. 48, fig. 1–4.
1990 *Burtonops* nom. nud. Struve, p.
1995 *Eldredgeops? africanus* Struve,
2012 *Hypsipariops? overwegi* Basse, p. 209

Type specimen.—Holotype: USNM 174072 from the *Wernoceras* limestone, Gor Loutad, Western Sahara (presently claimed by Morocco);

Diagnosis.—As for genus.

Genus *Eldredgeops* Struve, 1992

1990 *Eldredgeops?* nom. nud. Struve, p. 254.
1992 *Eldredgeops*; Struve, p.

Type Species—*Phacops rana* var. *milleri*, Stewart 1927, from the Middle Devonian Silica Shale Formation in Sylvania, Ohio. Holotype: OSU 16266A, the holotype specimen representing *Eldredgeops milleri* was originally designated as a lectotype for *Phacops rana* var. *milleri* by Babcock (1992) and is figured within.

Included Species—*Eldredgeops arkonensis* (Stumm 1953), *E. crassituberculatus* (Stumm 1953), *E. milleri* (Stewart 1927), *E. norwoodensis* (Stumm 1953), *E. paucituberculatus* (Eldredge 1972), *E. rana* (Green 1832), and *E. tindoufensis* (Burton & Eldredge 1974)

Diagnosis—Eyes bearing 15-18 dorso-ventral files (number invariant within individual species). Glabella furrow 1p deeply incised; separated from both preoccipital ring and glabella by strong furrows. Lateral nodes on 1p subquadrate; weakly to moderately separated from median portion of 1p. Glabella furrows 2p and 3p very weakly developed or absent. Subocular librigenal field shallow or absent anteriorly and shallow posteriorly. Among the genus, cephalon generally covered in low rounded tubercles. Lateral border may have granule to small tubercle sized projections. Tubercles on glabella large and pustular, with greatest concentration on composite glabellar lobe and 1p.

Axis of thorax covered with transversely elongate tubercles. Tuberculation on pleura variably developed.

Pygidium with seven to 10 axial rings and six or seven pleurae. Interpleural furrows generally obsolescent; anteriormost interpleural furrows shallow or absent. Pleural furrows shallow, moderately arched. Pygidium semicircular in outline, with tubercles reduced or absent towards margins.

Eldredgeops arkonensis (Stumm, 1953)

1927 *Phacops rana* var. *milleri*; Stewart, p. 58, pl. 5.
1940 *Phacops rana* var. *milleri*; Delo, p.23–24, pl. 1.
1953 *Phacops rana arkonensis*; Stumm, p.138–139, pl. 10.
1972 *Phacops rana milleri*; Eldredge, p. 79–80, fig. 14.

Type Material—Holotype: UMMP 28847 from the Middle Devonian Hamilton group of Ontario, Canada.

Diagnosis—Eye with 18 dorso-ventral files, six to seven lenses per file. Eye with elevated facets and thin sclera throughout. Reduction in overall ornamentation except on palpebral lobes and posterior portion of glabella.

Occurrence—Arkona shale (Middle Devonian, Hamilton group) of western Ontario, Canada.

Discussion—*Phacops rana arkonensis* was originally designated as its own subspecies of *Phacops rana* by Stumm (1953). Eldredge (1972) treated *Phacops rana arkonensis* as a synonym of *Phacops rana milleri*. While the two species share very similar eye morphology, the distinction in maximum number of lenses per file, combined with the relative difference in

proportions of the cephalon and reduction of overall tuberculation, suggest that each is uniquely diagnosible. Recognizable from other members of *Eldredgeops* by its unusually short, wide cephalon. Relative proportions of the cephalon increase the average axial furrow divergence to 65-70°. Pygidium as in other members of *Eldredgeops* apart from tuberculation.

Eldredgeops crassituberculatus (Stumm, 1953)

1953 *Phacops rana crassituberculata*; Stumm, p. 136–137, pls. 9–10.
1966 *Phacops rana crassituberculata*; Clarkson, p. 470, pl. 73.
1972 *Phacops rana crassituberculata*; Eldredge, p. 78–79, fig. 13.
1991 *Phacops rana crassituberculatus*; Ramsköld & Werdelin, p.
2011 *Eldredgeops crassituberculata*; Schoenemann & Clarkson, p. 102, fig. 1.E.

Type Material—Holotype specimen UMMP 25537

Diagnosis—See Eldredge (1972 p. 79).

Eldredgeops paucituberculatus (Eldredge, 1972)
ZooBank registration number

1972 *Phacops rana paucituberculata*; Eldredge, p. 80–81, fig. 16
1991 *Phacops rana paucituberculatus*; Ramsköld & Werdelin, p.73

Type material—Four specimens from the Plum Brook shale of Ohio. Holotype: UMMP 57135.

Specimens not examined in person. Holotype figured in Eldredge (1972, fig. 16).

Diagnosis—See Eldredge (1972, p. 80-81).

CHAPTER TWO:
UNDERSTANDING THE RELATIONSHIP BETWEEN TRAIT ASYMMETRY AND PHENOTYPIC VARIATION IN THE TRILOBITE GENUS *ELDREDGEOPS* STRUVE 1992 USING A MAXIMUM LIKELIHOOD METHOD

ABSTRACT—Variation is the raw material upon which natural selection operates. The degree to which symmetric phenotypic variation among individuals in a population operates as a driver of natural selection on both micro- and macro-evolutionary timescales is well known. Less clear is the effect that within-individual variation, expressed as fluctuating asymmetry (FA), may affect evolutionary trajectories. In order to understand this phenomenon, we must use the fossil record. The degree of precision needed to conduct studies of fluctuating asymmetry, combined with preservation biases of the fossil record, leaves few study systems in which large scale study of fluctuating asymmetry can be conducted. The schizochroal eye-lenses of phacopid trilobites meet these criteria but traditional metrics for determining fluctuating asymmetry may be artificially biased when using meristic character data. A maximum likelihood method has previously been proposed to overcome this bias; however, no studies to date have employed this method. The study herein applies both traditional FA metrics and the proposed maximum likelihood method to isolate the components of variation in two species of the Middle Devonian trilobite genus *Eldredgeops* Struve 1992. Both methods recovered similar estimates among the components of variation that were investigated, though results do not match precisely suggesting differences between the methods. Further investigating the patterns of variation suggests that the symmetric and asymmetric components of variation *may* be developmentally independent of each other. However, due to small sample sizes as a imposed by the COVID 2020-2021 pandemic, these results are not conclusive. The analyses presented herein constitute the first steps in the ongoing process of understanding the ancient developmental system of *Eldredgeops*.

INTRODUCTION—Phenotypic variation is the raw material that natural selection operates on (Darwin, 1859), and can be assessed among individuals or within an individual (e.g., left-right asymmetry). Phenotypic variation is regulated by developmental systems (Laland et al., 2015) through various types of morphological homeostasis or canalization (per Canon, 1932; Waddington, 1957). Phenotypic variation among individuals can arise from genotypic variation and/or from differing environmental influences over development for a given genotype (phenotypic plasticity). Buffering of developmental systems against such genetic and macroenvironmental variation is known as genetic and environmental canalization, respectively (Waddington, 1940; Palmer, 1994). Phenotypic variation within an individual is unlikely to arise from genetic or environmental sources, because the left and right sides of a bilaterally symmetric organism develop under the control of a single genotype and within the same external environment. However, left-right asymmetry within a nominally bilaterally symmetric individual can arise from stochastic developmental irregularities during development affecting each side independently (Møller & Swaddle, 1997; Polak, 2003; Leamy & Klingenberg, 2005; Klingenberg, 2015; Graham & Özener, 2016). Buffering of a developmental system against these stochastic perturbations is known as homeorhesis or developmental homeostasis and can be measured as fluctuating asymmetry (FA; random deviations from symmetry in an otherwise symmetric structure) (Waddington, 1957; Nijhout & Davidowitz, 2003; Webster, 2019).

Morphological homeostasis is relevant to evolution because it buffers developmental systems against sources of phenotypic variation. Indeed, morphological homeostasis has been suggested to be a mechanism by which species maintain morphological stasis over periods of hundreds of thousands or millions of years (Eldredge & Gould, 1972; Williamson & Foote, 1984; Foote & Cowie, 1988; Møller & Pomiankowski, 1993; Rutherford, 2000; Wagner, 2000;

Hansen & Houle, 2004). The potential for genetic canalization and environmental canalization to serve as constraints on evolution is clear (see reviews by Møller and Swaddle, 1997; Polak, 2003; Graham et al., 2010; Klingenberg, 2015; Webster, 2019 and references therein). However, whether and how homeorhesis relates to phenotypic evolution is not well known; nor is the degree to which genetic and environmental canalization relate to homeorhesis. Empirical studies of morphological homeostasis have almost exclusively been conducted by neontologists. However, to understand the macroevolutionary consequences of morphological homeostasis, and to determine the timescale over which morphological homeostasis limits the expression of phenotypic variation—both within a species and across clades—it is necessary to study homeostasis within the fossil record (see discussion by Webster, 2019).

A first step to investigate whether homeorhesis might constrain the evolution of a trait is to determine the relationship between the level of within-individual variation (FA) and the level of among individual (symmetric) variation for that trait (Webster, 2019). Here, I do that for a series of traits related to the development of the eyes in two species of the trilobite genus *Eldredgeops* Struve 1992. Exploring potential constraints on phenotypic evolution within *Eldredgeops* is of particular interest because that genus served as one of the original case studies in the formation of the theory of punctuated equilibria and morphological stasis (Eldredge & Gould, 1972; Gould & Eldredge, 1977, 1986, 1993; Eldredge, 2015). No previous study has explicitly tested whether morphological homeostasis played a role in the evolutionary stasis within *Eldredgeops*, although Gould (2002) speculated that morphological homeostasis may not be able to serve as a constraint on those timescales. Among trilobites, developmental asymmetries appear to be relatively common. Reporting file counts among three species of *Reedops* Richter & Richter 1925, Clarkson (1969) noted at least one occurrence of asymmetrical

counts between lenses. Among 17 lens counts reported by Fortey and Morris (1977), four of the five specimens that capture lens counts for both sides exhibited asymmetrical counts. Crônier et al. (2004) investigated multiple beds preserving specimens of the phacopid *Acuticryphops acuticeps* (Kayser 1889) and found that variation (both within and among-individuals) in lens counts through time generally increased, in the penultimate bed 3% of specimens examined exhibited some degree of fluctuating asymmetry increasing to 5% in the stratigraphically youngest bed. Right/left asymmetry in total number of dorso-ventral files appear to be less common (Clarkson, 1969; Thomas, 1998).

Using the maximum likelihood estimation model developed by Young (2007), I isolate the symmetric and FA components of variation in the number of lenses within each dorso-ventral file within the eyes of *Eldredgeops crasstiuberculatus* (Stumm 1953) and compare them to the values recovered for the sister species *Eldredgeops milleri* (Stewart 1927). If the underlying mechanisms that control within-individual variation through homeorhesis are the same as those that control the expression of symmetric phenotypic variation, then we should expect to find these values positively correlated in the traits considered in the analyses herein. If the recovered relationships are not positively correlated, this would suggest that mechanisms controlling within- and among-individual variation are to some degree independent of each other. This analysis aims to contribute to our understanding of eye development within trilobites and aids our understanding of developmental constraints on phenotypic evolution more broadly.

Further, this paper explores the significance of the "Swain Effect," a statistical non-independence between the observed trait mean and the estimate of FA that arises for meristic traits when the amount of asymmetry is low (Swain, 1987; Palmer, 1994; Palmer & Strobeck 2003; Young, 2007). The Swain Effect suggests that commonly used methods for quantifying

FA, such as those proposed by Palmer & Strobeck (1986, 2003), may be inappropriate for meristic traits such as eye lens number (the focus of this present study). Despite being known for more than 30 years, the Swain Effect is almost invariably ignored in studies of FA, which continue to use these traditional FA metrics on either entirely meristic or mixed (continuous and meristic) datasets. To understand the degree to which studies of FA in meristic traits may be biased in their estimate of FA, the level of FA was calculated for the *Eldredgeops* eye lens data using two methods: a two-factor mixed-model ANOVA (which does not correct for the Swain Effect), and a maximum likelihood model developed by Young (2007) (which does).

MATERIAL AND METHODS—

Material—All specimens used in this study belong to either the trilobite species *Eldredgeops milleri* (Stewart, 1927) or *Eldredgeops crassituberculatus* (Stumm, 1953). Specimens are housed in the following university and museum collections: American Museum of Natural History (AMNH), Bowling Green State University (BGSU), and the Field Museum of Natural History (FMNH).

All specimens were originally collected from the Silica Formation, a lower Givetian (Middle Devonian) deposit located in Sylvania, Ohio. The Silica Formation is approximately 20 meters thick, consisting of alternating beds of calcareous and argillaceous limestone, and is divided into 27 units (Kesling & Chilman, 1975; Brett 1999). Specimens of *E. crassituberculatus* are found in units 7-8, though possible occurrences in unit 6 and 9 have been reported (Kesling & Chilman, 1975). Specimens of *E. milleri* are confined to units 8-11, spanning a total stratigraphic thickness of approximately 3.2 meters in the type section (Figure 2.1; Eldredge, 1972; Kesling & Chilman, 1975). However, sampling efforts by the 'Friends of the University of

Michigan Museum of Paleontology' indicate that *E. milleri* is rare above unit 9a, and most *E. milleri* are sampled either from unit 8 (~20 cm thick) or the base of unit 9 (referred to as unit 9a; ~ 20 cm thick). The co-occurrence of *E. crassituberculatus* and *E. milleri* in Unit 8 represent the only known co-occurrence of these two species in any sampling locality (Eldredge, 1972). Units 5B-13 have been interpreted to be part of a single 'biotope sequence,' partially defined as the *Mucrospirifer*-transition zone (units 7-9a). Unit 8 is marked by a pause in argillaceous input from the Acadian Mountains, while unit 9a represents a densely fossiliferous bed marked by a return of argillaceous sediments that steadily increases throughout unit 9 (Kesling & Chilman, 1975). The disappearance of *Mucrospirifer* above unit 9a, combined with the increased supply of argillaceous sediments and volume of fossiliferous material in this thin bed, indicate that unit 9a is likely a flooding surface within a larger stratigraphic sequence (Patzkowsky and Holland, 2012; interpretation of the Silica Formation my own). Given present

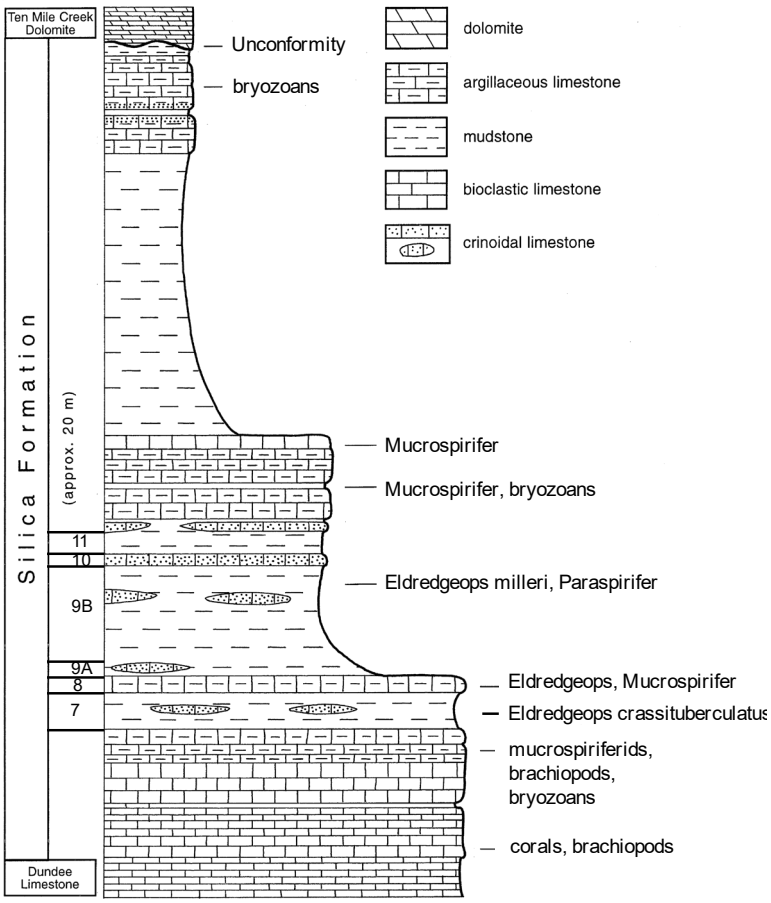

Figure 2.1—Composite of the type stratigraphic section of the Silica Formation as exposed in the Medusa Cement Quarry, Sylvania Ohio. Units 7-11, which contain *Eldredgeops crassituberculatus* and *E. milleri*, are highlighted. Section adapted and modified from Kesling & Chilman (1975) and Brett (1999).

interpretations of the Silica Formation, it is not clear how much time separates units 8 and 9a or if they represent a continuous deposition within a parasequence.

Each specimen was mounted laterally to expose an individual eye to the camera lens. Due to the curved nature of an individual visual surface (which wraps ~180° in plan view), specimens were photographed from two angles on each side, once to capture the anterior portion of the visual surface and once to capture the posterior portion. This process was repeated for the opposing side of the trilobite, resulting in four photographs to capture a composite of both visual surfaces of a single individual. In some cases, individual trilobites were first coated with ammonium chloride sublimate to enhance the contrast of the lenses against the intermediate sclera. Lens counts for a particular visual surface of a given individual were obtained by matching dorso-ventral files between photographs of that visual surface of that specimen (Figure 2.2). To account for possible error in lens counts, each side was counted on two separate occasions. The analyses herein are based upon lens counts on 18 specimens of *E. crassituberculatus* and 28 specimens of *E. milleri*.

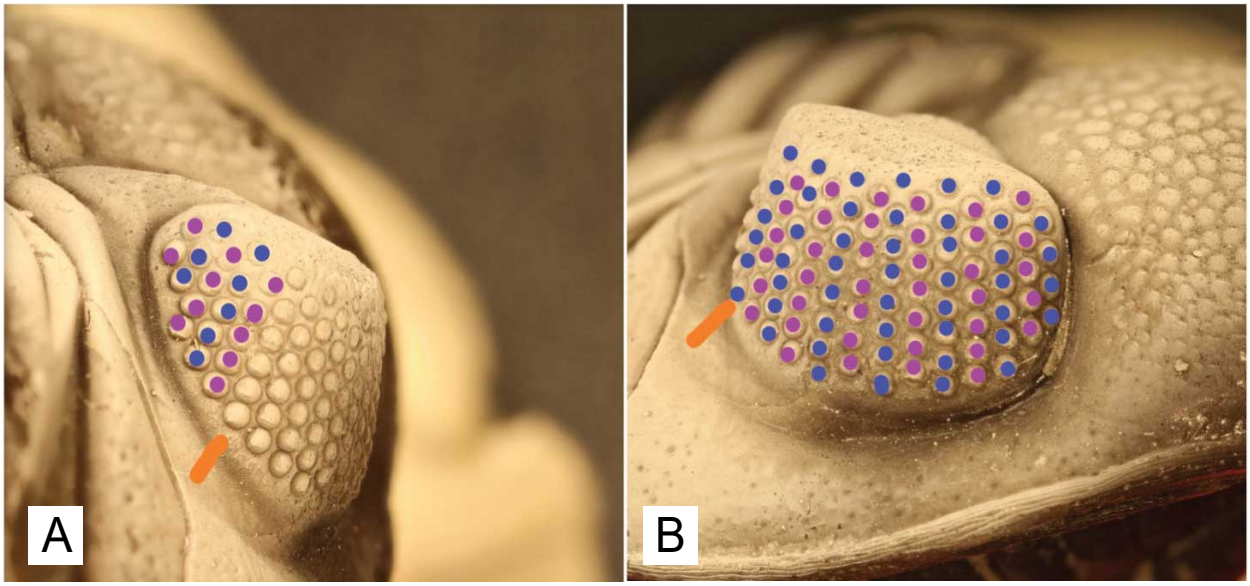

Figure 2.2—Photographs of the right eye of a specimen of *Eldredgeops milleri* illustrating the method used to align and count each individual eye. In both photographs the anterior of the cephalon is to the right. Purple and blue dots are used to highlight each lens of alternating dorso-ventral files in the eye. Orange marker highlights homologous dorso-ventral file between photographs used to maintain counts between photos. A: posterior-most region of the eye, B: anterior-most region of the eye.

Variables Assessed—Treatment and terminology for lens distributions follows Clarkson (1966a). Numbering of individuals proceeds from the anterior (File 1) to the posterior (File *k* for a given species).

Lenses within both *E. crassituberculatus* and *E. milleri* are arranged into a maximum of 18 dorso-ventral files in mature specimens. For *E. crassituberculatus,* the maximum number of lenses in a file is 6, though occasionally specimens with 7 lenses in a file may be reported (Stumm, 1953; Eldredge, 1972); the lenses are either reduced or flush with the scleral wall, thick sclera separate lenses from each other. Within *E. milleri* the maximum number of lenses in a file is either 8 or 9 (Stumm, 1953; Eldredge, 1972), a very rare instance of 10 lenses in a dorso-ventral file was observed in the material examined for this study; the lenses are bulbous and protrude well above the visual surface, and little to no sclera separates the lenses from each other. As with most phacopids, in both species of *Eldredgeops* the lenses are arranged in close

hexagonal packing; due to the curvature of the eyes, lenses increase in size towards the bottom of the visual surface to maintain packing arrangement.

Study of lens patterning over the last half-century suggests that the development of eyes in trilobites is coordinated under a developmental program (Clarkson, 1975; Zhang & Clarkson, 1990; Thomas, 1998, 2005; Crônier & Clarkson, 2001; Clarkson et al., 2006; Schoenemann & Clarkson, 2017). A unified lens-emplacement model (Chapter 3) suggests that the development of individual dorso-ventral files to some degree are semi-independent of each other. While a single row of lenses may be emplaced across multiple dorso-ventral files between successive molts (Zhang & Clarkson, 1990; Thomas, 1998, 2005), asymmetries between sides in individual columns, the addition of a series of lenses in a new file, and the curved nature of the generative zone in trilobites all suggest that to some degree the files are semi-independent of each other, though regulated under the same developmental program (Chapter 3). Therefore, lens counts and analyses were conducted treating each dorso-ventral file as independent trait.

Traditional Fluctuating Asymmetry Metrics—A wide variety of metrics have been used to estimate FA (Van Valen, 1962; Leamy, 1984; Palmer & Strobeck, 1986, 2003). Many of these metrics are variations on the standard equation (R_i-L_i [differences between sides of an individual trait]); some include a trait size correction by individual or by sample, others treat asymmetry as signed or unsigned (Palmer, 1994; Palmer & Strobeck, 2003). Among these indices, the currently preferred method of isolating the FA component of variation is a two-factor mixed-model ANOVA (Leamy, 1984; Palmer & Strobeck 2003), which incorporates replicate measures and thus includes an estimation of measurement error (ME). The magnitude of FA is often minor component of the total variation (generally < 5% and often < 1% of the trait size; Palmer, 1994) and is sometimes exceeded by the magnitude of measurement error, rendering the estimate of FA

unreliable. Under the two-factor mixed-model ANOVA there are two effects: the "Individuals" term is the symmetrical component of variation among individuals (i.e., the symmetric phenotypic variation within the sample); and the "Sides" term which is the variation between the two sides of the organism (equating to directional asymmetry). The interaction term ("Individuals x Sides") represents a difference in sides among individuals, which is the measure of developmental noise (FA). The significance of FA is determined by the F-ratio between the mean square of the interaction and the measurement error (Leamy, 1984; Palmer & Strobeck, 2003).

Maximum Likelihood Estimation—Young (2007) based his maximum likelihood method for estimating the strength of FA on the development model for meristic characters proposed by Falconer (1981) and Swain (1987). Under this model a meristic count is determined by the value of an underlying continuous distribution, termed the liability (L). Along this liability are thresholds that determine the translation of an underlying continuous liability into a series of integer character states. The integer character states, considered to be the realized liability, are the sum of the population mean liability (M), a fixed genotype effect (G), and the developmental error (E), such that: $L = M + G + E$, where E is normally distributed around a mean of 0 (Young, 2007, p. 486-487). Using this conceptual model, the ML method isolates the components of variation into the following parameters: the population trait mean for a bilateral character (μ), the genetic and/or environmental effects on the liability for the organism (GE [$N(0, \sigma^2)$]), and the independent developmental disturbance (A, [$N(0,\sigma^2)$]), where N is a normal distribution centered around a mean of zero.

Counts are replicated, so data are first subjected to a series of maximum likelihood estimations to evaluate the impact of measurement error on the sample (equations 2.10-2.12 in

Young, 2007, see also Appendix B) by maximizing the log-likelihood (equation 2.12 in Young, 2007). This is accomplished by fitting the data to either a geometric distribution (with parameter q) or a Poisson distribution (with parameter λ); those distributions were chosen as candidates because they are discrete and symmetric around 0, which may be appropriate because counting errors are inferred to impose no directional bias (Young, 2007).

The parameter estimate that maximized the log-likelihood of measurement error (either $\hat{q}$ or $\hat{\lambda}$) was then used in conjunction with the observed data of lens counts to minimize the weighted log-likelihood (equation 2.13 in Young, 2007, see also Appendix B) to estimate the following parameters: $\hat{\mu}$ (trait mean for the sample), $\hat{\sigma}_{GE}$ (also abbreviated sGE; the genetic and/or environmental components of variation summarizing the symmetric component of phenotypic variation), and $\hat{\sigma}_A$ (also abbreviated sA; 'developmental instability,' the fluctuating asymmetry term).

Optimization of all likelihood functions was accomplished using the NLIN procedure in SAS, using the Gauss method (Young, 2007). Starting values for the parameters were the same as Young (2007). Values for σ were derived from a one-way ANOVA with left and right counts treated as replicate observations such that the starting value for $\sigma_{GE} = \sqrt{SS_i/df_i}$ (SS_i = sum of squares between individuals) and the starting value for $\sigma_A = \sqrt{SS_{error}/df_{error}}$. The sample mean of the observed count was used as the starting value for μ, and a constant of 0.5 was used for the starting value for the error parameter. To reduce computation time, errors were evaluated over the interval (-5, 5) instead of (-∞, ∞), a valid assumption given the total magnitude of R/L count differences was never observed to be greater than 2 for either species considered herein.

Comparisons between Samples—To compare estimated parameter values between the two species, a likelihood ratio test (Sokal & Rohlf, 1995; Young, 2007) and multi-model inference

using the corrected Akaike Information Criterion (AIC_C) (J. Young, personal communication, 2021) were conducted. For both tests comparing populations, the sum of the log-likelihoods over both populations (where $\mu_1, \mu_2, \sigma_{GE1}, \sigma_{GE2}, \sigma_{A1}, \sigma_{A2}, (q_1 \text{ or } \lambda_1), (q_2 \text{ or } \lambda_2)$ are estimated) is compared to the sum of the log-likelihoods where all data were treated as a single population.

Under a likelihood ratio test, data were compared to critical values in a X^2-distribution with 4 degrees of freedom. Values deemed to be statistically significant (p=0.05) lead to rejection of the null hypothesis and suggest that the parameter estimates recovered treating the species separately are distinguishable and were not different due to chance.

Comparison of the two species using multi-model inference was conducted herein by summing log-likelihoods between populations and treating them as a model with 8 free parameters. They were compared to a second model which treated the two species as one population estimating a series of joint $\hat{\mu}, \hat{\sigma}_{GE}, \hat{\sigma}_A,$ and $(\hat{q} \text{ or } \hat{\lambda})$ parameter estimates (4 free parameters). Corrected Akaike Information Criterion (AIC_C) values (Akaike, 1973, 1974; Hurvich and Tsai, 1989) were calculated to determine which model is favored. Akaike weights were also calculated to evaluate the relative likelihood of each model.

To evaluate the relationship between symmetric phenotypic variation (σ_{GE} or sGE) and stochastic developmental instability (σ_A or sA), a series of regressions were performed against the parameter estimates using a model II regression to minimize the sum of squares of the normal deviates. Data were regressed in R using the *lmodel2* package (Legendre & Oksanen, 2018, v. 1.7-3).

Assessing the Role of Ontogeny in FA—It is possible that ontogeny could be a control on the expression of variation such that dorso-ventral files that develop throughout a longer interval of ontogeny have a greater degree of variation than dorso-ventral files that develop through a

shorter period of ontogeny. A single row of lenses is added between molts (Clarkson, 1975; Thomas 1998, 2005; Crônier & Clarkson, 2001; Clarkson et al., 2006; Harzsch & Hafner, 2006; Schoenemann & Clarkson 2015; Chapter 3). Therefore, it is possible that asymmetry values could correlate with the trait size such that dorso-ventral files which contain more lenses are more likely to be asymmetrical. Further, addition of new dorso-ventral files occurs out of order in *Eldredgeops* (and likely trilobites more broadly), such that central dorso-ventral files are present throughout ontogeny, the posterior-most two dorso-ventral files (files 17 and 18) are added next, and then the anterior-most file is added (file 1)(Chapter 3). Under this model of eye growth, we should expect the lowest values of FA in the anterior- and posterior-most files if FA is related to ontogeny.

RESULTS—Parameter estimates for $\hat{\mu}$, $\hat{\sigma}_{GE}$, $\hat{\sigma}_{A}$, the error term ($\hat{q}$ or $\hat{\lambda}$), and their respective likelihoods for *E. crassituberculatus* and *E. milleri* (Appendix B, Tables B.2-B.3 as well as the recovered values using the two-factor mixed-model ANOVA for *E. milleri* (Appendix B, Tables B.5-B.22). Parameter estimates for the fluctuating asymmetry term were found to be higher using the maximum likelihood method than those recovered using traditional FA10, while the estimates of symmetric phenotypic variation were found to be higher when using FA10 versus those recovered via maximum likelihood. Recovered values are generally lower in *E. crassituberculatus* than they are in *E. milleri*.

Comparisons between species—The recovered likelihoods for treating the data as a single population were moderately higher than the sum of likelihoods for the two species across all dorso-ventral files. When the likelihoods recovered for the samples of *E. crassituberculatus* and *E. milleri* are compared to each other using a likelihood ratio test, where a combined population

(see Appendix B, Table B.4 for parameter estimates and likelihoods for the 'combined' data set) of the two species is treated as a null hypothesis, none of the differences in the parameter estimate values were significantly different from each other for any trait (Table B.23). This conclusion was also true in the multi-model inference, in which the 4-parameter model treating the data as a single population was favored for all dorso-ventral files (Weight AIC=19.46-71.69 for separate species; Table B.24).

Examining trait correlations—On average, the recovered parameter estimates for *E. crassituberculatus* are lower than those recovered the homologous dorso-ventral file in *E.* milleri (Tables B.2-B.3). A series of regressions were conducted on the parameter estimates recovered for *E. crassituberculatus* and *E. milleri* to determine the relationship between developmental instability and the symmetric component of phenotypic variation.

A regression through the data for all dorso-ventral files, treating each species separately, serves as a proxy for testing for a species-level relationship between FA and the symmetric component of phenotypic variation (Figure 2.3). This approach assumes that all data points are independent of each other (Palmer, 1994; Polak, 2003; Graham et al., 2010; Klingenberg, 2015), which may not be the case for the dorso-ventral files in phacopid eyes (see discussions in Chapter 3). Using a model II regression, the coefficients of correlation and the coefficients of determination for both species indicate little support for a species-level relationship between FA and phenotypic variation (*E. crassituberculatus*: R=0.311, R^2=0.096, p=0.209; *E.milleri*: R=-0.154, R^2=0.0023, p=0.54).

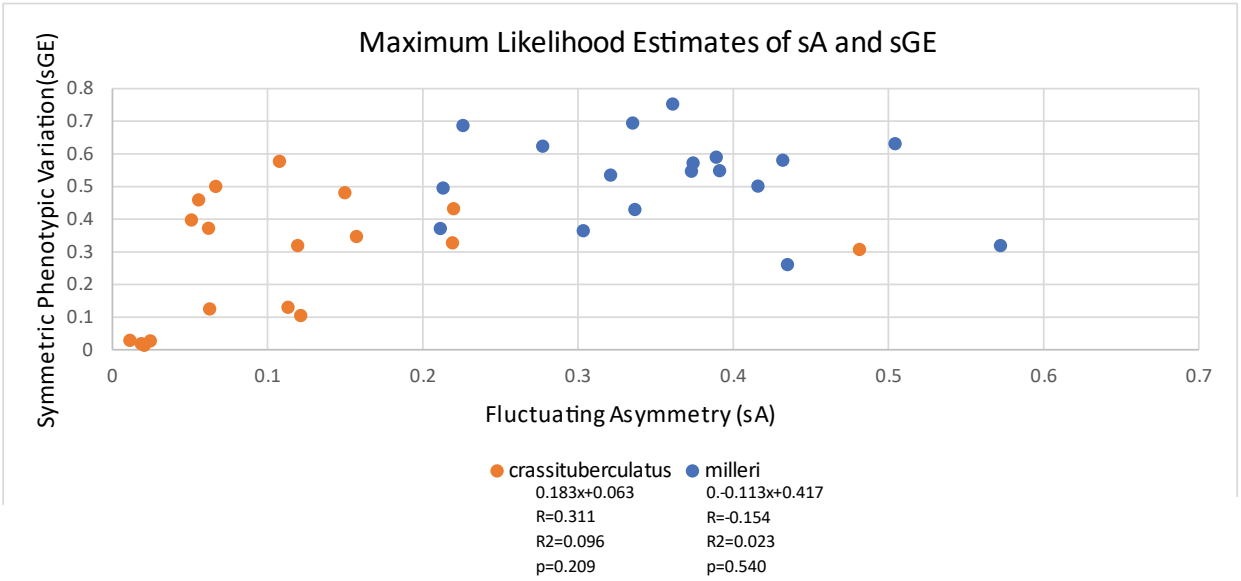

Figure 2.3-Graph comparing the recovered parameter values for fluctuating asymmetry and symmetric phenotypic variation by maximum likelihood estimation. Fluctuating asymmetry is expressed as sA and the symmetric variation is expressed as sGE. Each data point represents recovered parameter values for a single dorso-ventral file for each species. Model II regressions for each species are also indicated.

The species parameter estimates for FA (σ_A) and the symmetric component of variation (σ_{GE}) were isolated for each dorso-ventral file to determine file-specific relationships between these two parameters (Figure 2.4). Isolating the data in such a way can be used to infer the relative relationship between the components of variation and thus infer if they are being controlled by similar processes during development. It is important to note that confidence limits on these regressions cannot be determined because each was based on only two data points (one for each species per dorso-ventral file) and as such are necessarily correlated with a coefficient of determination (R^2) equal to 1.

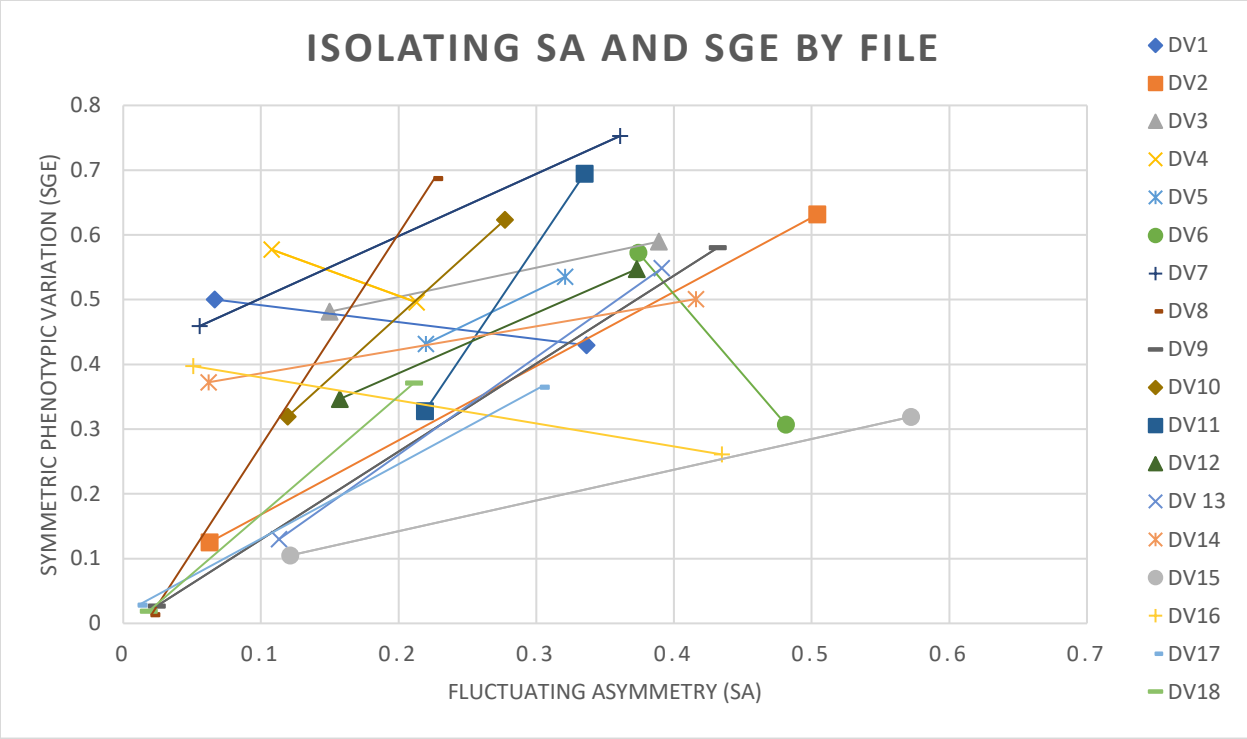

Figure 2.4 Graph comparing the recovered parameter values for fluctuating asymmetry and symmetric phenotypic variation by maximum likelihood estimation isolated by each dorso-ventral file. Each individual point represents the recovered parameter estimate for a single dorso-ventral file for a single species. Fluctuating asymmetry is expressed as sA and the symmetric variation is expressed as sGE. Regressions are made between the same dorso-ventral file in the two species of *Eldredgeops*.

Plotting the FA parameter estimates against their relative position in the eye reveals that in neither species of *Eldredgeops* did FA values correlate with their position given the ontogenetic development of the eye (Figure 2.5). Additionally, there was no relationship found when plotted relative to the mean number of lenses in a given dorso-ventral file (Figure 2.6). Regardless of trait size or timing of dorso-ventral file initiation, the occurrence of developmental irregularities is randomly distributed in a given dorso-ventral file throughout its ontogenetic development.

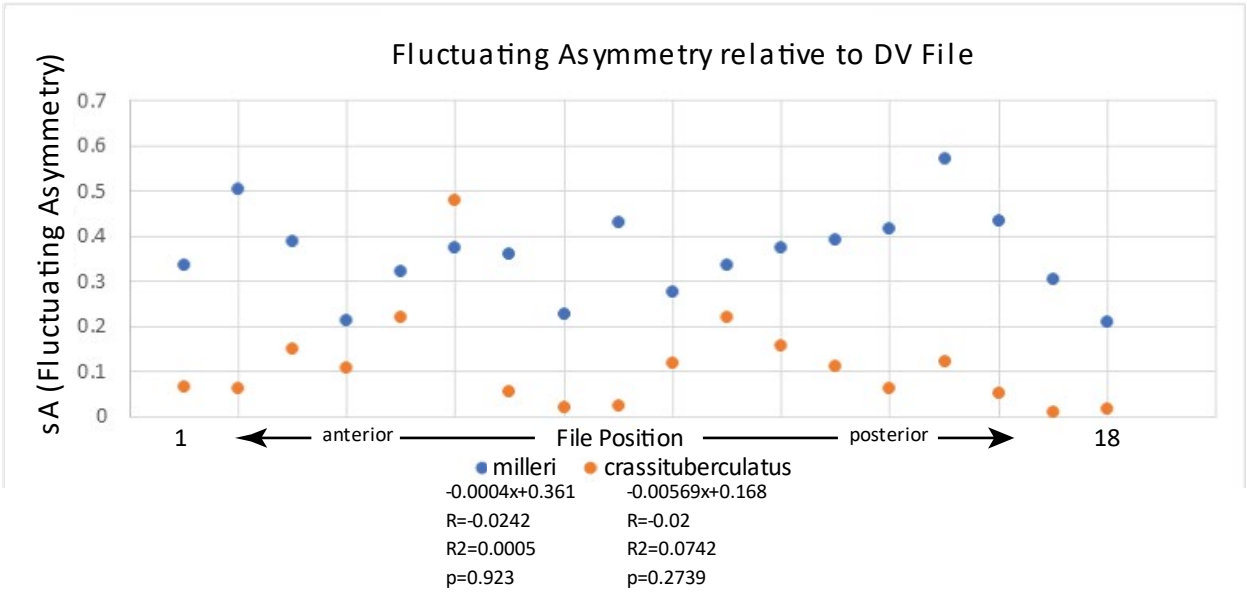

Figure 2.5— Comparison the recovered parameter values for fluctuating asymmetry by maximum likelihood estimation based on relative position of each dorso-ventral file in the eye. Fluctuating asymmetry is expressed as sA. Each data point represents recovered parameter values for a single dorso-ventral file for each species. Model I regressions for each species are also indicated.

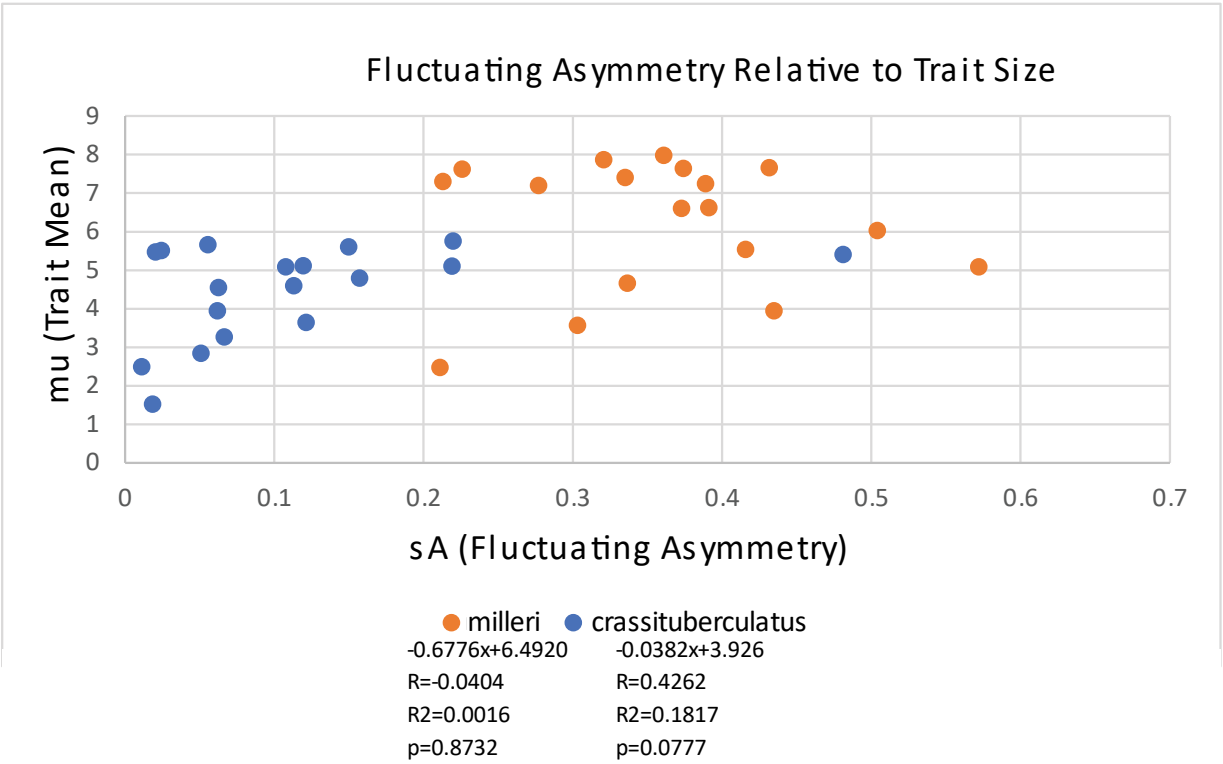

(Bottom of previous page) Figure 2.6— Comparison of the recovered parameter values for fluctuating asymmetry and by maximum likelihood estimation relative to the mean trait size. Fluctuating asymmetry is expressed as sA. Each data point represents recovered parameter values for a single dorso-ventral file for each species. Model II regressions for each species are also indicated.

Comparing recovered values between traditional and MLE methods—Recovered values for fluctuating asymmetry, symmetric variation, and trait means were compared for those found using the two-factor mixed-model ANOVA and those recovered using maximum likelihood estimation. The values recovered using both methods were similar, but not identical, for all components of variation in *E. milleri* (Figure 2.7). Recovered estimates for fluctuating asymmetry and symmetric variation are well correlated (R^2=0.812,0.901; p=3.286e-7, 8.1761e-10 respectively). Departures in the data from perfect correlation are relatively small in either direction (Figure 2.7A) making it difficult to infer where bias in natural data may be occurring (if any). Recovered trait means between the two methods are nearly identical and highly correlated (Figure 2.7B; slope= 0.9972x; R^2=0.997, p=6.3581e-31). As found in Young (2007), analysis using both MLE and traditional FA10 of natural data showed that recovered FA values were slightly different due to inherent differences in the methods but the overall trends in the FA values between MLE and traditional metrics were the same.

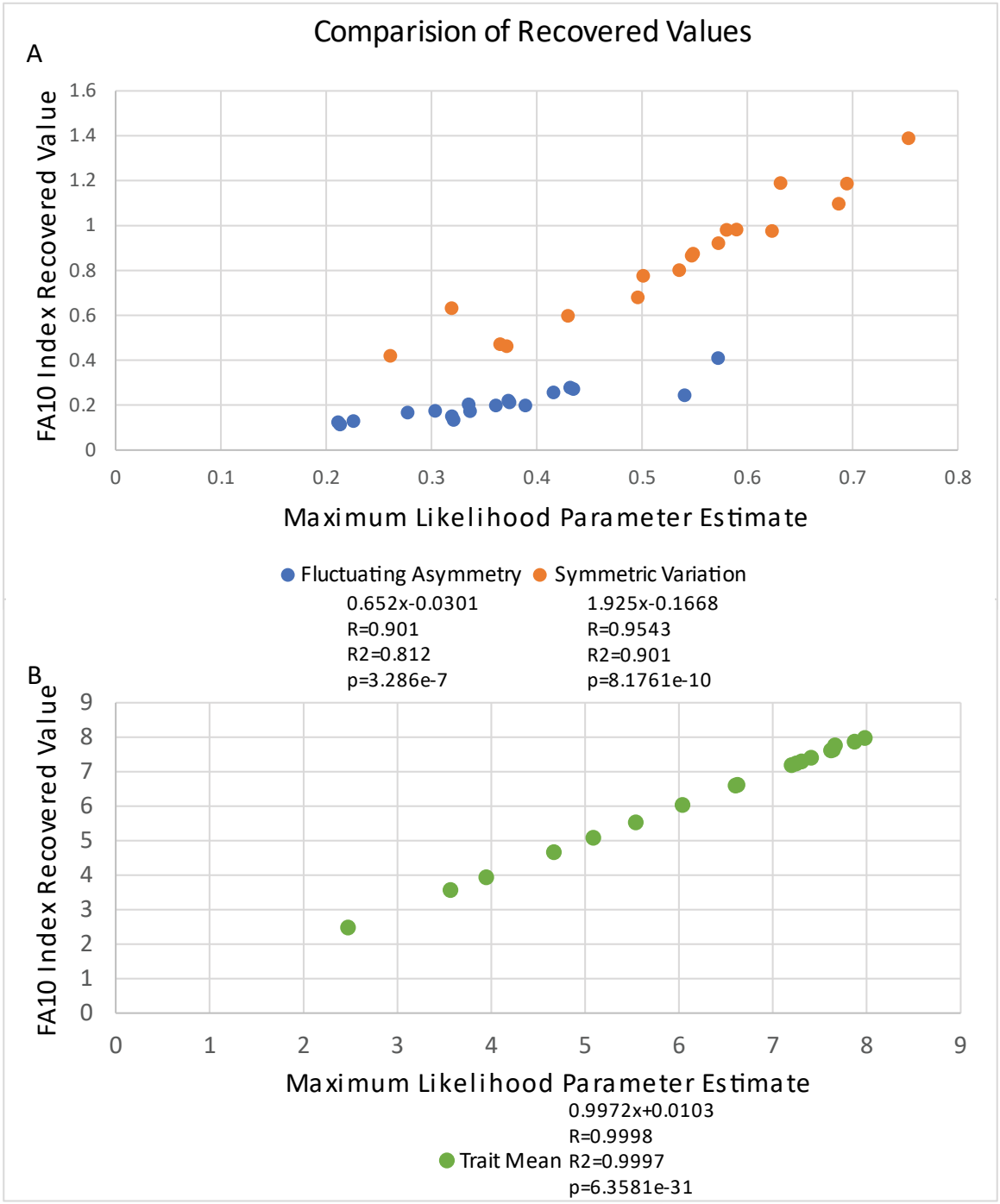

Figure 2.7- A: Comparison of the recovered parameter values for fluctuating asymmetry and symmetric phenotypic variation by maximum likelihood estimation and traditional FA10 index for *Eldredgeops milleri*. Fluctuating asymmetry is expressed as sA and the symmetric variation is expressed as sGE. FA is expressed as the Interaction mean square and the symmetric phenotypic variation is expressed as the Individual mean square for traditional FA10 index. B: Comparison of recovered estimates for trait means for both FA10 and MLE. Each data point represents recovered parameter values for a single dorso-ventral file for each species. Model II regressions for each species are also indicated.

Detecting the 'Swain Effect'—The "Swain Effect" states that as mean values of meristic traits are increasingly distant from an integer value, their corresponding level of asymmetry is biased upwards due to their nonindependence in traditional methods for calculating fluctuating asymmetry (see Swain, 1987; Palmer, 1994; Young, 2007). The components of variation were isolated using the traditional two-factor mixed-model ANOVA (FA10, Palmer & Strobeck, 2003) and using Maximum Likelihood Estimation (Young, 2007) for all dorso-ventral files for *E. milleri* and using the Maximum Likelihood Estimation method for *E. crassituberculatus*. The departure of each dorso-ventral file from the nearest integer value was plotted against the estimate of fluctuating asymmetry (Figure 2.8). Estimates of fluctuating asymmetry using both the traditional FA10 index and the MLE method for *E. milleri* show a slight negative relationship between the departure from the nearest integer and the value of FA; both regressions cannot be distinguished from a null model defining no relationship between the two variables (traditional $p=0.0844$; MLE $p=0.8732$). This is somewhat surprising, given that the mathematics of the "Swain Effect" would predict that the recovered FA values for FA10 should have a positive bias. For *E. crassituberculatus*, a weak but significant negative relationship was recovered ($p=0.001$).

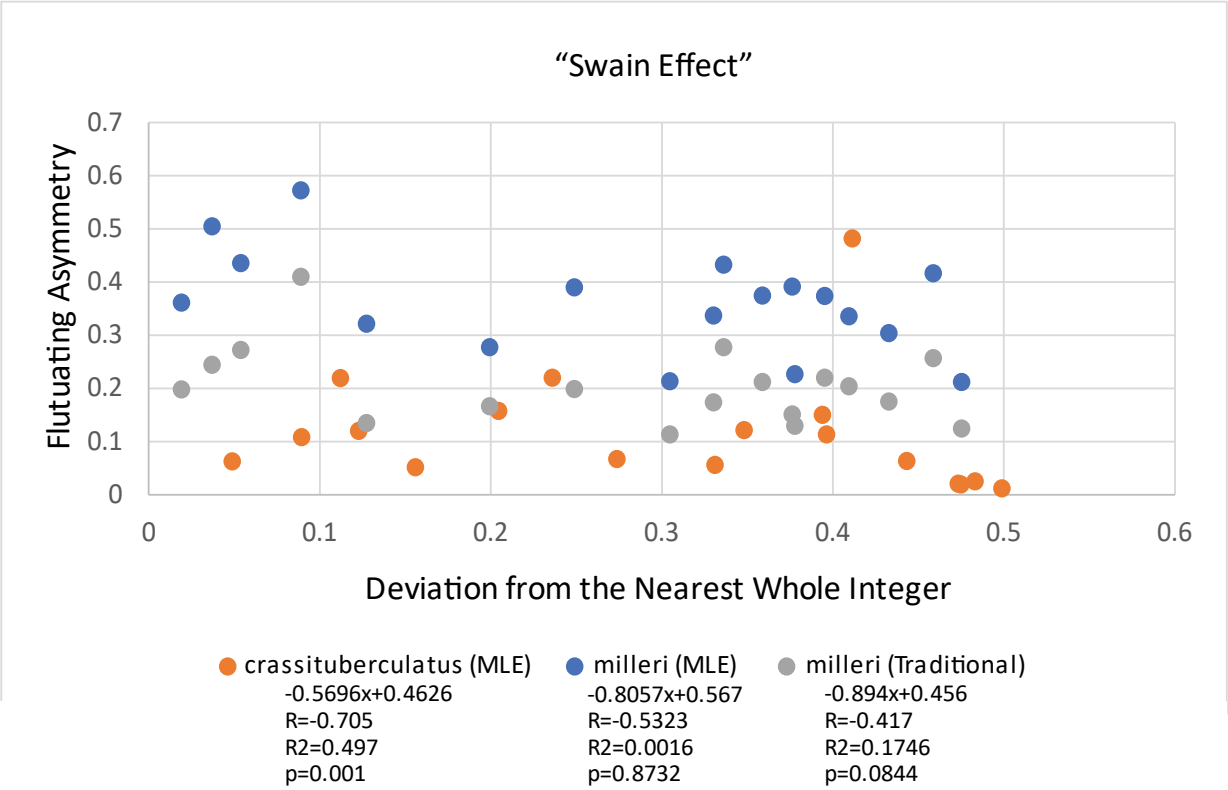

Figure 2.8— Comparison of the recovered parameter values for fluctuating asymmetry by maximum likelihood estimation. Fluctuating asymmetry is expressed as sA for the maximum likelihood estimates. FA is expressed as the Interaction mean square for the traditional FA10 index. Each data point represents recovered parameter values for a single dorso-ventral file for each species. Model II regressions for each species are also indicated.

INTERPRETATION AND DISCUSSION—

Comparison between species and the frequency of left-right asymmetry in lens number—

Differences in eye lens distribution are well established for species of *Eldredgeops* (Stumm, 1953; Eldredge, 1972; Burton & Eldredge, 1974): *E. crassituberculatus* specimens have a maximum of 6, rarely 7, lenses in a dorso-ventral file compared to the tightly packed eyes of *E. milleri* which commonly have either 8 or 9 lenses maximum in a dorso-ventral file (see analysis by Eldredge, 1972; Chapter 1). The results of the likelihood ratio test (Table B.23) and the multi-model inference (Table B.24) are therefore surprising. For each of the 18 dorso-ventral files examined, the tests found no significant differences in any of the recovered parameter estimates

between the two species. Low sample size might limit the statistical power of these tests (see below) but taken at face value these results suggest that intraspecific variation (including symmetric variation among individuals and left-right asymmetry within individuals) renders the purported interspecific differences non-significant.

Asymmetry in eye lens number is indeed rampant within *Eldredgeops* (this study) and other phacopid trilobites. Of all the *Eldredgeops* specimens examined in this present study (n=46), only one showed perfect symmetry in all 18 dorso-ventral files. No specimens in the present study were observed possessing differing numbers of files between sides. This is not surprising, because even the anteriormost file, which is last to be emplaced developmentally (Clarkson, 1975; Thomas, 2005; Clarkson et al., 2006; Chapter 3), usually consists of several lenses which must have been emplaced over several molts. Asymmetries in total number of files would thus indicate an early developmental failure that was not corrected over a long duration of the affected trilobite's life. It is clear that the developmental system of trilobites closely controlled the arrangement of lenses and resulted in efficient lens packing. However, the degree to which asymmetries might have been deleterious to the trilobites is not clear. It is noteworthy that Lesperance (1991, figures. 6.8-6.10) illustrated a mature specimen of *Eldredgeops rana* with two left eyes that exhibited normal lens packing in each.

Relationship between asymmetric and symmetric components of variation, and the implications for our understanding of the controls on phenotypic variation—Recovered likelihood ratios, when compared to a X^2-distribution, suggest that the differences observed in the parameter estimates of the two species of *Eldredgeops* may be due to chance (see above). However, it is noteworthy that estimates of both symmetric variation and FA are typically lower in *E. crassituberculatus* than they are in *E. milleri* (Tables B.2-B.3). Although I find no evidence for

species specific parameter estimates it is interesting to note that, to the extent that the recovered estimates represent true species differences, this would imply that the asymmetric and symmetric components tend to be positively correlated when compared across species (Figures 2.3, 2.4): the species that exhibits higher FA for a given trait tends to exhibit higher symmetric variation among individuals for that trait (with only four traits being exceptions). This might indicate shared mechanisms of developmental control over both homeorhesis and genetic and/or environmental canalization, lending support to a hypothesis that homeorhesis could limit phenotypic variation on a scale that is "visible" to natural selection and could thus serve as an evolutionary constraint on at least short geologic timescales (*E. crassituberculatus* and *E. milleri* being separated from their most recent common ancestor by several hundred thousand to a few million years [Chapter 1])(see Webster, 2019). It must be emphasized that further sampling is required to verify this possibility, both to obtain more reliable parameter estimates for each trait and to increase the number of species over which the correlation can be drawn (see below).

Empirical studies investigating the relationship between the symmetric phenotypic variation and within-individual variation are common in the neontological literature. However, a variety of patterns have been documented. Several studies have found congruence between among- and within-individual variation, including within skeletal elements and mandibles of mice (Hallgrímsson et al., 2002; Klingenberg et al., 2003; Gonzalez et al., 2016), wings traits of *Drosophila* (Klingenberg & Zaklan, 2000) and tsetse flies (Klingenberg et al., 2001), and cranial elements of snakes (Lazić et al., 2015). However, other studies using model neontological systems have found either a weak or no correlation between FA and among-individual variation, including within inbred mouse populations (Debat et al., 2000), limbs of crickets (Réale & Roff, 2003), various cranial elements of macaque skulls (Willmore et al., 2005), and investigations

into the effects of *Hsp90* in *Drosophila* (Rutherford & Lindquist, 1998; Rutherford, 2000). This has led to the repeated inference in the literature that the mechanisms controlling the various components of within- and among-individual variation are likely trait-, population-, or species-specific (Scheiner, 1993; Clarke, 1997, 1998; Polak, 2003; Leamy & Klingenberg, 2005; Muñoz-Muñoz et al., 2006; Van Dongen, 2006; Klingenberg, 2015; Klingenberg, 2019; Webster, 2019).

That inference is supported by the present study. If the relationship between the components of variation is modeled as a linear regression over all traits within a species (Figure 2.3), neither species of *Eldredgeops* showed a significant positive correlation between the amount of FA and the amount of symmetric variation. To the extent that these estimates of variation are reliable, this would suggest that within a given species the relationship between FA and symmetric variation is trait-specific.

Comparing traditional FA methods and maximum likelihood estimation—Swain (1987) was the first to show that using traditional metrics to estimate fluctuating asymmetry for meristic traits introduces a bias. This is due to the statistical non-independence of treating meristic traits as part of an underlying continuous distribution (mathematically demonstrated by Young, 2007). Trait means should inherently be a whole integer value, however the mean value recovered for the traits are not, and thus rounded to the nearest whole integer value. This phenomenon has been termed the "Swain Effect" (Young, 2007), and predicts that as the trait mean increasingly departs from the nearest integer the recovered FA estimate is biased upwards, inducing a positive correlation between these two factors. This problem has been well documented in the literature (Swain, 1987; Palmer, 1994; Palmer & Strobeck, 2003; Graham et al., 2010). Young (2007) proposed a maximum likelihood method that avoids the bias introduced by traditional metrics. However, no studies investigating fluctuating asymmetry since Young (2007) have used this

maximum likelihood method to estimate the components of variation. This study represents the first study since Young (2007) to estimate trait means, the symmetric components of phenotypic variation, and fluctuating asymmetry of a meristic trait using the MLE method.

When investigating the degree to which data may be biased by using traditional estimates of FA, an interesting pattern emerged. Extending the reasoning of Swain (1987) and Young (2007), we would predict a positive relationship between deviation from the nearest integer value and the corresponding measure of FA when estimating parameters using FA10. However, using the data for all 28 specimens of *E. milleri*, a weakly negative but non-significant relationship was recovered (p=0.0844; Figure 2.7). One reason for these results could be the magntiude of asymmetry relative to the overall trait size. Young (2007, p. 495), "the primary advantage of $\hat{\sigma}_A$ is that it is unbiased by shifts in the mean liability away from integer values, except when the amount of character variation is relatively low. Even then, it is much less biased than the traditional (*r*-*l*) metrics." For data used by Young (2007), both simulated and natural, the relative size of the traits used were orders of magnitude larger than the relative size of asymmetry between sides. This is not the case for the eye-lens data in the present study. The maximum trait size in *E. milleri* is nine (with the one exception of an individual with two dorso-ventral files that contain 10 lenses), the maximum range of lenses within a homologous file among-individuals was four, and the maximum range in asymmetric counts between sides was two; both among- and within-individual variation occurs on the same magnitude as the relative trait size.

The maximum likelihood method proposed by Young (2007) was applied to both species of *Eldredgeops*. The maximum likelihood method recovered a weakly negative relationship between the estimate of FA and the departure from the nearest whole integer for a trait mean for both species, though these parameter estimates are weakly correlated with one another

(R^2=0.497, *E. crassituberculatus*; 0.0016, *E. milleri*) and the correlation for *E. milleri* was not significant (p=0.8732). Simulations by Young (2007) suggest that using his ML approach eliminates the inherent bias caused by the departure from the nearest whole integer value in meristic traits. The correlations between the maximum likelihood estimates of FA and the relative departure for the trait mean from the nearest whole integer for both species would suggest that the data for *Eldredgeops* were unbiased by the "Swain Effect" (Figure 2.7). However, recovered FA values for *E. milleri* using traditional metrics were also not found to be biased by the departure from the nearest whole integer (Figure 2.7). Therefore, it cannot conclusively be determined whether this observation was due to the inherent nature of the data or if maximum likelihood estimation was truly able to eliminate the artificial inflation of FA due to the "Swain Effect".

The traditional FA metrics (Van Valen, 1962; Leamy, 1984; Palmer & Strobeck, 1986, 2003) and the maximum likelihood method proposed by Young (2007) are based on similar underlying assumptions about the distributions of the components of variation. However, the recovered estimates for both fluctuating asymmetry and symmetric phenotypic variation do not match 1:1, highlighting the underlying differences in the ways that the methods estimate the components of variation (Figure 2.8A). In all cases correlations between fluctuating asymmetry, symmetric variation, and trait means are highly correlated (FA: R^2=0.812, p=3.286e-7; symmetric variation: R^2=0.901, p=8.1761e-10; trait mean: R^2=0.997, p=6.3581e-31).

Using the data herein, it is not clear whether the maximum likelihood method proposed by Young (2007) appreciably improves estimates for the components of variation. Two major differences are present between the analyses presented herein and the analyses of Young (2007). The first is that the inferences made by Young (2007) were based almost entirely on simulated

datasets where the predicted values were known, whereas the data herein is measured from empirical data. The second is relative sample sizes: simulated data by Young were conducted using samples of 50 and 100 over 500 replicated datasets, whereas the data here was conducted 18 specimens of *E. crassituberculatus* and 28 of *E. milleri*. Empirical analyses often are conducted on 50-100 specimens or less, which limits the statistical power of FA methods to correctly estimate the 'true' values for the components of variation (Young, 2007). For the data observed for *Eldredgeops*, variation occurs on the same magnitude as the trait size, combined with the present sample sizes, neither the traditional FA methods nor the maximum likelihood method can be explicitly preferred.

Effects of small sample size on maximum likelihood estimation—Both the likelihood ratio test and multi-model inference are designed to test for differences in model likelihoods. Likelihoods recovered using the maximum likelihood method proposed by Young (2007) are calculated as the SS_{error} (Error Sum of Squares). Looking at the formula for the sum of squares the dependency on sample size becomes apparent:

$$TSS = \sum_{i=1}^{n}(y_i - \bar{y})^2 \qquad (2.1)$$

In the present study system, deviations from bilateral symmetry are small (less than 2) and for a given trait ideally are normally distributed around a mean of 0. Additionally, variation in the total number of lenses within a file is low, with the difference in total range of lenses in a single dorso-ventral file being less than or equal to 3. Therefore, if we are looking at the sum of squares of small deviations, the largest impact on the total sum of squares is that of sample size. Small likelihoods are to be expected for small sample sizes, which was observed.

It is therefore important to acknowledge that the inferences and discussion of the results presented herein are tentative. Interpretations are based on the data at hand, though it is clear that

larger sample sizes are needed to improve the robustness of the results. Due to the ongoing 2020-2021 COVID pandemic at the time of writing, I was unable study specimens from the Cleveland Museum of Natural History (CMNH), the Paleontological Research Institute (PRI), and the University of Michigan Museum of Paleontology (UMMP). Each of these institutions has an extensive collection of specimens from the Silica Formation that would have greatly increased the overall sample size of the data.

It is possible that a minimum sample size needed is on the order of either 50, 100, or more samples to have the statistical power to detect differences between the two species. Simulations using a sample size of 200 specimens show that as the relative measure of FA increases, the statistical power of being able to detect differences between populations decreases (Young, 2007). If each species requires a minimum of 50 pristine specimens, with each specimen needing to be photographed four times and each eye counted twice, this will require a significant investment in time and sampling effort. That is not to say that the effort can't be made, nor that the specimens do not exist. From experience working with *Eldredgeops* in multiple museum collections and field sampling, there is a wealth of data that can still be collected from current museum stocks. Given enough patience and investment, the payoff for continued sampling among *Eldredgeops* is great: understanding the relationship between FA and symmetric variation in fossil populations would have numerous implications for our understanding of macroevolution and the expression of trait variation in populations (see discussion by Webster, 2019).

CONCLUSION—Developmental asymmetries are common in the species of *Eldredgeops* investigated herein, and in trilobites more broadly (Clarkson, 1966a; Clarkson, 1969; Fortey & Morris, 1977; Ludvigsen, 1979; Owen, 1985; Ludvigsen, 1991; Thomas, 1998; Crônier & Clarkson, 2001). Continued study of eye-lens asymmetries in phacopid trilobites may prove to be

a fruitful avenue of research. The preliminary analyses presented herein suggest that developmental patterns in fossil clades like *Eldredgeops* may be similar to those in neontological studies in that the mechanisms controlling the various components of within- and among-individual variation are likely trait-, population-, or species-specific (Scheiner, 1993; Clarke, 1997, 1998; Polak, 2003; Leamy & Klingenberg, 2005; Muñoz-Muñoz et al., 2006; Van Dongen, 2006; Klingenberg 2015; Klingenberg, 2019; Webster, 2019).

This analysis is the first to apply the maximum likelihood method to estimate the components of variation since Young (2007) developed that method. Young (2007) demonstrated that the MLE method can overcome the "Swain Effect" bias that arises when traditional methods of estimating FA are applied to meristic traits (Van Valen, 1962; Leamy, 1983; Palmer & Strobeck, 1986, 2003). In the present study, the recovered estimates for FA, symmetric variation, and trait mean do not seem to be appreciably improved by using the maximum likelihood as opposed to the traditional FA10 method, nor can it be explicitly stated that maximum likelihood was able to overcome the "Swain Effect". This may be due to the low sample sizes of the two species used herein and the size of the traits used relative to the amount of variation observed; planned additional sampling was hindered due to the COVID 2020-2021 pandemic. With larger sample size, as suggested by Young (2007), the maximum likelihood methods may be a better alternative to traditional FA metrics when using meristic traits. Future studies investigating fluctuating asymmetry should continue to use and investigate the maximum likelihood method proposed by Young (2007).

CHAPTER THREE:
VARIATION OF EYE-LENS DISTRIBUTION IN TWO SPECIES OF *ELDREDGEOPS* STRUVE 1992 AND ITS IMPLICATIONS FOR MODELING EYE DEVELOPMENT IN TRILOBITES

ABSTRACT—The calcified lenses of trilobites are one of the oldest preserved visual systems in the animal kingdom. Schizochroal lenses, found only in the Suborder Phacopina, represent a unique visual system with no exact modern counterpart. Over the past half-century, a number of developmental models have been proposed to for both the development of the lens itself and how a series of these lenses were emplaced across the visual surface of the eye during ontogeny. This paper reviews models of lens emplacement within trilobites, discusses predictions and limitations of the models, and then, using new data from the visual surface of two species of *Eldredgeops*, evaluates and proposes a developmental model for lens emplacement and growth within trilobites. Development of the visual surface and emplacement of eye-lenses in trilobites were likely regulated by similar but semi-independent processes. New lenses were emplaced within the generative zone, with the first lenses being emplaced near the palpebral suture. Throughout ontogeny, new lenses were added below previous lenses and usually maintain a close hexagonal packing arrangement. Current models of eye development in trilobites largely disagree on the shape of the generative zone, whether curved or horizontal. Observation of eye-lens distributions in *Eldredgeops*, including analysis of left-right asymmetries within-individuals, suggests that the generative zone traced the advancement of the visual surface and was curved convex ventrally. Further, asymmetries observed in *Eldredgeops* suggest that, at least within this genus, individuals were not capable of compensatory growth to repair developmental abnormalities throughout ontogeny.

INTRODUCTION—Trilobites were a successful group of marine arthropods, comprising some 20,000 named species (Adrain, 2011). First appearing in the early Cambrian (~521 Ma), trilobites possess one of the earliest records of visual systems in the fossil record. Among oculate trilobites, lenses were composed of the mineral calcite, allowing for exceptional cases of preservation and extensive study over the last century and a half (Packard, 1880; Beecher, 1895; Lindström, 1901; Clarkson, 1975; Thomas, 2005; Schoenemann, 2021; among others). Three types of eye morphology have been distinguished among trilobite clades: the most common being the holochroal type, the more derived schizochroal type restricted to the Suborder Phacopina, and the abathochroal type being found only in some eodiscids (Clarkson, 1975, 1979; Zhang & Clarkson, 1990; Thomas, 1998, 2005; Crônier & Clarkson, 2001; Schoenemann & Clarkson, 2015; Schoenemann, 2021).

Meticulous study of lens patterning in trilobites has led to a developmental model for trilobite eyes (Clarkson, 1975; Zhang & Clarkson, 1990; Thomas, 1998, 2005). While this model was based primarily on study of schizochroal lenses, comparative morphology and phylogenetic considerations suggest that all three eye-types were underlain by a common developmental regimen (Thomas, 2005; Harzsch & Hafner, 2006). Formulation of this model occurred in phases over the last half-century. Models for trilobite eye development are here treated under two main categories. The original model was proposed by Clarkson (1975, 1979) and was later supported with ontogenetic evidence by Zhang and Clarkson (1990). A modified version of Clarkson's (1975) model was proposed by Thomas (1998) and subsequently expanded to integrate developmental information from modern arthropods (Thomas, 2005). These two models were developed from observations of many of the same trilobites and are similar in many of their proposed developmental mechanisms, but differ in the way in which lenses are hypothesized to

have been emplaced within the visual surface of trilobites (see below). It remains unclear which, if either, of these models is accurate. Further, while discussions on trilobite eye development have advanced greatly in recent decades, a consensus on the how the generative zone moved through ontogeny is not clear (Crônier & Clarkson, 2001; Clarkson et al., 2006; Harzsch & Hafner, 2006; Schoenemann & Clarkson, 2015).

This paper reviews the proposed developmental models (Clarkson, 1975, 1979; Zhang & Clarkson, 1990; Thomas, 1998, 2005), then details the developmental model of eye growth in three modern arthropod clades which have been suggested as analogues for development in trilobites. Eye variation within two species of the Middle Devonian phacopid *Eldredgeops* Struve 1992 is investigated; right and left eyes of individuals of *Eldredgeops* commonly show abnormalities. Abnormalities of the eyes provide an under-exploited source of data regarding variation in eye-lens emplacement that might shed light on the underlying developmental mechanisms. Reviewing abnormalities in other trilobites, lens-distribution models from the literature and the two species of *Eldredgeops,* and common developmental mechanisms in modern arthropods, I propose a model for the growth and development of eyes within trilobites that draws on developmental abnormalities to unify previous models of eye-lens emplacement.

BACKGROUND—

Trilobite Eye Morphology—In all trilobites, eye lenses were originally composed of the birefringent mineral calcite (Lindström, 1901; Clarkson, 1975; Thomas, 2005; Lee et al., 2007, 2012; Torney et al., 2008, 2014; Schonemann & Clarkson, 2011, 2015; Schoenemann, 2021 [though recently questioned by Lindgren et al. (2019) who argue the calcitic nature of the eyes are secondary rather than primary features]). Individual lenses have long been thought to be single crystals of calcite oriented with the optical axis perpendicular to the visual surface to

avoid the double-refraction of light through the calcite crystal lattice (Thomas, 2005). Recent analysis of schizochroal lenses revealed the calcite was underlain by multiple alterations to the crystal that aligned to the curvature of the lens and may have internally possessed organic ommatidia-like structures that corrected for any spherical aberration of light to visual processing (Schoenenann & Clarkson, 2011; Torney et al., 2014). Within the small lenses typical of holochroal eyes (≤1μm lens diameter) the receptor diameter was smaller than that of the spherical aberration that would be produced by the misalignment of the ordinary and extraordinary ray passing through the lens (Schoenemann et al., 2019; Schoenemann, 2021).

Three eye types are known for trilobites. Considered apomorphic, the primary eye type among trilobites is the holochroal eye (Clarkson et al., 2006). The visual surface of these eyes sat upon a socle and was covered by many small, closely spaced lenses that were covered by a thin cornea; no sclera separated individual lenses (Thomas, 2005; Schoenemann & Clarkson, 2015). Ommatidia-like units probably underlay the individual lenses, which likely approximated vision similar to the compound eye found in most modern arthropods (Clarkson, 1997; Thomas, 2005; Schoenemann & Clarkson, 2015; Schoenemann et al., 2019; Schoenemann, 2021).

Abathochroal eyes were originally described by Jell (1975) and are only known from some members of the Eodiscina. Investigated by Zhang and Clarkson (1990) and Gál et al. (2000), some authors have questioned whether the abathochroal structure represents a distinct eye type (Crônier & Clarkson, 2001; Clarkson et al., 2006; Schoenemann & Clarkson, 2015). Each lens was small and covered by an individual cornea; lenses were separated from each other by sclera that were no deeper than the lens itself. The cornea likely did not extend into the sclera itself (Gál et al., 2000). Comparisons with juvenile holochroal eyes of other Eodiscina suggest

that abathochroal eyes developed neotenically from a holochroal ancestor (Zhang & Clarkson, 1990).

Trilobites within the Suborder Phacopina possess schizochroal eyes. Due to their structure and size, schizochroal lenses have been studied in particular detail (Clarkson, 1975, 1979; Clarkson & Levi-Setti, 1975; Miller & Clarkson, 1980; Horváth & Clarkson, 1993; Thomas, 2005; Clarkson et al., 2006; Schonemann & Clarkson, 2011, 2015; Torney et al., 2014; Schoenemann, 2021). The lenses in schizochroal eyes are much larger and fewer in number than those in holochroal eyes and are separated from each other by an 'interlensar sclera' (Clarkson, 1967, 1997; Schoenemann & Clarkson, 2015). The lenses were of a doublet structure and were overlain by a corneal covering that extended into the interlensal sclera; they were underlain by an interlensar bowl that may have reduced reflectivity and enhanced light transmission (Figure 3.1)(Horváth, 1996; Thomas, 2005). This internal bowl may also have been involved in image formation, functioning in a similar role as the retina (Egri & Horváth, 2012). Within the lens, internal trabecula, simple organic sheaths, may have acted to guide light through towards the interlensar bowl through complete internal reflection and working as a light-guided lens (Schoenemann & Clarkson, 2008, 2011, 2015).

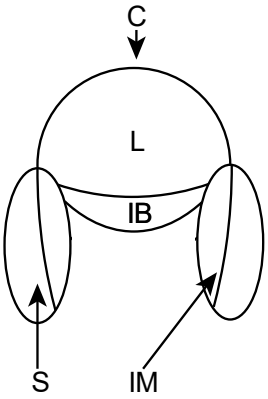

Figure 3.1—Schematic cross section through a schizochroal lens doublet bounded on either side by intralensar sclera (S), identical in composition to the general cuticle which separates lens from adjacent ones. Each lens is covered in a thin corneal membrane (C) which intersects the sclera as the intrascleral membrane (IM). The lens proper (L) is bounded below by a Cartesian surface, below which is the intralensar bowl (IB) which may have acted as a rudimentary retina.

Lens arrangement within the trilobite eye is regular often occurring in a close hexagonal packing system, particularly for schizochroal eyes in which the lenses are ordered into vertical files and horizontal rows (Figure 3.2)(Clarkson, 1975; Thomas, 2005). Within schizochroal eyes,

the visual surface itself takes the shape of a lunate section of a logarithmic spiral (Clarkson, 1975; Crônier & Clarkson, 2001; Thomas, 2005; Clarkson et al., 2006; Harzsch and Hafner, 2006). Being arthropods, trilobites molted frequently throughout ontogeny. It is likely that between individual molts, trilobites added a single row of lenses to the visual surface of the eye (Clarkson, 1975; Zhang & Clarkson, 1990; Thomas, 1998, 2005; Harzsch & Hafner, 2006). The outward expansion of the visual surface during growth meant that a simple lens packing arrangement would become disrupted; this was commonly solved by a progressive increase in lens size towards the ventral rows, thus allowing the packing arrangement of the eye to be maintained (Clarkson, 1975).

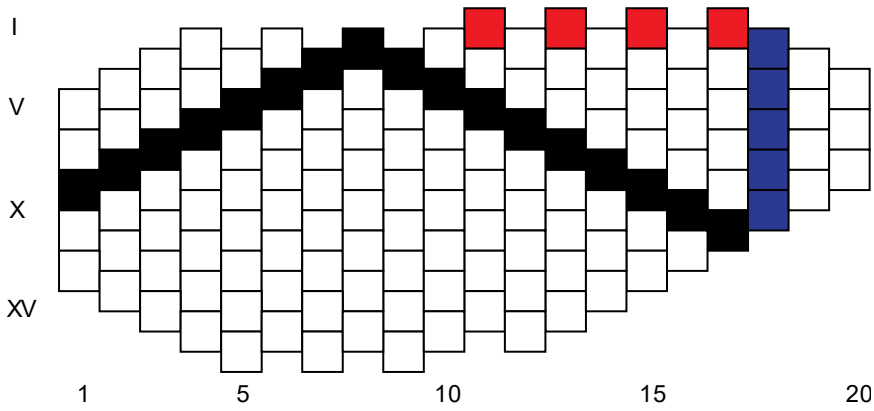

Figure 3.2—Eye lens diagram of the visual surface for the paralectotype of *Eophacops musheni* (Salter, 1864) (BU59a), diagraming the terminology of Clarkson (1966a). Front of the eye is to the left; Roman numerals correspond to the numbering of individual *horizontal rows*. Arabic numerals below the diagram correspond to individual *dorso-ventral files*, counting proceeds from anterior to posterior; individual dorso-ventral file indicated by blue boxes. Black boxes indicate single examples of *ascending* and *descending diagonal rows*; red shading indicates the *accessory upper horizontal row*. Diagram adapted and modified from Thomas (1998).

Some of the structural and functional aspects of schizochroal lenses discussed herein have been questioned by Bruton & Haas (2003), who proposed a separate functional model of schizochroal lenses termed the Graded Refractive Index (GRIN) model. However, their model lacks sufficient evidence and has not been supported by subsequent authors (Thomas, 2005; Lee et al., 2007; Torney et al., 2014; Schoenemann & Clarkson, 2015; Schoenemann et al., 2015; Schoenemann, 2021).

Eye Lens Diagrams—Eye lens diagrams are a simplified means of interpreting variation in trilobite eye lens patterning; these diagrams are commonly employed by phacopid workers to represent the packing arrangement within the schizochroal eye. Terminology for diagraming the position of lenses within trilobites follows Clarkson (1966a); see Figure 3.2. In an eye lens diagram, the characteristic close hexagonal packing arrangement is easily represented and allows for comparison between eyes of the same individual, multpile individuals of the same species, or across species (Campbell, 1977; Clarkson & Tripp, 1982; Howells, 1982). These diagrams depict the characteristic arrangement of lenses into dorso-ventral columns (= dorso-ventral files), horizontal rows, and the ascending and descending diagonal rows that form as a consequence of the packing arrangement (Thomas, 1998). While it is possible to represent the size and separation of lenses with minimal distortion into a two-dimensional representation, stereographic plots are needed for this process (Clarkson, 1966a).

Trilobite Eye Development—Much of our knowledge of trilobite eye development has been based on study of schizochroal and abathochroal eye-types (Clarkson, 1966a, 1975, 1979; Zhang & Clarkson, 1990; Thomas, 1998; 2005; Schoenemann & Clarkson, 2015). However, the schizochroal eyes of phacopids are argued to be a paedomorphic modification of the juvenile ancestral holochroal eye suggesting that eye development in all trilobites was regulated through a common developmental program with similar developmental pathways (Clarkson, 1975; Thomas, 2005; Schoenemann & Clarkson, 2015; Schoenemann et al., 2017, 2019; Schoenemann, 2021). A developmental model for trilobite eyes was first proposed by Clarkson (1975) and has been revised over the last half-century (Clarkson, 1979; Clarkson & Tipp, 1982; Thomas, 1998; Thomas, 2005; Clarkson et al., 2006; Harzsch & Hafner, 2006; Schoenemann & Clarkson, 2011, 2015). As a result of these revisions, two models of eye development have emerged: (1) a model

that essentially follows the original developmental model proposed by Clarkson (1975), but was modified using ontogenetic evidence of abathochroal lenses of Cambrian eodiscine trilobites (Zhang & Clarkson, 1990)[herein to be referred to as the 'Clarkson model']; (2) an alternative model that proposes a different style of advancement of the generative zone through ontogeny, which incorporates information from possible shared developmental mechanisms with modern arthropods (Thomas, 1998, 2005)[herein to be referred to as the 'Thomas model'].

In oculate trilobites, eyes first appear in the protaspid stage of the life cycle and form near the anterior margins of the cephalon. Throughout subsequent ontogeny, the eyes migrate posteriorly, and in schizochroal eyes particularly, may rotate downward, often asymmetrically such that the posterior of the eye rotates to a greater degree than the anterior portion of the eye (Clarkson, 1975; Miller & Clarkson, 1980; Horváth & Clarkson, 1993; Clarkson, 2005; Clarkson et al., 2006). It is possible that prior to the development of the visual surface and first lenses, immature trilobites might have possessed photoreceptors capable of basic light sensing to aid blind larvae in avoiding predation similar to that found in the earliest 'trilobite-larvae' stages of *Limulus* (Harzsch at al., 2006); however, this remains conjectural. With each successive molt the calcite visual surface had to be re-formed alongside the rest of the trilobite cuticle (Clarkson, 1975; Thomas, 2005; Schoenemann & Clarkson, 2015).

Post-ecdysial development and calcification of individual lenses has been described in detail for *Eldredgeops milleri* by Miller and Clarkson (1980) and Horváth and Clarkson (1993). Immediately post-ecdysis, while the cuticle remained flexible, the lens was conical and lay directly beneath a thin corneal covering. As calcification continued, the lens expanded laterally becoming biconvex and filled the void between the cornea and sclera. Between molts, the cornea continued to expand laterally and downward, so that the lens became increasingly bulbous; this

resulted in the lateral thickening of the calcite lens as described by Torney et al. (2014). It is unclear whether the development of the interlensar bowl and the sclera proceeded synchronously with the growth of the lens and cornea or sequentially (Thomas, 2005). Simulations by Horváth and Clarkson (1993) suggest that optical function of the lens was optimized soon after the early conical stage had passed, possibly synchronously with the hardening of the trilobite cuticle. Even while the lens was in the conical phase, the lens was sensitive to light, allowing for the post-ecdysial trilobite to remain hidden while in a vulnerable and metabolically stressed state (Horváth & Clarkson, 1993; Thomas, 2005; Clarkson & Schoenemann, 2008, 2011, 2015).

The growth of the visual surface and the emplacement of lenses through ontogeny were long viewed to be regulated independently (Clarkson, 1975; Zhang & Clarkson, 1990; Thomas, 1998). However, using developmental evidence from *Drosophila*, Thomas (2005, p.89) argued that this view is "unnecessarily complex" and that the size and shape of the eye, including the emplacement of new lenses, were likely regulated together by controlling the proliferation of cells destined to make up the eye probably analogous to undifferentiated cells in larval *Drosophila* that later form the eye following metamorphosis. However, evidence suggests that the growth of the visual surface and the emplacement of new lenses were likely to

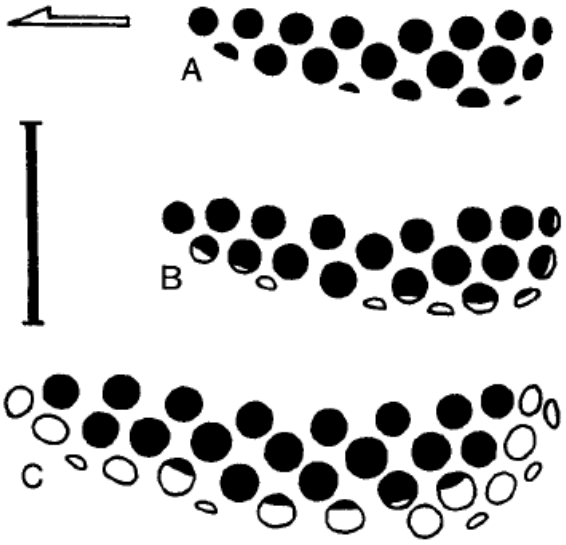

Figure 3.3—Schematic diagram showing the early growth stages of the eye of *Schizhudiscus longquanensis* adapted from Zhang and Clarkson (1990). Anterior of the eye is to the left. Scale bar =0.2mm A: smallest librigena from the study, eye comprising 19 lenses including six half-lenses. B: Somewhat larger librigena containing a total of 22 lenses. C: larger librigena with a total of 34 lenses, showing either full or half-lenses. Blank lenses represent an increase in either size or number of lenses during growth (per Zhang and Clarkson, 1990).

some degree independent. The eodiscids *Shizhudiscus longquanensis* and *Neocobboldia chinlinica* show a series of half-lenses near the bottom of the visual surface (Figure 3.3); these lenses have been interpreted as being in the process of development and could only become functional over two successive molts (Zhang & Clarkson, 1990). Separation of the growth of the visual surface from lens differentiation has also been documented in the phacopid *Nephranops? franconicus* (see Alberti, 1970b, fig. 3a-c), where the holotype specimen shows a normally proportioned and fully developed visual surface, but the both the left and right eyes have no lenses or interlensar bowls due to the independent failure to differentiate. This same phenomenon was documented by Feist and Clarkson (1989) in the proetid (holochroal eye-type) *Erbenicoryphe parvula*. Ludvigsen (1979, p.77, fig. 51c) documented an asymmetrical specimen of (schizochroal eye-type) *Viaphacops crastatus*, the right eye showing normal development with 67 lenses, but the left eye containing only 20 lenses, though the visual surface is slightly smaller than that found on the right. While originally attributed to an injury, it is likely that this asymmetry was due to a genetic or developmental abnormality (Owen, 1985; Thomas, 1998) in which differentiation of further lenses was arrested separately from the growth of the visual surface.

'Clarkson model' of lens emplacement—The early models proposed by Clarkson (1975, 1979; Zhang & Clarkson, 1990) and later models proposed by Thomas (1998, 2005) propose a similar mechanism for the differentiation of the first lenses. Active lens emplacement occurred in the *generative zone*. Early models treated the outward expansion of the visual surface and the generative zone as synonymous (Clarkson, 1975; Harzsch & Hafner, 2006). However, it is now clear that the growth of the visual surface and the emplacement of lenses were semi-independent of each other and the generative zone refers to only the region of lens emplacement on the visual

surface (Thomas, 2005; Clarkson et al., 2006; Schoenemann & Clarkson, 2015). The first lenses were emplaced at the top of the eye near the palpebral suture, forming a single horizontal row (the accessory lens row in Figure 3.2; Row 1 in Figure 3.4). As the visual surface expanded, largely to the anterior and ventrally but also to the posterior, the active sections of the generative zone moved in response. In all cases, new lenses were added ventrally and emplaced below previously-formed lenses (Clarkson, 1975; Zhang & Clarkson, 1990; Thomas, 1998, 2005; Crônier & Clarkson, 2001; Schoenemann & Clarkson, 2015). The relative movement of the generative zone is the main difference between the models of development discussed early in the literature (Clarkson, 1975, 1979; Zhang & Clarkson, 1990) and the subsequently proposed developmental models (Thomas, 1998, 2005; Crônier & Clarkson, 2001; Clarkson et al., 2006; Schoenemann & Clarkson, 2015).

In these earlier developmental models (Clarkson, 1975, 1979; Zhang & Clarkson, 1990), the generative zone is hypothesized to have advanced in a manner that follows the propagating front of the visual surface (Figure 3.3). In this model, a new horizontal row of lenses may be added below the previous lenses. However, the curvature of the visual surface meant that the generative zone was not necessarily strictly horizontal and new active centers may have formed additional dorso-ventral files if there was enough space in the anterior or posterior regions of the visual surface (Figure 3.3B-C). Thus, the generative zone advanced as a modified parabola. Clarkson (1975, 1979) and Clarkson & Tripp (1982) argued that homologous lenses among specimens can be identified by aligning specimens starting with their posteriormost dorso-ventral file and moving towards the anterior. However, if new dorso-ventral files could have been added at either end of the visual surface depending on the accommodation of the visual surface,

accurate homology between specimens would not necessarily be achieved if immature species did not share the full complement of dorso-ventral files.

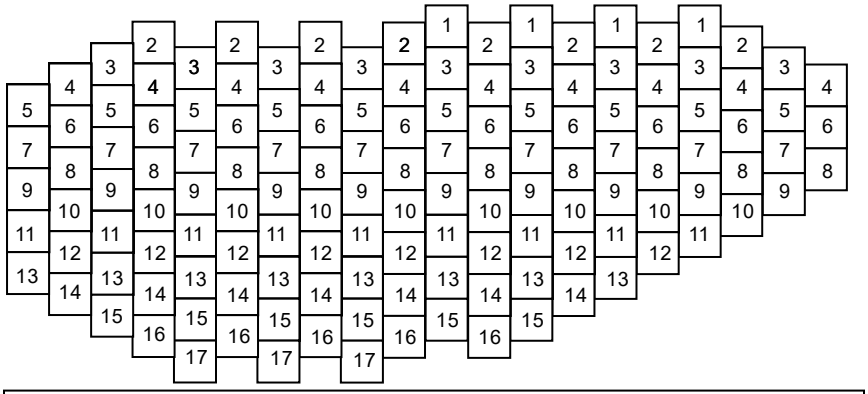

Figure 3.4—Schematic representation of visual surface in a paralectotype of *Eophacops musheni*. Front of the eye to the left. Numbers represent individual horizontal rows. Every lens in an individual horizontal lens is emplaced at the same point during ontogeny per Thomas (1998). Development proceeds in numerical order. Figure adapted and modified from Thomas (1998).

'Thomas model' of lens emplacement—Under the developmental models proposed by Thomas (1998, 2005) and accepted in the literature since (Crônier & Clarkson, 2001; Clarkson et al., 2006; Schonemann & Clarkson, 2015), the advancement and emplacement of new lenses is hypothesized to have occurred in a different manner to that of the Clarkson model. The first lenses to be emplaced are still hypothesized to form the uppermost horizontal row ('the accessory lens row'). However, Thomas (1998) proposed that the generative zone remained horizontal during its progressive movement away from the palpebral suture during ontogeny. As in the Clarkson model, active centers of the generative zone may have expanded towards either the anterior or posterior edge of the visual surface, but this only occurred when new lenses were being emplaced across the entire horizontal lens row (Figure 3.4). Such a hypothesized movement of the generative zone can be supported by conserved mechanisms of lens emplacement found in modern arthropod clades, where the propagation of new lenses occurs on an entirely 'row by row' (ex. *Limulus*) or 'column by column' (ex. *Drosophila*) basis (Thomas, 2005).

The strictly horizontal orientation of the generative zone under this model is at odds with the ontogenetic data provided by Zhang and Clarkson (1990; Figure 3.3). The model proposed by Thomas (1998, 2005) would suggest that in Figure 3.3C, the generative zone had moved to the bottom of the visual surface and the new lenses in the upper horizontal rows could not be emplaced because the generative zone had already migrated away from that area. Under the Thomas (1998, 2005) model, the variation in Figure 3.3 would be explained by variation among individuals that resulted from differential developmental timing in the onset of lens emplacement in the earliest stages of eye development (Thomas, 1998, 2005; Crônier & Clarkson, 2001; Clarkson et al., 2006).

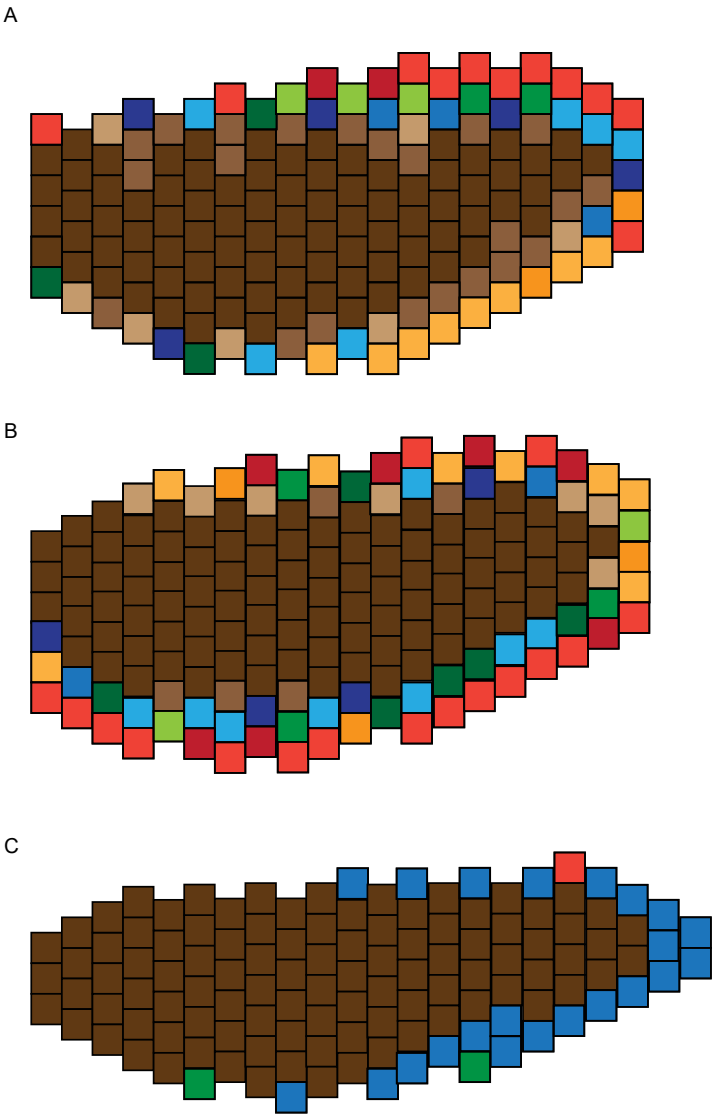

Figure 3.5—Schematic representations of the visual surfaces in *Eophacops musheni* (A-B) and *Acaste inflata* (C). Anterior of the eye is to the left. Colors correspond to the number of specimens in a population that share the individual lens. A: sample from the Much Wenlock Formation representing 27 eye across 26 specimens. B: sample from the Coalbrookdale Formation (?), representing 13 eyes across 13 specimens. Data adapted from Thomas (1998); where ranges of shared lenses were reported in the original paper, they are represented herein with the minimum number of the range.

Studying lens variation in two populations of *Eophacops musheni* (Fig. 3.5A-B) and a population of *Acaste inflata* (Fig. 3.5C), Thomas (1998) found that the greatest amount of variation in lens distribution occurs dorsally, posteriorly, and ventrally. However, this interpretation is not surprising given the method he used to identify homologous lenses. Instead of the "posterior-first" lens homology suggested by Clarkson & Tripp (1982), specimens were aligned using an anterior-to-posterior alignment. By doing so, the upper rows of the anterior dorso-ventral files would be aligned and considered to be homologous among specimens, so that variation among individuals would only be interpreted as occurring dorsally, posteriorly, and ventrally. Furthermore, Thomas's (1998, 2005) proposed method of homology and movement of the generative zone are complicated by issues regarding the initiation of differentiation of new lenses. Under all models proposed [both Clarkson and Thomas] the first lenses are emplaced in the first horizontal row, to which new lenses are then added sequentially below. This would suggest that all specimens of *Acaste* and *Eophacops* should share the accessory lens row. However, the first several horizontal rows show few shared lenses between specimens (Fig. 3.5), in Fig. 3.5A the first row emplaced during ontogeny could be any one of the first six horizontal rows of the composite data. Thomas (1998) attributed this variation to natural population variation and differential variation in the timing and onset of eye lens emplacement between specimens.

It is equally possible given Thomas's (1998; Figure 3.5) data that the generative zone was shaped like a backwards C in which the generative zone arcs around the posterior margin, such that during growth the active centers of lens emplacement could radiate outward from the anterior central cluster of lenses. This conclusion would violate the assumption that new lenses were emplaced exclusively *below* existing lenses in the horizontal row (Clarkson, 1975, 1979;

Clarkson & Tripp, 1982; Thomas, 1998, 2005; Crônier & Clarkson, 2001; Harzsch & Hafner, 2006; Clarkson et al., 2006; Schoenemann & Clarkson, 2015). Nor do the data rule out the curved nature of the generative zone that was suggested by Clarkson (1975, 1979) and Zhang and Clarkson (1990).

The study by Thomas (1998) remains an important contribution to our understanding of eye-lens variation in trilobites and aids our understanding of development in trilobites. However, the data presented do not unequivocally support either the strictly horizontal movement of the generative zone as proposed by Thomas (1998, 2005) nor do they falsify the possible parabolic movement of the generative zone as proposed by Clarkson (1975) and Zhang and Clarkson (1990).

Testing model assumptions—Under Thomas's model, the number of lenses in any given horizontal row would be fixed throughout subsequent ontogeny, because the downwardly-moving and strictly horizontal generative zone would never again impinge upon that particular row. The total number of dorso-ventral files in the eye could increase through ontogeny from one horizontal row down to the next (e.g., if the generative zone elongated anteriorly and/or posteriorly), but the number of lenses within a given horizontal row could not increase through ontogeny.

One way to test the observations proposed by Thomas (1998) requires understanding the relative ontogeny of multiple specimens. While Thomas (1998) provided information on the relative size of specimens and their total number of dorso-ventral files (see text-figure 3, Thomas, 1998, p. 903), this does not necessarily equate to the pattern of lens emplacement that a single individual would follow. Figure 3 in Thomas (1998, p. 903) also reveals that the study was based only on rather large specimens (having a cephalic length ≥7mm).

Further, if a strictly horizontal generative zone is the favored model, we should expect a skewed distribution in the total number of dorso-ventral files in morphologically mature specimens. Where morphologically immature specimens are observed which lack the full complement of doro-ventral files, they have already emplaced several horizontal rows, by which adult specimens have emplaced all dorso-ventral files. Therefore, the logical extension of this observation would be that the sub-adult specimens would not be capable of adding new files during ontogeny because the generative zone has moved passed the position to do so resulting in an adult distribution where most specimens exhibit the maximum number of files with a tail of adults showing some number less.

MATERIAL AND METHODS—

Focal Species— Lens patterning and distributions were observed for two species of the Middle Devonian trilobite genus *Eldredgeops* Struve, 1992; *E. crassituberculatus* (Stumm, 1953) and *E. milleri* (Stewart, 1927). The species considered here have been fully described elsewhere (see Chapter 1; Eldredge, 1972). This section is included to illustrate the differences in lens distribution of the two included species of *Eldredgeops*.

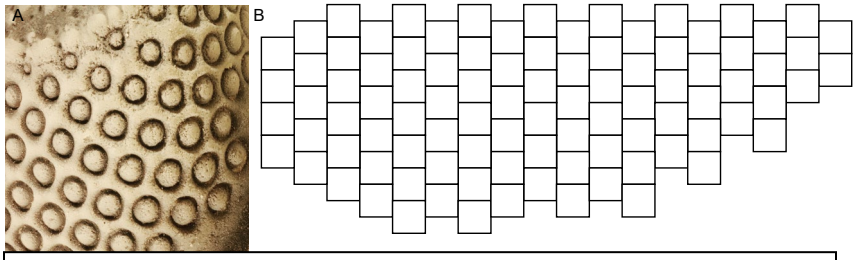

Figure 3.6—A: visual surface of the eye in a specimen of *Eldredgeops crassituberculatus* highlighting the regular arrangement of lenses into dorso-ventral files. Note the characteristic lens shape where the lens is reduced or flush with the scleral wall and a thick sclera is developed between individual lenses. B: Schematic representation of the visual surface of the eye of *E. crassituberculatus* assembled from 36 eyes of 18 specimens.

Lenses within *E. crassituberculatus* are arranged into a maximum of 18 dorso-ventral files in morphologically mature specimens. Maximum number of lenses in a file is 6, though occasionally specimens with 7 lenses in a file may be reported. As with most phacopids, lenses are arranged in close hexagonal packing; due to the curvature of the eyes, lenses increase

in size towards the bottom of the visual surface to maintain the packing arrangement. The lenses are either reduced or flush with the scleral wall, thick sclera separate lenses from each other (Figure 3.6A). A composite distribution of lenses for specimens studied illustrated in Figure (3.6B).

Lenses in *E. milleri* are arranged into a maximum of 18 dorso-ventral files in morphologically mature specimens. Maximum number of lenses in a file is either 8 or 9, very rare instance of 10 lenses in a dorso-ventral file was observed in the material examined for this study.

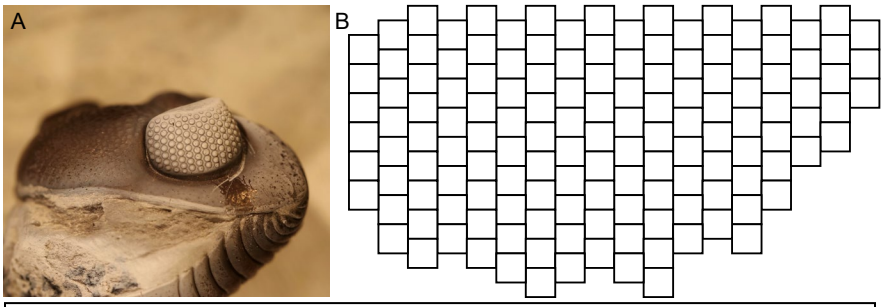

Figure 3.7— A: visual surface of the eye in a specimen of *Eldredgeops milleri* highlighting the regular arrangement of lenses into dorso-ventral files. Note the characteristic lens shape where the lens protrudes above the visual surface and a thin sclera is developed between individual lenses. B: Schematic representation of the visual surface of the eye of *E. milleri* assembled from 56 eyes of 28 specimens.

Lenses arranged in typical close hexagonal packing; lenses increase in size towards the bottom of the visual surface to maintain packing arrangement. The lenses are bulbous and protrude well above the visual surface, little to no sclera separates the lenses from each other (Figure 3.7A). The packing arrangement and distribution of lenses of the specimens studied is illustrated in Figure 3.7B).

Material Collection and Specimen Preparation—Specimens belonging to *E. crassituberculatus* and *E. milleri* were selected from the following museum and university collections: the American Museum of Natural History (AMNH), Bowling Green State University (BGSU), and the Field Museum of Natural History (FMNH). Specimens included in this study are the same as those used in Chapter 2, with some additional specimens from the BGSU collection. All

specimens of *E. crassituberculatus* and *E. milleri* examined herein were collected from the Silica Formation located in Sylvania, Ohio. The museum records do not contain information about which unit(s) within the Silica Formation the specimens were collected from.

Each specimen was mounted laterally to expose an individual eye to the camera lens. Due to the curved nature of an individual visual surface (which wraps ~180° in plan view), specimens were photographed from two angles on each side, once to capture the anterior portion of the visual surface and once to capture the posterior portion. For specimens where both eyes are well preserved, this process was repeated for the opposing side of the trilobite, resulting in four photographs to capture a composite of both visual surfaces of a single individual. In some cases, individual trilobites were first coated with ammonium chloride sublimate to enhance the contrast of the lenses against the intermediate sclera. Lens counts for a particular visual surface of a given individual were obtained by matching dorso-ventral files between photographs of that visual surface of that specimen (see Chapter 2). To account for possible error in lens counts, each side was counted on two separate occasions. Full lens counts (i.e., on both left and right eyes) were obtained for 18 specimens of *E. crassituberculatus* and 28 specimens of *E. milleri* (same as Chapter 2). The number of dorso-ventral files for at least one eye was counted on 20 *E. crassituberculatus* and 63 *E. milleri* BGSU specimens.

Glabella length, glabella width, eye length, and eye height were recorded for each specimen within the BGSU collection. These measurements help facilitate an understanding of the ontogeny of eye lens emplacement for both *E. crassituberculatus* and *E. milleri*.

RESULTS—

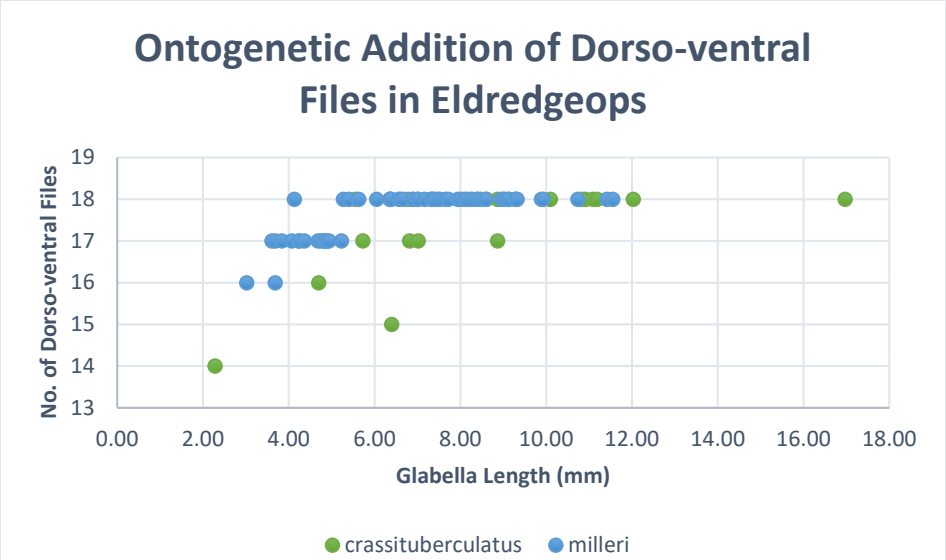

Figure 3.8—Relative addition of lenses throughout ontogeny in both species of *Eldredgeops*. Data represent the number of dorso-ventral files in a single eye taken from BGSU specimens. Size [a proxy for developmental age] is quantified as the length of the glabella measured from the frontal margin to the preoccipital furrow.

Ontogenetic Addition of Eye-Lenses and Files—Samples of both species of *Eldredgeops* studied herein include specimens of a fairly wide size range, which permits the inference of ontogenetic patterns of lens emplacement (Figures 3.8, 3.9, 3.10). There is variation in the size at which new dorso-ventral files were added to the visual surface, both within and between the two species. For example, among *E. milleri* specimens, BGSU4052A has a glabella length of 4.13 mm, yet possesses 18 dorso-ventral files while the slightly larger BGSU4032B has a glabella length of 4.69 mm and possesses only 17 dorso-ventral files. All specimens of *E. milleri* with glabella length > 5.27 mm possess 18 dorso-ventral files. Specimens of *E. crassituberculatus* show a greater range of variation in the size at which dorso-ventral files were added (Figure 3.10). For example, BGSU4037A has a glabella length of 6.40 mm and has 15 dorso-ventral files, BGSU4064A has a glabella length of 4.70 mm and has 16 dorso-ventral files, and BGSU4057C has a glabella length of 5.55 mm and has 18 dorso-ventral files. Specimens of *E. crassituberculatus* with glabella length larger than 8.87 mm all possess 18 dorso-ventral files.

To facilitate comparisons, positionally equivalent lenses must be identified between sides of the same individual and between specimens. In previous hypotheses of homology, Clarkson

(1975) aligned lens arrays using the posteriormost dorso-ventral file as a reference, whereas Thomas (1998) aligned lens arrays using the anteriormost portion of the eye as a reference (see above). Examination of immature eyes of *Eldredgeops* (here defined as those lacking the full complement of 18 dorso-ventral files) revealed that in rare cases neither the posterior-to-anterior recommendation of Clarkson (1975) nor the anterior-to-posterior recommendation of Thomas (1998) can be used to align homologous lenses between specimens. In morphologically mature specimens, the first lens in the 18th file was always observed to belong to the second horizontal row. Therefore, in immature specimens, if the first lens in the posteriormost file belonged to the first horizontal row, then it would be highly unlikely that this file was truly homologous to the 18th dorso-ventral file. Further, in some cases using either posterior-first or anterior-first matching, a homologous file in a smaller specimen would have an unexpectedly larger number of lenses than the next largest specimen.

Under the assumption that size equates to ontogenetic age (see above), an ontogenetic sequence of lens emplacement was constructed for both species of *Eldredgeops* (Figures 3.9, 3.10). For each ontogenetic sequence, specimens were arranged based on relative size and positional homology was matched using the method proposed herein. Under this hypothesis of lens homology, lenses that are present in one specimen but that were absent in the next smallest specimen (color-coded in Figures 3.11 and 3.12) are interpreted to have been added as part of an ontogenetic growth pattern for the species. It is conceivable that such differences in lens number represent among-individual static variation (i.e., that those individuals would have differed in lens number at the same size [or age]) (see Hughes et al., 2021 for an analogous cautionary note

regarding conflation of ontogenetic with static variation in segment number in trilobites). However, the ontogenetic interpretation is favored because it prioritizes a system of regular developmental expression as suggested by observations of shared lens-distributions in morphologically mature specimens of *Eldredgeops*.

For *E. crassituberculatus* (Figure 3.11), the smallest specimen (BGSU4058) has 14 dorso-ventral files and six horizontal rows of lenses. Through subsequent ontogeny, a fifteenth dorso-ventral file was added at the anterior margin of the eye (BGSU4037A), with several additional lenses being emplaced below the common lens core that was shared with BGSU4058. The sixteenth and seventeenth dorso-ventral files were subsequently added to the posterior region of the eye, with the final (eighteenth) dorso-ventral file later being emplaced anteriorly. Throughout ontogeny, lenses were never added above another in the same dorso-ventral file: the

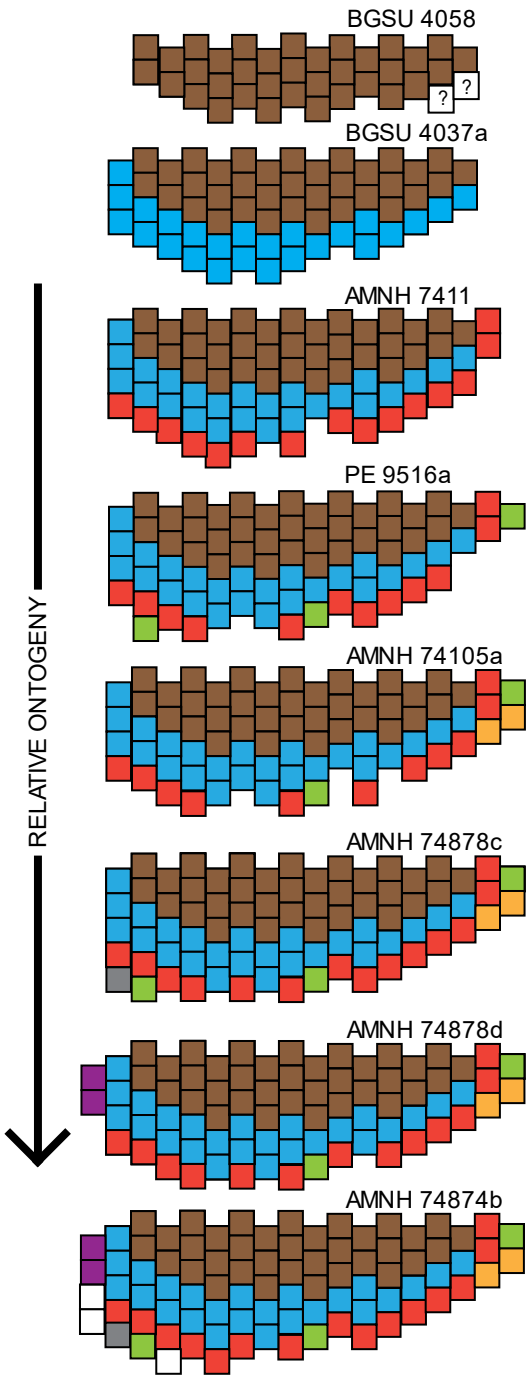

Figure 3.9—Inferred addition of lenses throughout ontogeny for *E. crassituberculatus*. Specimens are arranged in order of size. Brown lenses represent the '*common core*' of lenses, inferred to be shared across all trilobites regardless of age [at least within the size range observed in the sample]. Subsequent addition of colors represents the series of lenses shared by larger trilobites and so on. Positional homology and lens matching is aided by the observation that in all morphologically mature specimens the first lens of the first dorso-ventral file belongs to the third horizontal row, the first lends in the 17th dorso-ventral file belongs to the first horizontal row, and the first lens in the 18th file belongs to the second horizontal row.

lower margin of the visual surface was the site of new lens emplacement. However, new lenses were sometimes emplaced at the anterior or posterior ends of otherwise older horizontal rows, associated with the creation of new dorso-ventral files.

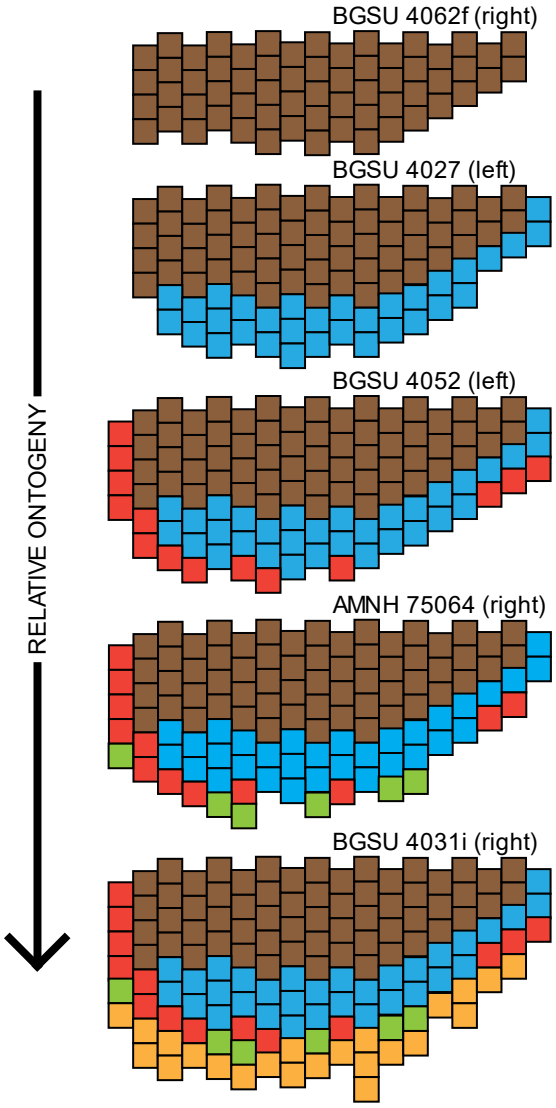

Figure 3.10—Inferred addition of lenses throughout ontogeny for *E. milleri*. Specimens are arranged in order of size. Brown lenses represent the '*common core'* of lenses, inferred to be shared across all trilobites regardless of age [at least within the size range observed in the sample]. Subsequent addition of colors represents the series of lenses shared by larger trilobites and so on. Positional homology and lens matching is aided by the observation that in all morphologically mature specimens the first lens of the first dorso-ventral file belongs to the third horizontal row, the first lens of the 17th dorso-ventral file belongs to the first horizontal row, and the first lens of the 18th file belongs to the second horizontal row.

For *E. milleri* (Figure 3.10), the smallest specimen for which an accurate lens count could be made (BGSU4062F) possesses a total of 16 dorso-ventral files. Like *E. crassituberculatus*, the addition of a seventeenth dorso-ventral file occurred at the posterior margin of the visual surface and the eighteenth dorso-ventral file was emplaced in the anteriorly. New lenses were always emplaced below an existing lens at the lower margin of a dorso-ventral file; new lenses were sometimes emplaced at the anterior or posterior ends of otherwise older horizontal rows associated with the addition of new dorso-ventral files. The interpretation that new lenses were emplaced in multiple horizontal rows at the same time suggests that the generative zone must have been curved—following the lower margin of the visual surface from the

anterior margin to the posterior margin—rather than strictly horizontal.

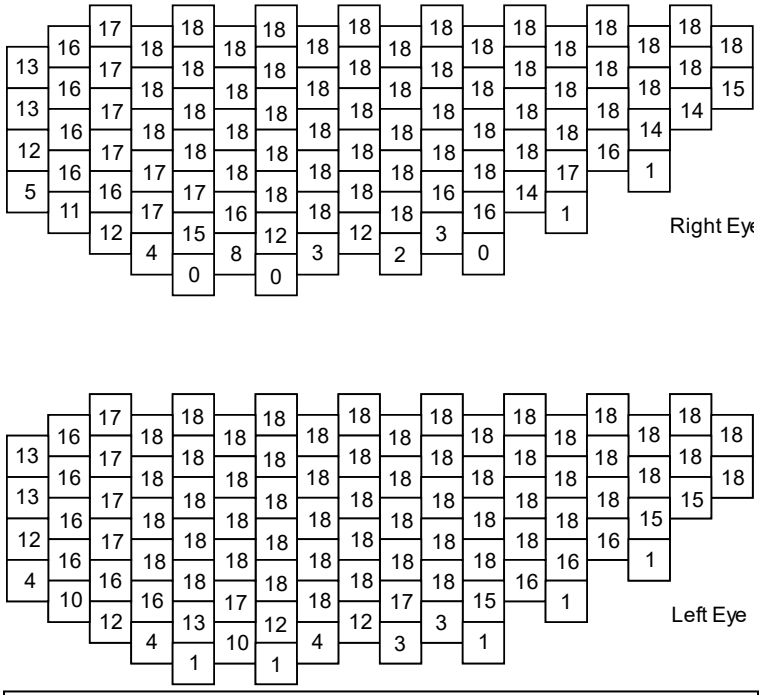

Figure 3.11—Schematic representation of the left and right eyes of *E. crassituberculatus* across 18 specimens in which lens counts for both eyes could be obtained. Front of the eye is to the left. Numbers in the boxes represent the number of specimens having that lens on that eye.

Right-Left Eye-Lens Distributions—As described in Chapter 2, right-left distributions of the same individuals commonly show asymmetries, with observed right-left differences in a single dorso-ventral file ranging from one to two lenses. Figure 3.11 shows the right-left eye-lens distribution for 18 specimens of *E. crassituberculatus*. The total number of dorso-ventral files ranges from 16 to 18; none of the 18 specimens show right-left asymmetry in the total number of dorso-ventral files. In most cases the maximum number of lenses in a file is 6, though a single specimen had two dorso-ventral files that reached a maximum number of 7 lenses, both within the left eye of the specimen. The smallest specimen of *E. crassituberculatus* on which both the right and left eyes were counted had 16 dorso-ventral files and a minimum number of 60 lenses in the right eye; due to asymmetries within several dorso-ventral files, the same specimen had a total of 64 lenses in the left eye.

Figure 3.12 shows the right-left eye-lens distribution for 28 specimens of *E. milleri*. The total number of dorso-ventral files ranges from 17 to 18 (only 16 files were countable on one specimen due to the anteriormost two files being partially obscured by matrix). None of the 28

specimens show right-left asymmetry in the total number of dorso-ventral files. As reported by previous workers, the typical number of lenses in a dorso-ventral file is either eight or nine (see Stumm, 1953; Eldredge, 1972). One specimen shows previously unrecognized maximum counts of ten lenses in two dorso-ventral files (files 7 [left eye] and 11 [right eye]), but both instances represent cases of asymmetry where the homologous file in the other eye exhibits the typical count of nine lenses. The smallest specimen in which both the left and right eyes could accurately be counted possessed a total of 17 dorso-ventral files, with a minimum of 93 lenses (BGSU4037a). On an even smaller specimen (BGSU 4062f) the lenses could only be counted on a single side; that eye possessed 16 dorso-ventral files with 61 lenses. As with *E. crassituberculatus,* the greatest amount of left-right asymmetry in lens number was concentrated ventrally.

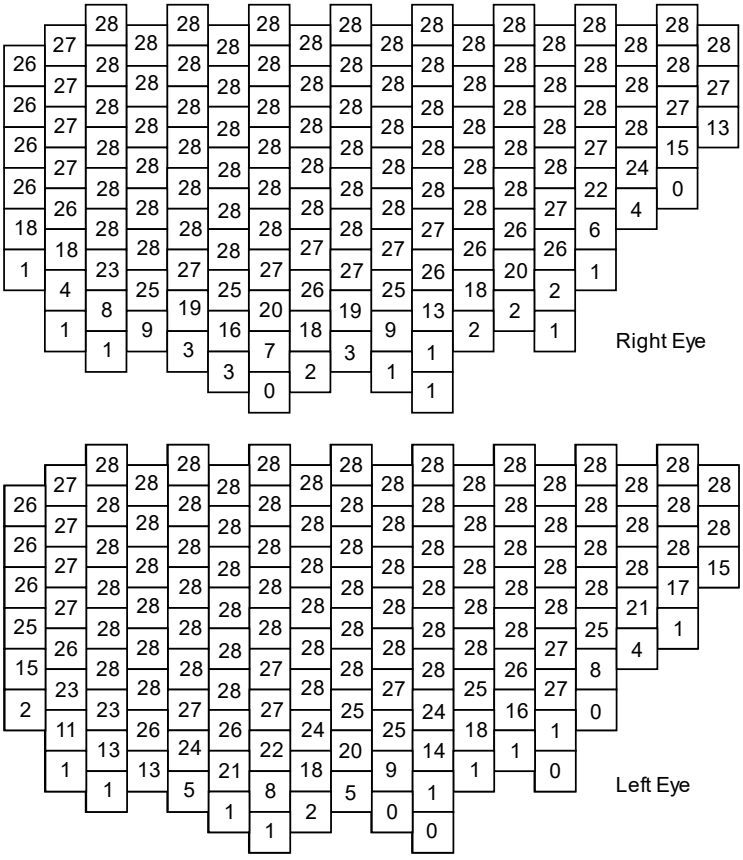

Figure 3.12—Schematic representation of the left and right eyes of *E. milleri* across 28 specimens in which lens counts for both eyes could be obtained. Front of the eye is to the left. Numbers in the boxes represent the number of specimens having that lens on that eye.

INTERPRETATION AND DISCUSSION—

Eye Development in Trilobites—Though much of our understanding of development in modern arthropods comes from holometabolous insects, it is entirely possible that trilobites shared

similar developmental controls (Thomas, 2005). The similarities in eye-lens development between *Drosophila* and *Limulus* suggests that developmental mechanisms are conserved among disparate modern arthropods. As such, initiation of eye development in trilobites was likely facilitated using *Eyeless* (*ey*) and its homologues (Thomas, 2005) and likely involved a complex series of gene regulatory networks and signaling pathways to begin differentiation of the visual surface and emplacement of lenses.

As observed in previous studies (Clarkson, 1975, 1979; Clarkson & Tipp, 1982; Thomas, 1998; Crônier & Clarkson, 2001), the first lenses to develop in the trilobite eye probably formed the uppermost horizontal row of lenses. Some authors have noted diminutive lenses in the uppermost horizontal row of the mature eye (Harzsch & Hafner, 2006). These lenses have been interpreted as being emplaced at some point late in ontogeny (Harzsch & Hafner, 2006). However this would not have been possible if—as proposed by other workers (Clarkson, 1975, 1979; Thomas, 1998, 2005; Clarkson et al., 2006) and herein—the generative zone moved away from the palpebral suture during ontogeny because new lenses could then only be emplaced below previously-formed lenses. In some specimens of *Eldredgeops* diminutive (or sometimes half-formed) lenses were observed in the first horizontal row. In the model of lens emplacement proposed herein, those lenses are interpreted as (irregularities in) the earliest-formed lenses rather than as late additions to the visual surface. As the trilobite grew, those lenses remained fixed in place but could continue to grow.

The downward migration of the generative zone through ontogeny was likely controlled by similar developmental principles as the morphogenic furrow in modern *Drosophila* (Thomas, 2005). In three common modern analogues to trilobites (*Drosophila, Limulus*, and Strepsiptera), emplacement of lenses is governed by the passage of a wave of differentiation across a

previously unpatterned nascent visual surface (Thomas, 2005; Bushbeck, 2005; Harzsch & Hafner, 2006; Harzsch et al., 2006). As with *Drosophila*, it is possible that the relative downward migration of the generative zone of the trilobite eye triggered release of protein signals from developing lenses that inhibited lens cell clusters from developing as a means of maintaining the close hexagonal packing. This is further supported by the rare occurrence of intercalated lens files in trilobite eyes (Clarkson, 1975; Thomas, 1998), which suggests that lens development was regulated by the distance between centers of previously formed lenses (Thomas, 2005).

A strictly horizontal generative zone, as proposed by Thomas (1998), is not supported by the data for either species of *Eldredgeops*. Under Thomas's model, the number of lenses in any given horizontal row would be fixed throughout subsequent ontogeny, because the downwardly-moving and strictly horizontal generative zone would never again impinge upon that particular row. The total number of dorso-ventral files in the eye could increase through ontogeny from one horizontal row down to the next (e.g., if the generative zone elongated anteriorly and/or posteriorly), but the number of lenses within a given horizontal row could not increase through ontogeny. Thus, for *E. crassituberculatus*, the difference in number of lenses in the second horizontal row between BGSU 4058 (seven lenses, forming a total of 14 dorso-ventral files with the lenses in the first horizontal row) and the slightly larger BGSU 4037a (eight lenses, forming a total of 15 dorso-ventral files with the lenses in the first horizontal row) would have to be interpreted as static variation among individuals rather than as the ontogenetic addition of a new dorso-ventral file. Under Thomas's model, some large individuals of *E. crassituberculatus* should be expected to show as few as seven lenses in the second horizontal row. Such a prediction is not observed within the sample examined herein: indeed, all large specimens

possess nine lenses in the second horizontal row. A similar failed prediction of the Thomas model holds for *E. milleri*.

Observations of left-right asymmetries within *Eldredgeops* and other trilobites similarly do not support a strictly horizontal generative zone. If we consider the advancement of the generative zone on a horizontal 'row by row' basis as implied by the Thomas model, stochastic perturbations during development in which lenses fail to propagate would be expressed as an absence of lenses within medial positions of the file where the generative zone moved past without emplacing a lens during a molt. Clarkson (1966a) described one specimen of *Acaste downingiae* with two extra lenses on the right eye and a hiatus on the center of the left eye in which no lenses propagated. This is the only case where this has been observed. As observed in both species of *Eldredgeops*, asymmetries in lens counts between homologous files were not the result of temporary arrests in development confined to the medial positions of the file. Instead, lens packing remains regular, such that asymmetries could only be inferred by taking differences in lens numbers between the left and right sides of the same individual.

As suggested by previous authors, it is likely that only a single (curved) row of lenses was added between successive molts (Clarkson, 1975; Zhang & Clarkson, 1990; Thomas, 1998, 2005; Crônier & Clarkson, 2001; Clarkson et al., 2006; Schoenemann & Clarkson, 2015). That is to say, only a single new lens was added within a given dorso-ventral file per molt (and only if there was sufficient space to accommodate that lens in the visual surface). If that hypothesis is true, then the presence of left-right asymmetry of more than one lens within a given dorso-ventral file of a given individual would indicate that trilobites were not capable of corrective repair or compensatory (targeted) growth. If the processes controlling symmetric (among-individuals) and asymmetric (within-individual) variation operate under similar developmental

mechanisms (Chapter 2), then we would expect that species failing to correct development using compensatory growth would have a greater range of populational variation upon which natural selection can act. From the specimens observed in this study, the presence of multiple occurrences of intra-individual, intra-file, left-right asymmetries of two lenses indicates that at least for *Eldredgeops*, developmental asymmetries were not repaired and were additive throughout ontogeny (see lens counts in Appendix C, Table C.1). However, the extent to which this might apply to eye development in other trilobites is unknown. Changes in variance of size for successive instars of a Cambrian olenellid trilobite and a Silurian aulacopleurid trilobite are consistent with the prediction of compensatory (targeted) growth in those trilobites (Fusco et al., 2004; Webster, 2015). Among other arthropods, compensatory growth has been documented in earwigs (Tomkins, 1999), but was not found in studies of crabs (Chippindale & Palmer, 1993; Swaddle and Witter, 1997).

SUMMARY AND CONCLUSIONS—Developmental models of eye lens emplacement proposed by Clarkson (1975, 1979; Zhang & Clarkson, 1990) and Thomas (1998, 2005), are similar in many respects. Both models propose that: (1) the development of the visual surface and the emplacement of eye lenses was likely controlled by similar developmental mechanisms; (2) active lens emplacement occurred in the 'generative zone,' shown to be analogous to lens emplacement in modern *Drosophila, Limulus*, and Strepsiptera (Thomas, 2005; Bushbeck, 2005; Harzsch & Hafner, 2006); (3) the first lenses were emplaced near the palpebral suture; and, (4) additional lenses were emplaced below previous lenses. These two models differ in their proposal for the form and movement of the generative zone through ontogeny. The 'Clarkson model' suggests that movement of the generative zone traces the advancement of the lens surface and is to some degree parabolic (convex ventrally). The 'Thomas model' argues that the

generative zone is strictly horizontal with new lenses being added on a "row by row" basis. The ontogenetic series of lens emplacement interpreted herein suggest that, for both species of *Eldredgeops*, new lenses could be simultaneously added to different horizontal rows of different dorso-ventral files. This does not support the horizontal "row by row" generative zone hypothesis argued by Thomas (1998, 2005). The observed data for *Eldredgeops* are similar to the ontogenetic series presented by Zhang and Clarkson (1990), in that new lenses seem to have been added to the anterior and/or posterior ends of pre-existing horizontal rows throughout ontogeny, in addition to being added as new rows at the bottom edge of existing dorso-ventral files. The generative zone of lens emplacement was therefore apparently curved (convex ventrally), extending along the entire lower margin of the visual surface and intersecting the anterior and/or posterior ends of multiple rows.

Further, the presence of asymmetries in *Eldredgeops* suggests that movement of the generative zone was not uniform between successive molts. Variation in lens emplacement between left-right homologous files suggest that even between sides stochastic perturbations in developmental signaling could be different enough to prevent the emplacement of a lens on a single side. As lenses could be added across multiple files during a single molt, we would expect that any developmental disturbance should affect multiple dorso-ventral files. As asymmetries are found in some, but not all, dorso-ventral files, this would suggest that developmental signaling is semi-independent from each other. Continued examination of asymmetries in trilobite eye-lens development, and other tetratologies, would prove to be a fruitful avenue of research to aid our knowledge of these and other ancient developmental systems. One such avenue would be to examine developmental asymmetries at both a mico- (within genus) to

macro-(bove the genus) phylogenetic scale could reveal on what time scales developmental patterns are regulated.

CONCLUSIONS

The trilobite genus *Eldredgeops* has held an important place in our understanding of patterns of macroevolution. Trilobites belonging to this genus were integral to the foundations of the concept of punctuated equilibrium and evolutionary stasis (Eldredge & Gould, 1972; Gould & Eldredge, 1977, 1986, 1993). Here I presented a three-part investigation of *Eldredgeops* and explored the role of developmental regulation and expression within this enigmatic fossil clade.

Chapter 1 presented a large-scale exploration of the trilobite family Phacopidae using both Bayesian and parsimony-based phylogenetic methods to determine phylogenetic support for monophyly of *Eldredgeops* and the broader relationships of that genus. As with previous studies, the analyses presented herein found little support for the purported phacopid tribes. Based on an increased number of characters and expanded taxonomic sampling relative to previous studies, this present study found a greater degree of phylogenetic signal and recovered more stable relationships, particularly within genera. Recovered phylogenetic relationships in *Eldredgeops* were similar in branching pattern to those found by Eldredge (1972), confirming the phylogenetic hypothesis behind one of the original case studies of punctuated equilibrium (Eldredge, 1971, 1972; Eldredge & Gould, 1972). However, *Eldredgeops africanus* (=*Phacops rana africanus*) was not recovered within the otherwise monophyletic *Eldredgeops* and is henceforth assigned to *Alloeldredgeops africanus* n.g. Additionally, the results of this study support the phylogenetic hypothesis presented by Eldredge (1973) that *Phacops iowensis* is more closely related to *Viaphacops* and *Paciphacops* (then *Phacops cristatus* and *P. logani* respectively), than it is to *Phacops latifrons s.s.* All species/subspecies of *P. iowensis* are therefore now assigned to *Smithops* n.g. Furthermore, the "small-eyed variant" of *Paciphacops invius* was suggested by Ramskold and Werdelin (1991) to be distinct from *P. invius* but was

never reassigned. Following inclusion in this phylogenetic analysis, that variant of *P. invius* is designated as *Paciphacops wallacki* n.s. This chapter provides a backbone phylogenetic tree upon which future phylogenetic studies may build. Two particular areas of focus may be particularly rewarding: (1) incorporation of more species belonging to the Silurian genera *Acernaspis* and *Ananaspis* to help polarize the early branching relationships within the Phacopidae; and (2) inclusion of phacopids that show either reduced eyesight or were completely blind.

The subsequent chapters of this dissertation focused on developmental regulation, and methods for studying such regulation, using *Eldredgeops* as the principal study organism. Chapter 2 investigated a maximum likelihood method proposed by Young (2007) to estimate fluctuating asymmetry when using meristic traits. These results were compared to traditional fluctuating asymmetry metrics proposed by Palmer and Strobeck (1986, 2003; Palmer, 1994). The results of this chapter represent the first steps in trying to understand the macroevolutionary relationship between symmetric phenotypic variation and within-individual left-right developmental asymmetries. Limited sample sizes imposed by the shuttering of museum collections in response to the COVID 2019-2021 pandemic resulted in low statistical power to infer the relationships between the components of variation at this time. Continued sampling efforts would prove fruitful.

At present, competing models of eye development disagree on the shape and movement of the generative zone throughout ontogeny in trilobites (Clarkson, 1975, 1979; Zhang & Clarkson, 1990; Thomas, 1998, 2005). Study of eye-lens patterning and developmental asymmetries in two species of *Eldredgeops* (Chapter 3) provide evidence that the generative zone was likely parabolic (convex ventrally) as it advanced from the dorsal to the ventral side of

the eye during ontogeny. The presence of asymmetries that are not shared between multiple doro-venteal files that were likely emplaced at the same time in development—the result of stochastic perturbations during development—suggests that individual dorso-ventral files are to some degree developmentally independent of each other. Furthermore, the presence of left-right asymmetries of ≥2 lenses within a single file suggests that, at least within the genus *Eldredgeops*, trilobites were not capable of compensatory growth between successive molts. Similar expression of eye-lens emplacement has been observed in modern *Drosophila, Limulus,* and Strepsiptera, suggesting common developmental mechanisms for euarthropod eyes.

I believe that Niles Eldredge put it best in his memoir *Eternal Ephemera* (2015, p. 243): "the ontogeny of those roughly 380-million-year-old trilobites was clearly a complex, genetically controlled process." The research presented herein shows how the fossil record can be used to test hypotheses regarding evolutionary developmental biology in ancient taxa, an approach that offers a valuable compliment to studies using solely extant taxa. Continued research on developmental regulation and patterning within *Eldredgeops* and other fossil clades will be of great benefit, informing us on what timescales developmental constraints may guide the trajectories of traits through evolutionary time.

APPENDIX A:

SUPPLEMENTAL INFORMATION FOR CHAPTER ONE

This appendix contains a list of the characters and character states used in phylogenetic analyses for the family Phacopidae, a table of specimen references and stage information (Table A.1), and a fully discretized character-taxon matrix (Table A.2).

List of characters and character states—

Applicable characters from Ramsköld & Werdelin, 1991, McKellar & Chatterton, 2009, and Oudot et al., 2019 have been included and are indicated as follows: α indicates characters used in Ramsköld & Werdelin, 1991; † indicates characters used in McKellar & Chatterton, 2009; ‡ indicates characters used in Oudot et al., 2019; * indicates that the character or character state has been modified to better encompass the range of data in the present study.

Terminology is based on previous phacopid work such as Eldredge 1972, Chlupáč 1977, Crônier et al., 2011, van Viersen et al., 2017.

1. ‡ Cephalon. Length vs. width of the cephalon, excluding genal spines if present, expressed as a percentage. 0: <54%; very wide, 1: 54-59%, 2: 60-66%, 3: >66%; very narrow.
2. α † ‡ * Glabellar width. Transverse width (maximum) of the frontal lobe of the glabella as a percentage of total cephalic width. 0: <50%, 1: 50-59%, 2: 60-69%, 3: 70-75%.
3. ‡* Glabella. Ratio of the glabellar width at the L1 relative to the maximum width at the frontal lobe. 0: <50%; narrow, 1: 50-60%, 2: >60%; very wide.

4. † Granules on the glabella. Presence and concentration of granules on the various surfaces and sculpture of the glabella. 0: granules present on all convex surfaces; *Acernaspis orestes*, 1: granules reduced between tubercles; *Paciphacops logani*, 2: granules absent between tubercles; *Austerops punctatus.*
5. α†* Tubercles on the glabella, Generalized class of large sculpture elements and their distribution on the glabella. 0: tubercles absent or bordering on granule size, 1: tubercles weak or sparse, 2: tubercles distinct, medium-high density, 3: tubercles pustular, dense, 4: tubercles pustular, sparse.
6. † Degree of glabellar overhang, Qualitative judgement of how much the glabella overhangs the anterior border furrow and adjacent anterior border, usually taking into account the position of the vincular furrow as well. 0: no overhang, 1: frontal face of the glabella vertical or with mild overhang, 2: high degree of overhang.
7. α†‡* Occipital ring width. Transverse width of the occipital ring, measured between axial furrows, expressed as a percentage of cephalic width. 0: <32%, 1:32-36%, 2: 36-40%, 3: >40%.
8. α* Occipital ring length. Measured from the posterior margin of the ring to the deepest part of the occipital furrow, expressed as a percentage of sagittal cephalic length. 0: ≤ 13%, 1: 14-17%, 2: >17%.
9. ‡ Occipital lateral ring nodes. Also corresponds to the thoracic axial rings. 0: lobes absent or poorly defined. 1: weak to distinctly inflated; moderately defined, 2: strongly defined, furrow runs halfway across the occipital ring.
10. †‡ Axial furrow divergence. Angel between the axial furrows on either side of the glabella in front of the S1. If the axial furrow is not linear, the angle of divergence

does not include the anterior part of the furrow. 0: low, <60°, 2: moderate, 60-70°, 2: high, >70°.

11. ‡ Axial furrow depth adjacent to the L1. 0: shallow, 1: deep.

12. ‡ Axial furrow depth between the S1 and the front of the palpebral furrow. 0: shallow, 1: deep.

13. α†‡* L1–Sagittal length. 0: Much shorter (sag.) than the occipital ring, 1: as long (sag.) or nearly as the occipital ring.

14. α†‡* L1–shape and definition of the lateral node. 0: subcircular, separated from median portion of L1 by weak exsagittal furrow, 1: subcircular, inflated, separated from median portion of L1 by a strong exsagittal furrow, 2: subquadrate, not strongly inflated, separated from the median portion of L1 by weak exsagittal furrow, 3: subquadrate, not differentiated from the median portion of L1 by independent inflation or exsagittal furrow, 4: subquadrate, about as wide as long, not strongly inflated, separated from the median portion of L1 by strong exsagittal furrow, 5: transverse (wider than long) separated from the median part of L1 by an exsagittal furrow.

15. ‡ L1 width (tr.) of median portion relative to total width. Measured as width between exsagittal furrows defining the lateral nodes; if nodes are not differentiated from the remainder of L1, width of median portion is measured as width between inner ends of S1 apodemal pits. 0: 45-55%, narrow, 1: 56-65%, wide, 2: >65% very wide.

16. ‡* Inflation of the median portion of L1. 0: depressed, 1: not inflated or slightly inflated, 2: inflated.

17. †‡ S1 medial continuity. Whether or not the medial portion of the S1 furrow is continuous and easily traceable between the intercalating ring and the more anterior portions of the glabella. 0: discontinuous or effaced furrow, 1: continuous furrow.

18. ‡ S1 adaxial curvature (towards axis). 0: curved more strongly forwards adaxially than the occipital furrow, 1: subparallel to occipital furrow, 2: transverse or curved convex backwards.

19. ‡ Presence of the S2 and S3 as expressed on exterior of the exoskeleton, not on internal mold or as dark patches on the exoskeleton. 0: present, relatively well-developed, 1: present, poorly defined or indicated by a break in sculpture, 2: absent.

20. ‡ Length of the L2 relative to L3. Maximum exsagittal length of L2 (usually in line with the center or adaxial edge of lateral node on L1) expressed as a percentage of L3 measured along the same line. 0: >70%, 1: 60-69%, 2: 50-59%, 3:40-49%, 4: absent

21. ‡ Anterolateral border shape. Used to separate the ingroup Phacopidae from the outgroup members, only used in parsimony analyses. 0: curved with apex, *Calyptaulax,* 1: evenly curved in outline, Phacpoidae.

22. ‡* Anterolateral angle of glabella. 0: rounded, semicircular, *Eldredgeops crassituberculatus*, 1: sub-angular, *Eldredgeops norwoodensis*, 2: angular, *Pedinopariops vagabundus*.

23. ‡ Glabella transverse sculptural elements on anterior face of composite lobe. Any modification of tubercular sculpture in region above anterior border furrow. 0:

absent (granulation or tuberculation unmodified in shape). 1: scale-like granules/tubercles or very short ridges, 2: relatively long terrace ridges.

24. α†‡ Postocular area length. Exsagittal length of area between the back of the eye and posterior border furrow, measured at the posterior extreme of the eye when viewing the specimen dorsally, expressed as a fraction of posterior border length (exsag.), directly behind the first measurement. 0: less than half the length of the posterior border, 1: half or equal to the length of the posterior border, 2: longer than posterior border.

25. α†* Palpebral furrow definition. Depth of the palpebral furrow in the median one-third of its course. 0: faint to absent–weak, *Austerops kermiti–Morocops ovatus,* 1: distinct–deep, *Morocops forteyi–Paciphacops birdsongensis.*

26. α†* Palpebral sculpture. Presence of pitting on palpebral lobe and palpebral area. Includes sculpture on the palpebral lobe and palpebral rim. 0: even surface/ smooth between tubercles, 1: pitted surface, 2: deeply pitted surface.

27. α† Palpebral area height. In frontal view, height of the palpebral lobe relative to the dorsal surface of the palpebral area and glabella. 0: regions are about level, 1: palpebral area lower than the palpebral lobe, 2: palpebral area markedly higher than the palpebral lobe.

28. †* Number of dorso-ventral files within the eye. Typical number of vertical columns of lenses within the eye. Populations tend to reach a stable number of lenses in the holaspid stage. 0: 13-16 columns, 1: 17, 2: 18, 3: 19, 4: 20-23, 5: 24-26.

29. † Maximum number of lenses per dorso-ventral file. May be variable within species, coding represents that maximum number of lenses reported for a species in their holaspid stage of development. 0: 3-4 lenses, 1: 5, 2: 6, 3: 7, 4: 8, 5: 9, 6: ≥10.

30. † Accessory lens row. Presence of a single additional horizontal row of lenses beginning near the middle of visual surface and continuing posteriorly. This is usually composed of diminutive lenses, as opposed to possessing a consistently top-level row proceeding from the anterior corner of the eye. 0: absent, 1: present.

31. † Subocular pad. Presence and relative inflation of a raised pad beneath eye and dorsal to the genal field. 0: absent, 1: present, weakly inflated, 2: present, strongly inflated.

32. Characterization of facet depth. Characterizes how the individual facets project above or below the sclera on the visual surface of the eye. 0: reduced below or flush with the scleral wall, 1: protruding above the scleral wall.

33. α† Sclera in the eyes. Thickness of the interlensar sclera within the visual surface of the eye. 0: thin sclera throughout, 2: sclera slightly thickened, dorsally only, 2: sclera considerably thickened dorsally, only weakly ventrally, 3: sclera thickened throughout.

34. † Sculpture on sclera. Presence of tubercles upon the sclera surface. 0: absent, 1: present.

35. † Base of visual surface with tubercles. Presence or absence of row of coarse tubercles along the ventral margin of visual surface, often these are broad and rounded in nature. 0: absent, 1: present.

36. ‡ Subocular librigenal field. Width and relative inflation of the librigenal field below the eye, as seen in lateral view. 0: very narrow and concave at front of the eye, wide and concave at the posterior (subocular inflation an lateral border furrow separately distinguishable), 1: absent at front of eye, very narrow towards the posterior, 2: narrow or relatively narrow at front of the eye, moderately narrow and concave towards the back, 3: relatively wide at the front of the eye, wide towards the back of the eye.

37. ‡ Postocular genal field inflation. 0: not swollen, 1: swollen.

38. α†‡ Genal angle. Shape of the genal angle and any prominences it may bear. 0: drawn out, with acute tip or spine, *Viaphacops cristatus*, 1: drawn out with small spine, *Reedops pembertoni*, 2: rounded, angular, with/without distinct node at corner, *Morocops stelcki*, 3: rounded, with/without node, *Morocops forteyi.*

39. ‡ Lateral border sculpture. 0: granules, 1: prominent coarse granules/ fine tubercles, rather uniform in size, 2: prominent coarse granules/ fine tubercles, heterogenous in size, 3: granules or tubercles absent or weak, intervening pits, 4: scaly granules or short ridges, 5: smooth, 6: anastomosing terrace ridges(more extensive than just in the marginal zone) with pits.

40. ‡ Lateral border furrow depth behind the posterior branch of the facial suture. 0: shallow and narrow, 1: effaced or almost effaced, 2: moderately deep to deep, narrow, 3: moderately deep to deep, rather broad, 4: shallow and wide.

41. †‡ Margination. Presence of laterally raised bead along the ventral margin of the cephalon, to position behind that of eye and usually extending to genal angle without disappearing into gena or disintegrating into component suture elements.

0: rim incomplete or absent, 1: rim complete, reaching almost fully to the genal angle.

42. † Posterior border spines. Presence of locally prominent concentrations of coarse tubercles or spines along posterolateral margin of the posterior border. 0: absent. 1: present.

43. α†‡* Vincular furrow depth, measured in the medial part of the furrow. 0: wide, shallow, 1: deep, distinct, 2: completely absent medially.

44. α* Vincular notches. Presence of deep notches that extend laterally in the vincular furrow. 0: absent or weakly developed, 1: distinct, very strong with near separate pits.

45. † Terrace lines. Presence of terrace lines or generally elongate sculpture (either fragmentary or continuous) on various regions of dorsal surface of cephalon. 0: absent or nearly so, 1: ventral margin only, 2: on glabella, cheek, and vincular margin.

46. † Doublure sculpture. Nature of the sculpture elements upon doublure, especially its medial portion beneath the glabella. 0: relatively equidimensional, granule dominant, 1: short, broken terrace lines, or granules severely elongated transversely, 2: fully developed, largely continuous terrace lines dominant.

47. †‡ Thorax shape. 0: strong taper, <80% of first segment's total width, 1: weak taper, last segment >80% of first segment's total width.

48. Sculpture on thorax. Presence of granulation or tubercles on axial and pleural furrows. 0: absent, 1: axial rings only, 2: axial rings and pleural furrows, 3: pleural furrows only.

49. Sculpture on axial rings. Characterization of the shape of the granulation or tubercles on the axial rings of the thorax. 0: absent, 1: present, arranged in low, generally rounded projections, 2: present, arranged in sharp, conical projections, 3: granules.

50. ‡ Pygidium–Length/width ratio. Length excluding the articulating half ring. 0: very long, >60%, 1: 50-60%, 2: 40-49%.

51. ‡ Posterior outline of the pygidium. 0: subangular medially, 1: broadly rounded, 2: almost transverse medially.

52. ‡ Position of maximum pygidial width. 0: in front of the midlength (sag.), 1: behind the midlength, 2: at or about the midlength.

53. α†‡* Pygidial axis width. Width (tr.) of pygidial axis across its first axial ring, as expressed as a percentage of total pygidial width (tr.) excluding articulating facets. 0: 25-30%, 1: 31-35%, 2: 36-40%.

54. α†‡* Pygidial axis length. Length (sag.) of pygidial axis from the base of the first axial ring to the tip of its terminal piece, expressed as a percentage of total pygidial length (sag.) from base of first axial ring to pygidial margin. 0: exceptionally short, <78%, 1: short, 78-84%, long, 84-89%, 3: exceptionally long, >89%.

55. †‡ Closure of the pygidial axis. Degree of closure of axial furrows behind the terminus of the pygidial axis and attendant postaxial ridge this sometimes creates. 0: completely distinct or nearly so, 1: incomplete.

56. ‡ Taper of the pygidial axis. Measured as an angle between the axial furrows, excluding the posteriormost region where axis tapers more strongly towards the

terminus. 0: moderate to strong taper, >20°, 1: sub-parallel to weakly tapered, ≤20°.

57. α†‡* Pygidium–interannular ring. Presence or absence of interannular rings behind anteriormost axial rings in the pygidium, as well as their general appearance. 0: strong ring, near level with axial ring in front and sculpted, *Calptaulax glabella,* 1: distinct ring present, *Austerops kermiti*, 2: widened furrow or hint of ring, *Morocops forteyi*.

58. †‡ Number of axial rings. Generalized number of axial rings in the pygidial axis, roughly corresponding to use of 'richly' or 'poorly' segmented in axis descriptors. 0: 7-11 well defined rings, relatively numerous, 1: 4-6 well defined rings, relatively few.

59. † Number of pleural ribs. Generalized number of clear pleural ribs in the pygidium, based on independent inflation, roughly corresponding to use of 'richly' or 'poorly' segmented pleural field descriptions. 0: 2-5 clear ribs, comparatively few, 1: 6-10 clear pleural ribs, comparatively many.

60. α†‡ Depth of pleural furrows. 0: weak, thin pleural furrows; *Struveaspis micromma,* 1: deep, thin pleural furrows, *Austerops kermiti*, 2: deep, steep-sided to medium-wide pleaural furrows, *Morocops* oatus, 3: deep, wide pleural furrows, usually semicircular in profile, *Phacops araw*.

61. α†‡ Depth of the interpleural furrows. 0: weak to completely absent, 1: moderately impressed.

62. †‡* Description of the sculpture located on the pygidium. 0: tubercles developed in pleural ribs and axis, 1: granules, 2: tubercles restricted to axis, 3: granules and

tubercles absent, 4: granules and pits, 5: pits only, 6: tubercles moderately to strongly developed on the pleural border axis.

63. Height of the visual surface of the eye (height of the lenses), as expressed as a percentage of the total height of the eye including sclera and the subocular pad. 0: 60-69%, 1: 70-79%, 2: 80-89%, 3: 90-99%.

64. Length of the palpebral lobe relative to the total length of the cephalon (sag.), expressed as a percentage. 0: <30%, 1: 30-34%, 2: 35-39%, 3: 40-45%, >45%.

65. Width of the palpebral lobe expressed as a percentage of the total width of the ocular platform (axial furrows to the distal margin). 0: <30%, 1: 30-39%, 2: 40-49%, 3: >50%.

66. Presence of tubercles or granules on the palpebral lobe or the palpebral area. 0: absent, 1: granules or sparse tubercles, 2: coarse tubercles or sharp conical projections.

67. Ornamentation on the subocular pads. 0: absent, 1: present.

68. Relative inflation of the glabella. 0: depressed, *Eophacops trapeziceps*, 1: weak to moderated inflation, *Morocops ovatus*, 2: highly inflated, *Viaphacops bombifrons.*

69. Comparison of the length of the medial portion of the preocciptial lobe relative to the lateral length of the L1. 0: medial portion is smaller than the lateral, 1: medial portion is roughly equal to the lateral, 2: medial portion is larger than the lateral portion.

Table A.1—Geologic time series/stage information used to calibrate minimum FAD in BEAST, as well as references for each taxon included in the analysis. Species designated with an asterisk (*) reflect systematic taxonomy that reflects the results of the analyses conducted in Chapter 1.

Species	Publication	Member/ Formation	Event Hor./ Conodont	Age Model (GTS 2011-2012)
Acernaspis becsiensis	Chatterton & Ludvigsen 2004	Becscie Fm.	Base Rhuddanian	443.8
Acernaspis copperi	Chatterton & Ludvigsen 2004	uppermost Jupiter Fm.	Base Telychian	438.5
Acernaspis orestes	Chatterton & Ludvigsen 2004	East Point Mb.	Base Aeronian	440.8
*Alloeldredgeops africanus**	Burton & Eldredge 1974	Crispiforme zone	*australis*	389.23
Ananaspis fecunda	Chlupáč 1977	Kopanina Fm.	base Ludfordian	425.6
Ananaspis feunda aspera	Chlupáč 1977	Kopanina Fm.	base Ludfordian	425.6
Austerops kermiti	McKellar & Chatterton 2009	El Otfal mbr. (Upper)	*australis*	389.23
Austerops salamandar	McKellar & Chatterton 2009	El Otfal mbr.	*australis*	389.23
Boeckops boecki	Chlupáč 1977	base Dvorce-Prokop LS	*E. sulcatus*	410.78
Chotechops hoseri	Chlupáč 1977	Acanthopyge LS	*P. costatus partitus*	393.25
Chotecops auspex	Chlupáč 1977	Choteč Ls	*P. costatus partitus*	393.25
Droptops armatus	Struve, 1995	Bou Dib Fm.	*P. varcus*	386.92
Drotops megalomanicus	Struve, 1995	Bou Dib Fm.	*P. varcus*	386.92
Eldredgeops arkonensis	Stumm, 1953	Arkona Fm.	*timorensis*	387.3
Eldredgeops crassituberculatus	Eldredge, 1972	Delaware (Blue Shale)/ Dundee	*P. costatus costatus*	391.5
Eldredgeops milleri	Eldredge, 1972	Bell Shale	*ensensis*	388.18
Eldredgeops norwoodensis	Eldredge, 1972	Tull Fm.	*semialternans*	385.41
Eldredgeops paucituberculatus	Eldredge, 1972	Plum Brook Shale	*timorensis*	387.3
Eldredgeops rana	Eldredge, 1972	Cardiff (Solsville) Mbr.	*hemianstatus*	387.72
Eldredgeops tindoufensis	Burton & Eldredge 1974	Crispiforme zone	*australis*	389.23
Eophacops bulliceps	Chlupáč 1977	loweer Ludlow	base Gorstian	427.4
Eophacops trapeziceps	Chlupáč 1977	upper Wenlock	base Homerian	430.5
Geesops fabrei	Khaldi et al., 2015	ZGE1	base Daleje Ev.	399.5
Geesops schlotheimi	Schraut 2000, Basse 2006	Ardorf Fm.	*australis*	389.23
Geesops sparsinodosus	Schraut 2000, Basse 2006	Ardorf Fm.	*australis*	389.23
Hypsipariops kowalskii	Strüve, 1992	Freilingen-Schihten	*ensensis*	388.18
Hypsipariops lyncops	Van Viersen, 2007	Loogh Fm.	*hemianstatus*	387.72
Liolophops sublevatus	Strüve, 1970	Freilingen-Schihten	*ensensis*	388.18
Lochkovella misera	Chlupáč 1977	Radotin LS	base Lochovian	419.2
Morocops forteyi	McKellar & Chatterton, 2009	Tazoulati equiv.	*serotinus*?	397.68
Morocops granulops	Chatterton et al. 2006	ZGE1	base Daleje Ev.	399.5
Morocops lebesus	Chatterton et al. 2006	ZGE3	*serotinus*	397.68
Morocops ovatus	McKellar & Chatterton, 2009	ZGE1	base Daleje Ev.	399.5
Morocops spinifer	van Viersen, Holland, Koppka, 2017	ZGE1	base Daleje Ev.	399.5
*Morocops stelcki**	McKellar & Chatterton 2009		*serotinus*?	397.68
Morocops struvei	van Viersen, Holland, Koppka, 2017	ZGE1	base Daleje Ev.	399.5
Morocops torkozensis	van Viersen, Holland, Koppka, 2017	ZGE1	base Daleje Ev.	399.5
Nyterops nyter	Basse, 2006		*hemianstatus*	387.72
Nyterops yeteifliensis	Basse, 2006	Eilenberg mb.	*ensensis*	388.18
Paciphacops birdsongensis	Delo 1940; Eldredge 1973; Campbell 1977	Birdsong Shale	*postwoschmidti*	417.27
Paciphacops cambelli?	Eldredge 1973, Campbell 1977	Haragan Fm.	*postwoschmidti*	417.27
Paciphacops eldredgei?	Eldredge 1973, Campbell 1977	Birdsong shale	*postwoschmidti*	417.27
*Paciphacops invius**	Campbell, 1977	Fittstown Mbr.	*delta*	415.38
Paciphacops logani	Eldredge 1973, Campbell 1977	Kalkberg F.	*postwoschmidti*	417.27
*Paciphacops raymondi**	Eldredge, 1973	Haragan Fm.	*postwoschmidti*	417.27
*Paciphacops wallacki**	Campbell, 1977	Fittstown Mbr.	*delta*	415.38
Pedinopariops lentigifer	Strüve, 1970	Junkerberg Fm.	*kockelianus*	388.97
Pedinopariops superstes	Chlupáč 1977; Crônier et al. 2015	Daleje Shale	base Daleje Ev.	399.5
*Pedinopariops vagabundus**	Strüve, 1992, McKellar &Chatterton 2009	Bou Dib Fm.	*P. varcus*	386.92
Phacopidella glockeri	Chlupáč 1977	upper Wenlock	base Homerian	430.5
Phacops araw	McKellar & Chatterton, 2009	El Otfal mbr. (Upper)	*australis*	389.23
Phacops degener	Chlupáč 1977	upper Zlichov	*E. gronbergi*	404.55
Phacops latifrons	Basse, 2006	Junkerberg Fm.	*kockelianus*	388.97
Phacops major	Chlupáč 1977	upper Zlichov	*E. gronbergi*	404.55
Phacops regius	Chlupáč 1977		base Daleje Ev.	399.5
Reedops bronni	Chlupáč 1977	base Dvorce-Prokop LS	*E. sulcatus*	410.78
Reedops cephalotes	McKellar & Chatterton 2009; Halamski & Balinski 2018	Kess-Kess Mounds	*P. inversus*	400.86
Reedops decorus	Chlupáč 1977	Zlichov Fm.	*E. excavatus*	406.11
Reedops modestus	Chlupáč 1977	upper Zlichov	*E. gronbergi*	404.55
*Smithops alpenensis**	Eldredge, 1972	Bell Shale	*hemianstatus*	387.7
*Smithops iowensis**	Eldredge, 1972	Dock Street	*rheanus*	386.92
*Smithops southwerthi**	Eldredge, 1972	Hungry Hollow Fm.	*timorensis*	387.3
Struveaspis fugitiva	Chlupáč 1977	Choteč LS	*P. costatus partitus*	393.25
Struveaspis micromma	Chlupáč 1977	lower Trebotov LS	*P. inversus*	400.86
Viaphacops bombifrons	Eldredge, 1973	Onondaga Fm.	*P. costatus costatus*	391.5
Viaphacops stummi	Eldredge, 1973	Bois Blanc	*P. costatus costatus*	391.5

Table A.2—The fully discretized matrix used in BEAST and PAUP*.

Species/ Character	1	2	3	4	5	6	7	8	9	10	11	12	13	14	15	16	17	18	19	20	21	22	23	24	25	26	27	28	29	30	31	32	33	34	35
Acernaspis becsiensis	1	2	1	0	0	0	2	1	1	0	1	1	0	1	1	0	0	0	0	0	1	1	0	1	1	1	0	0	0	1	1	1	1	0	0
Acernaspis copperi	0	1	1	0	0	0	0	2	1	0	1	1	0	1	1	0	0	0	0	0	1	0	0	0	1	0	0	0	1	1	1	1	0	0	0
Acernaspis orestes	1	1	1	0	0	0	1	0	2	1	1	1	0	4	1	0	0	1	0	0	1	0	0	0	1	0	0	0	2	1	1	1	0	0	0
*Alloeldredgeops africanus**	2	2	1	1	3	1	2	0	0	2	1	1	0	4	1	2	1	1	2	2	1	0	0	0	1	1	0	2	2	0	2	0	3	0	0
Ananaspis fecunda	0	1	1	0	2	1	0	0	2	2	1	0	1	0	1	1	0	1	0	2	1	0	0	1	1	2	2	3	3	0	1	1	0	0	0
Ananaspis feunda aspera	1	1	0	0	1	1	0	0	2	1	1	1	1	1	2	1	0	1	0	0	1	0	0	2	1	1	2	4	3	0	1	1	0	0	0
Austerops kermiti	2	1	0	2	0	1	0	1	0	0	0	0	1	2	1	1	0	1	2	4	1	2	2	0	0	0	0	2	5	1	0	1	0	0	0
Austerops salamandar	2	2	1	2	0	1	2	1	0	0	0	0	1	2	2	1	0	1	2	4	1	1	1	0	0	0	0	2	3	0	0	1	0	0	0
Boeckops boecki	1	1	1	0	0	2	0	2	2	1	1	0	0	4	2	0	0	1	2	4	1	1	?	1	0	0	0	4	4	0	0	1	0	0	0
Chotecops auspex	2	2	1	0	1	2	2	0	0	0	0	0	1	2	0	0	1	1	1	?	1	0	1	2	0	1	2	0	2	0	0	1	0	0	0
Chotecops hoseri	0	1	1	0	1	2	1	1	1	1	0	1	0	2	1	1	1	1	1	1	1	0	1	1	0	1	2	2	2	0	1	1	0	0	0
Droptops armatus	0	1	0	1	3	2	0	1	0	2	1	1	0	2	0	2	1	0	0	1	1	2	0	1	1	1	2	2	3	0	1	0	3	1	1
Drotops megalomanicus	1	2	1	1	3	2	1	1	0	2	1	1	0	2	0	2	1	0	1	?	1	2	0	1	1	1	2	2	2	0	1	0	3	1	1
Eldredgeops arkonensis	0	2	0	1	3	1	0	1	0	1	1	0	0	2	0	2	1	0	1	?	1	0	?	0	0	0	0	2	3	0	0	1	0	0	0
Eldredgeops crassituberculatus	1	2	1	1	3	1	1	1	0	0	1	0	0	2	1	2	1	1	1	?	1	0	1	0	0	0	0	2	2	0	0	0	2	0	0
Eldredgeops milleri	0	1	0	1	3	1	0	1	0	0	1	0	0	2	0	2	1	1	1	3	1	0	1	0	0	1	0	2	5	0	0	1	0	0	0
Eldredgeops norwoodensis	0	1	1	1	3	1	0	1	0	2	1	0	0	2	1	2	1	1	1	?	1	1	0	0	0	0	0	0	2	0	1	0	2	0	0
Eldredgeops paucituberculatus	0	1	1	2	4	1	1	1	0	1	1	0	0	2	1	2	1	1	1	?	1	0	0	0	0	0	0	0	?	0	0	0	2	0	0
Eldredgeops rana	0	2	1	1	3	1	1	1	0	2	1	0	0	2	1	2	1	1	1	?	1	1	0	0	0	0	0	1	2	0	1	0	2	0	1
Eldredgeops tindoufensis	?	?	0	1	3	1	?	1	1	1	1	0	0	2	1	2	1	0	1	1	1	0	0	0	1	0	2	5	1	0	1	0	0	0	0
Eophacops bulliceps	2	2	0	2	0	0	1	1	0	0	0	0	1	5	1	0	0	1	0	0	1	0	0	1	0	0	1	4	1	1	1	1	0	0	0
Eophacops trapeziceps	2	2	0	2	0	0	0	1	0	0	0	0	1	5	2	1	0	1	0	1	1	0	0	1	0	0	1	4	2	1	1	1	0	0	0
Geesops fabrei	2	1	0	1	4	0	2	1	1	1	1	1	0	1	1	0	1	1	0	3	1	0	0	0	1	1	0	3	2	0	0	0	1	0	0
Geesops schlotheimi	1	1	1	1	4	1	1	1	1	1	1	1	0	4	1	2	1	0	1	2	1	1	0	0	0	1	0	2	2	0	1	0	2	0	0
Geesops spariodosus	1	1	0	1	4	1	0	2	1	1	1	1	0	4	1	2	0	0	1	0	1	1	0	0	0	1	0	2	2	0	1	0	2	0	0
Hypsipariops kowalskii	1	2	0	1	3	1	0	0	1	1	1	1	1	2	1	2	1	0	0	2	1	0	1	1	1	1	0	2	3	1	1	0	2	0	0
Hypsipariops lyncops	0	1	1	1	3	1	1	1	1	2	1	1	1	2	1	2	1	0	1	1	1	0	0	0	0	1	0	2	3	0	2	0	2	0	0
Liolophops sublevatus	1	2	0	0	3	1	1	1	1	1	1	1	1	4	1	2	1	0	0	1	1	0	1	0	0	1	0	2	2	0	1	0	2	0	0
Lochkovella misera	1	1	1	0	0	2	0	2	1	1	0	1	0	2	1	1	1	1	1	0	1	0	?	2	0	0	2	0	2	0	0	1	0	0	0
Morocops forteyi	2	3	0	0	2	1	3	2	2	2	1	0	0	0	1	2	0	0	0	0	1	0	0	1	1	0	2	2	0	0	1	1	0	1	1
Morocops granulops	1	2	0	0	2	1	0	2	2	2	1	0	0	1	2	2	1	1	0	2	1	1	0	1	0	0	0	2	3	2	0	0	1	1	0	1
Morocops lebesus	3	2	1	0	1	1	1	1	0	0	1	0	0	1	2	1	0	1	0	1	1	2	0	0	0	0	0	3	2	0	1	1	1	0	1
Morocops ovatus	0	2	0	0	2	1	1	2	2	2	1	0	0	0	1	2	0	1	0	1	1	1	0	1	0	0	2	3	2	1	1	1	0	0	1
Morocops spinifer	1	3	1	0	2	1	2	2	2	2	1	1	1	1	1	2	1	1	0	1	1	0	0	1	1	0	2	2	0	0	1	1	0	0	1
*Morocops stelcki**	3	3	1	0	1	1	3	2	2	2	1	1	0	0	2	1	0	0	1	1	1	0	0	0	1	0	0	2	4	0	0	1	0	0	0
Morocops struvei	1	1	1	0	2	1	1	2	2	1	1	1	0	1	1	2	1	0	0	2	1	1	0	0	1	1	2	3	2	0	1	1	0	0	0
Morocops torkozensis	2	3	0	0	2	1	2	0	2	2	1	1	0	1	1	2	0	0	0	0	1	1	0	1	1	0	2	2	0	0	1	1	0	1	1
Nyterops nyter	2	2	1	1	4	1	1	0	1	2	1	1	0	4	1	2	1	0	1	?	1	1	2	0	0	1	1	0	2	0	1	1	2	0	0
Nyterops yeteifliensis	3	3	0	1	4	1	1	0	1	2	1	1	0	4	1	2	1	0	1	?	1	1	0	0	1	1	1	0	0	0	0	0	2	0	0
Paciphacops birdsongensis	1	2	1	1	2	2	1	2	2	2	1	1	0	4	2	0	0	1	0	0	1	2	0	1	1	1	0	0	0	1	2	0	2	0	0
Paciphacops cambelli	1	2	1	1	2	2	2	2	2	2	1	1	0	4	2	0	0	1	0	0	1	2	0	1	1	1	0	0	0	1	2	0	2	0	0
Paciphacops eldredgei	2	2	1	1	2	2	2	1	1	2	1	0	0	4	1	1	0	1	0	0	1	2	0	1	1	1	0	1	1	1	2	0	1	0	0
*Paciphacops invius**	0	1	1	1	2	1	1	2	1	1	1	1	1	2	2	1	0	1	0	0	1	2	0	2	1	2	2	0	2	0	2	1	0	0	0
Paciphacops logani	1	2	0	1	2	2	1	1	2	2	1	0	0	5	1	0	0	1	0	0	1	2	0	1	1	?	0	1	2	1	2	1	1	0	0
*Paciphacops raymondi**	0	1	0	1	2	2	1	1	0	1	1	1	0	5	2	0	0	1	0	0	1	1	0	0	1	2	1	0	1	1	1	0	3	0	0
*Paciphacops wallacki**	1	1	1	1	2	1	1	2	1	1	1	1	0	5	0	1	0	1	0	0	1	0	0	1	1	2	0	1	2	0	2	1	0	0	0
Pedinopariops lentigifer	1	2	0	1	3	2	0	1	0	2	1	1	1	4	2	1	1	0	1	?	1	2	1	1	0	1	0	2	3	0	1	0	0	0	1
*Pedinopariops vagabundus**	0	0	2	0	2	1	0	1	0	2	1	1	1	4	1	2	1	0	0	0	1	2	0	1	1	1	0	2	2	1	1	0	2	0	0
*Phacopidella glockeri**	1	1	0	2	0	0	0	0	2	1	1	1	1	2	1	2	0	1	0	0	1	0	0	2	0	0	0	4	2	0	0	1	0	0	0
Phacops araw	2	2	0	1	4	0	2	1	1	2	1	0	0	1	2	0	0	1	1	?	1	1	1	0	0	1	0	0	0	0	1	0	2	0	0
*Phacops degener**	2	2	0	1	2	1	1	2	1	2	1	1	0	1	1	1	1	1	1	1	1	0	0	1	1	1	0	4	2	0	1	1	0	0	0
Phacops latifrons	1	2	1	2	3	0	1	2	1	2	1	1	0	1	0	2	1	0	1	2	1	0	2	1	1	1	0	0	0	0	1	0	3	0	1
Phacops major	1	2	0	2	2	1	1	0	?	2	1	0	1	2	2	1	1	0	1	2	1	0	0	1	1	1	0	3	1	0	1	0	2	0	1
Phacops regius	1	2	1	1	2	1	1	0	1	2	1	1	0	1	2	2	1	0	1	?	1	0	?	1	1	1	0	3	4	0	1	0	0	0	0
Reedops bronni	3	2	0	0	0	2	2	1	2	2	1	0	0	4	2	1	0	1	0	0	1	2	0	2	1	0	2	0	4	0	0	1	0	0	0
Reedops cephalotes	3	2	0	0	0	2	1	0	2	2	1	0	0	4	1	1	0	1	2	4	1	2	1	2	0	0	0	5	4	0	1	1	0	0	0
Reedops decorus	2	2	0	0	0	2	2	2	2	0	1	0	0	3	1	1	0	1	1	0	1	2	0	2	0	0	0	5	4	0	1	1	0	0	0
Reedops modestus	3	2	1	0	0	1	2	2	2	0	1	0	0	4	1	1	0	1	1	0	1	2	0	1	0	0	0	5	4	0	0	1	0	0	0
*Smithops alpenensis**	1	3	0	0	2	0	1	1	0	2	1	1	1	3	1	0	1	0	0	2	1	1	?	1	1	0	1	0	0	1	2	0	3	0	1
*Smithops iowensis**	?	?	1	0	2	1	?	1	0	2	1	1	1	3	1	0	0	0	0	3	1	1	?	1	1	0	1	0	0	1	2	0	3	0	1
*Smithops southwerthi**	1	2	0	0	2	0	0	0	0	2	1	1	0	3	1	0	0	1	1	?	1	0	?	1	1	0	1	0	1	1	2	0	3	0	1
Struveaspis fugitiva	1	1	0	2	0	0	0	0	0	0	0	0	0	3	0	0	0	2	2	4	1	0	0	2	0	1	2	0	3	0	0	1	0	0	0
Struveaspis micromma	3	2	0	2	0	0	1	1	0	0	0	0	1	3	1	0	0	1	2	4	1	2	0	2	0	0	2	0	0	0	0	1	0	0	0
Viaphacops bombifrons	0	1	0	0	2	2	0	0	1	2	0	0	0	5	1	0	0	1	1	?	1	2	?	1	0	?	0	0	1	1	2	?	3	0	1
Viaphacops stummi	0	2	0	0	2	2	0	1	0	2	0	0	0	5	1	0	0	1	1	?	1	2	0	1	0	0	0	0	0	1	2	0	3	0	0
Calyptaulax callicephala	1	0	1	0	2	0	0	0	0	1	1	1	1	4	2	1	0	0	0	0	0	2	?	0	1	0	0	5	4	?	2	1	0	0	0
Calyptaulax glabella	1	0	1	0	0	0	0	1	1	1	1	1	0	4	1	1	0	0	0	0	0	2	?	0	1	0	0	5	6	?	0	1	0	0	0
Eomonorachus intermedius	2	0	1	0	1	0	0	1	0	0	1	1	0	4	2	0	0	0	0	0	0	2	?	1	1	0	0	1	4	?	?	1	0	0	0
Podowrinella christiei	2	0	2	0	?	0	0	1	0	1	1	1	1	4	0	?	0	0	0	0	0	2	1	0	?	0	0	3	2	?	2	1	1	0	0
Podowrinella straitonensis	2	1	0	0	0	0	0	0	0	1	1	1	0	1	2	0	0	0	0	0	0	2	?	0	1	?	0	2	3	?	0	1	1	0	0

Table A.2 (cont.)—The fully discretized matrix used in BEAST and PAUP*.

Species/ Character	36	37	38	39	40	41	42	43	44	45	46	47	48	49	50	51	52	53	54	55	56	57	58	59	60	61	62	63	64	65	66	67	68	69
Acernaspis becsiensis	1	1	2	0	3	0	0	0	1	0	0	?	1	3	0	1	2	2	1	1	0	0	1	0	1	0	1	0	2	1	0	0	1	2
Acernaspis copperi	1	1	2	0	2	0	0	0	1	0	0	0	0	0	2	1	1	2	2	1	0	0	1	0	0	0	1	0	3	1	0	0	1	2
Acernaspis orestes	1	1	2	0	3	0	0	0	1	0	0	0	0	0	0	1	2	2	1	1	0	0	1	0	1	1	1	1	4	1	0	0	1	2
*Alloeldredgeops africanus**	3	0	2	3	0	1	0	1	1	0	?	?	0	0	1	1	0	2	3	0	0	1	0	1	3	0	3	0	2	0	1	0	1	2
Ananaspis fecunda	1	1	3	3	3	0	0	0	?	0	?	1	0	0	2	2	0	0	1	0	1	0	0	0	3	1	3	1	4	0	2	1	1	1
Ananaspis feunda aspera	1	1	2	0	3	0	0	0	0	0	0	1	0	0	1	2	0	0	1	0	1	0	0	0	3	1	3	2	0	1	2	0	1	2
Austerops kermiti	1	0	2	4	1	0	0	2	0	1	2	?	0	0	1	1	0	1	2	1	1	0	1	0	1	1	5	3	3	1	0	0	1	0
Austerops salamandar	1	0	3	4	1	0	0	1	0	1	2	?	0	0	1	1	2	1	3	1	1	0	1	0	1	0	3	3	3	1	0	0	1	1
Boeckops boecki	1	0	2	2	2	0	1	0	0	0	1	?	1	3	1	2	2	2	1	1	0	0	1	0	1	1	1	1	0	0	1	0	2	0
Chotecops auspex	1	0	3	0	4	0	0	0	?	0	1	0	0	0	2	2	2	0	0	1	1	0	1	0	1	0	5	3	2	0	0	0	1	1
Chotecops hoseri	2	0	2	3	1	0	0	0	?	0	1	0	1	3	1	2	2	0	3	2	1	0	0	0	3	1	5	2	3	0	1	0	1	1
Droptops armatus	3	0	2	1	4	1	1	1	1	0	?	1	2	2	0	0	0	1	3	0	0	0	0	1	3	1	0	1	2	1	2	1	1	1
Drotops megalomanicus	3	0	2	1	4	1	1	1	1	0	?	1	2	1	0	0	0	1	3	0	0	0	0	1	3	1	0	2	2	2	2	1	1	1
Eldredgeops arkonensis	1	0	2	0	4	1	0	1	1	0	?	?	0	0	2	1	2	2	3	0	1	1	0	0	2	0	2	3	4	1	1	0	1	1
Eldredgeops crassituberculatus	1	0	2	0	4	1	0	1	1	0	2	1	1	1	2	1	0	0	3	0	1	1	0	1	2	1	2	3	3	1	2	0	1	1
Eldredgeops milleri	1	0	2	3	4	1	0	1	1	0	2	1	0	0	1	1	2	0	3	1	1	1	0	0	2	0	2	3	4	1	1	0	1	1
Eldredgeops norwoodensis	2	0	2	0	4	1	0	1	1	0	?	0	1	1	1	1	2	0	3	?	1	1	0	1	2	0	2	3	4	1	2	0	1	1
Eldredgeops paucituberculatus	1	0	2	3	4	1	0	?	?	0	?	1	1	1	1	1	2	0	2	0	1	1	0	1	2	0	2	2	4	1	1	0	1	2
Eldredgeops rana	2	0	2	1	4	1	0	1	1	0	?	?	2	1	1	1	2	0	2	0	1	1	0	1	2	0	0	2	3	1	2	0	1	1
Eldredgeops tindoufensis	1	0	2	0	4	1	0	1	1	0	?	?	1	1	?	?	?	?	?	1	?	?	0	1	?	?	1	2	2	1	2	0	1	1
Eophacops bulliceps	0	1	2	5	0	0	0	2	0	0	0	?	0	0	0	1	2	1	1	0	1	0	0	0	1	1	1	0	3	1	0	0	0	1
Eophacops trapeziceps	0	0	2	5	0	0	0	2	0	0	0	1	0	0	0	1	2	2	1	0	1	0	1	0	0	1	1	2	2	1	0	0	0	1
Geesops fabrei	2	0	3	3	4	1	0	1	1	0	2	?	1	1	2	1	2	0	2	0	1	1	1	1	2	0	1	2	2	2	1	0	1	1
Geesops schlotheimi	2	0	3	3	4	1	0	1	1	0	2	0	1	1	1	1	2	2	3	0	1	0	1	0	2	0	1	0	2	1	1	0	1	2
Geesops spariodosus	2	0	3	3	4	1	0	1	1	0	?	0	0	0	1	1	1	1	2	0	1	0	1	0	2	0	1	1	2	1	1	0	1	2
Hypsipariops kowalskii	2	0	2	3	4	1	0	1	?	0	?	?	?	?	0	1	1	0	2	?	1	1	0	1	3	0	4	1	3	1	2	0	1	2
Hypsipariops lyncops	2	0	2	3	4	1	0	?	?	0	?	?	1	3	2	1	2	0	3	0	1	0	0	0	2	0	1	1	2	0	2	0	1	2
Liolophops sublevatus	2	0	2	5	2	1	0	1	1	0	2	?	?	?	0	1	2	0	2	1	1	1	0	1	3	0	5	2	3	1	1	0	1	1
Lochkovella misera	1	1	2	1	3	0	0	0	1	0	0	?	?	?	2	1	2	0	1	0	0	0	0	1	2	1	1	2	0	0	1	0	1	1
Morocops forteyi	0	1	3	2	3	1	1	1	1	0	1	?	2	1	2	1	0	1	2	0	0	1	0	0	2	1	0	1	1	0	2	1	1	1
Morocops granulops	1	1	3	2	3	1	1	1	1	1	1	1	2	3	1	2	2	0	1	0	0	0	0	0	2	1	1	2	2	1	2	1	1	1
Morocops lebesus	2	0	2	2	4	1	1	0	1	0	2	?	2	3	1	1	2	0	0	0	0	0	1	0	2	0	1	1	2	2	2	1	1	1
Morocops ovatus	0	1	3	2	4	1	1	1	?	1	?	1	2	3	1	2	2	2	2	0	0	1	0	0	2	0	0	0	4	1	2	1	1	1
Morocops spinifer	0	1	3	2	4	1	1	1	1	0	?	?	2	1	1	2	2	1	1	0	0	0	0	0	2	1	0	1	2	1	2	1	1	1
*Morocops stelcki**	1	0	2	2	3	0	1	1	1	0	2	?	2	3	1	2	2	2	2	1	0	0	0	0	1	1	0	2	1	0	1	1	1	0
Morocops struvei	0	1	3	2	3	1	1	?	?	0	?	?	2	3	?	?	?	?	?	?	?	?	?	?	?	?	?	1	3	1	2	1	1	1
Morocops torkozensis	0	1	3	1	3	1	1	1	1	0	1	?	2	1	?	?	?	?	?	?	?	1	0	?	2	1	0	1	2	0	2	1	1	1
Nyterops nyter	2	0	2	3	4	1	0	1	1	0	2	?	0	0	1	0	0	0	2	0	1	1	0	1	2	0	3	0	3	1	1	0	1	2
Nyterops yeteifliensis	3	0	2	1	4	1	1	1	1	0	2	1	0	0	?	?	0	0	2	0	?	1	0	0	2	0	3	1	2	1	1	0	1	2
Paciphacops birdsongensis	3	1	2	0	3	0	0	?	?	0	?	0	0	0	?	1	?	?	2	0	0	0	0	1	2	1	3	0	2	1	2	0	2	1
Paciphacops cambelli	3	1	2	5	3	0	0	1	1	0	0	0	0	0	1	1	2	1	2	0	0	0	0	0	3	1	3	0	2	1	2	0	2	1
Paciphacops eldredgei	2	1	2	0	2	0	0	1	1	1	0	?	0	0	2	1	2	2	3	0	0	0	0	1	2	1	1	1	1	1	1	0	2	1
*Paciphacops invius**	1	1	3	0	3	0	0	0	0	0	0	?	2	1	0	1	0	2	2	0	0	0	0	1	2	1	3	1	2	1	2	0	1	1
Paciphacops logani	2	1	1	5	3	0	0	1	1	0	?	0	0	0	2	1	2	2	1	0	0	0	0	1	3	1	3	1	1	1	2	0	2	1
*Paciphacops raymondi**	2	1	2	0	2	0	0	1	0	0	0	?	?	?	?	?	?	?	?	?	?	?	?	?	?	?	?	1	3	2	2	0	2	2
*Paciphacops wallacki**	0	1	3	0	3	0	0	0	0	0	1	?	?	3	1	1	0	2	2	0	1	0	0	1	2	1	3	1	1	2	2	0	1	1
Pedinopariops lentigifer	2	1	2	2	4	1	0	?	?	1	?	?	1	1	2	1	0	0	3	1	0	0	0	1	2	0	2	0	2	0	2	1	1	1
*Pedinopariops vagabundus**	2	1	2	3	4	1	1	1	1	0	2	1	2	1	1	1	0	0	3	1	0	0	0	1	2	1	0	1	2	1	2	1	1	1
*Phacopidella glockeri**	2	0	5	1	0	0	0	2	0	0	0	1	0	0	1	1	0	0	2	0	0	1	0	1	0	1	3	0	1	1	0	0	0	1
Phacops araw	2	0	3	2	3	0	0	0	1	1	2	?	0	0	2	1	2	1	3	0	0	1	0	0	2	0	5	1	1	1	2	0	1	2
*Phacops degener**	2	0	3	2	3	0	0	0	1	0	0	?	?	1	0	1	2	1	2	0	0	0	0	0	2	0	0	1	3	3	2	1	1	1
Phacops latifrons	2	1	3	3	3	0	0	1	1	1	2	?	0	0	?	?	?	?	?	?	?	1	?	?	?	?	?	0	1	0	2	1	1	1
Phacops major	2	1	2	3	4	0	0	0	1	1	?	?	?	?	1	1	2	1	2	0	0	0	0	1	2	0	0	0	1	0	2	1	1	1
Phacops regius	1	1	2	1	0	0	0,1	1	1	0	2	?	?	?	1	1	2	1	2	0	0	0	0	1	2	0	0	1	2	1	2	1	1	1
Reedops bronni	1	1	2	5	4	0	0	0	0	0	1	0	1	3	1	2	2	0	3	1	0	?	1	0	0	0	3	3	0	0	1	1	2	1
Reedops cephalotes	2	1	3	0	3	1	0	2	0	1	2	1	1	3	2	1	0	1	1	1	0	0	1	0	0	0	1	1	0	0	1	1	2	0
Reedops decorus	2	1	1	5	3	0	0	2	0	0	0	1	0	0	1	1	0	0	3	0	0	0	1	0	0	1	3	1	0	0	0	0	2	0
Reedops modestus	1	1	2	0	4	0	0	2	0	0	1	?	1	3	1	1	0	0	1	0	0	0	0	0	2	1	1	2	1	2	1	0	2	1
*Smithops alpenensis**	2	1	2	2	3	0	1	?	?	0	?	1	0	0	1	2	2	0	0	1	1	0	0	1	3	1	0	1	0	0	1	1	1	2
*Smithops iowensis**	2	1	2	2	3	0	1	?	?	1	?	?	2	1	1	2	2	0	2	1	1	0	0	0	3	1	0	1	2	2	1	1	1	2
*Smithops southwerthi**	3	1	3	2	3	0	0	?	?	0	?	?	0	0	2	1	0	0	?	1	1	0	0	1	3	1	0	1	2	1	1	1	1	2
Struveaspis fugitiva	1	1	3	5	1	0	0	?	?	0	?	1	0	0	0	1	0	0	3	0	1	?	0	1	0	0	5	3	0	0	0	0	0	0
Struveaspis micromma	1	1	3	5	1	0	0	?	?	0	?	1	0	0	?	1	0	?	1	0	1	?	?	?	0	0	5	0	0	0	0	0	0	0
Viaphacops bombifrons	?	1	0	5	?	0	0	0	0	1	1	?	0	0	1	2	2	2	3	1	0	0	0	1	3	1	3	?	2	0	0	0	2	1
Viaphacops stummi	3	1	0	5	3	0	0	1	1	0	0	?	?	?	1	2	1	0	2	1	1	0	1	0	0	1	1	1	2	0	2	0	2	1
Calyptaulax callicephala	3	0	2	5	3	0	0	2	0	0	0	0	0	0	0	0	0	0	3	0	1	0	0	1	3	1	1	1	3	0	1	1	0	1
Calyptaulax glabella	1	0	2	5	3	0	0	2	0	?	?	?	0	0	0	0	0	1	1	0	0	0	0	1	3	1	1	3	4	0	0	0	0	1
Eomonorachus intermedius	?	0	0	5	3	0	0	2	0	?	?	0	0	0	0	0	0	2	3	0	0	0	0	1	3	1	1	?	1	0	0	0	0	2
Podowrinella christiei	3	1	2	5	3	0	0	2	0	?	?	?	?	?	0	0	0	2	2	0	0	0	0	0	3	1	1	?	2	0	0	0	0	1
Podowrinella straitonensis	1	0	2	5	3	0	0	2	0	?	?	?	?	?	0	0	0	2	3	0	0	0	0	0	3	1	4	2	3	0	0	0	0	2

APPENDIX B:
SUPPORTING DOCUMENTATION FOR CHAPTER TWO

For supporting mathematic theory behind determining fluctuating asymmetry by maximum likelihood estimation, see Young (2007). The following equations and definitions are adapted from that text.

Definitions:

μ= population mean liability for a bilateral character
GE_i=$N(0, \sigma^2{}_{GE})$ genetic and/or environmental effect on the liability for organism i
L_i= organismic liability for the character for organism i=μ+GE_i
$A_{ij=}$ independent $N(0, \sigma^2{}_A)$ developmental disturbance on side j of organism
L_{ij}= realized liability for the character on side j of organism i=L_i+A_{ij}
R_{ij}= random amount by which Lij is rounded to an integer value
Y_{ij}= true character state on side j of organism i=L_i+A_{ij}+R_{ij}
E_{ij}= discrete counting error on side j of organism i
O_{ij}= observed count of character on side j of organism i= Y_{ij}+E_{ij}

When calculating the maximum likelihood using replicant counts, distributions of count differences are first compared to candidate discrete distributions. The first distribution used was a geometric distribution, where $0 \leq q \leq 1$ and:

$$\Pr(E_{ij} = x) \begin{matrix} = q & \text{for } x=0 \\ = \frac{q(1-q)^{|x|}}{2} & \text{for } x=-\infty,\ldots,-3,-2,-1,1,2,3,\ldots,\infty \end{matrix} \quad \text{(B. 1)}$$

The second candidate distribution selected was a Poisson distribution, where $\lambda \geq 0$ and:

$$\Pr(E_{ij} = x) \begin{matrix} = \exp(-\lambda) & \text{for } x=0 \\ = \frac{\exp(-\lambda)\lambda^{|x|}}{2|x|!} & \text{for } x=-\infty,\ldots,-3,-2,-1,1,2,3,\ldots,\infty \end{matrix} \quad \text{(B. 2)}$$

Maximum likelihood estimates for the counting error parameter are found by determining the value of q or λ that minimizes:

LL_l (q or $\lambda|d$)

$$= -\sum_{i=1}^{N} \sum_{k=1}^{K_i-1} \log\Big(\sum_{x=-\infty}^{\infty} \Pr(E_{ij1} = x | q \text{ or } \lambda) \Pr\,(E_{ij2} = x - d_{ijk} | q \text{ or } \lambda)\Big) \quad \text{(B. 3)}$$

Where $d_{ijk} = o_{ijk+1} - o_{ijk}$, which produces $2(K_i - 1)$ values for d_{ijk} for an organism with K_i replicated counts.

Once the count error distribution and its parameter are estimated, the maximum likelihood estimates for $\hat{\mu}$ (trait mean), $\hat{\sigma}_{GE}$ (symmetric phenotypic variation), and $\hat{\sigma}_A$ (fluctuating asymmetry) are found by minimizing the following weighted log-likelihood:

$LL_2(\mu, \sigma_{GE}, \sigma_A | o_r, o_l, \hat{q} \text{ or } \hat{\lambda})$

$$= -\sum_{i=1}^{N}\sum_{k=1}^{K_i}\frac{1}{K_i}\log[\sum_{e_{il}=-\infty}^{o_{il}}\sum_{e_{ir}=-\infty}^{o_{ir}}\Pr\left(E_{irk} = e_{irk0}|\hat{q} \text{ or } \hat{\lambda}\right) \text{x} \Pr\left(E_{ilk} = e_{ilk}|\hat{q} \text{ or } \hat{\lambda}\right) \text{x} \Pr(Y_{ir}$$

$$= o_{irk} - e_{irk}, Y_{il} = o_{ilk} - e_{ilk}|\mu, \sigma_{GE}, \sigma_A)] \text{ (B. 4)}$$

Comparisons of populations (species) were conducted using a log-likelihood ratio test and multi-model inference using Akaike weights (recommended by Young, 2007, Young 2021 [personal communication]):

Log likelihood ratio test:

$$G = 2\ln L = 2\ln\left(\frac{Likelihood_1}{Likelihood_2}\right) \text{(Sokal \& Rohlf, 1995)(B.5)}$$

Corrected Akaike Information Criterion:

$$= 2K - 2(\ln(likelihood)) \text{ x}\frac{2k(k+1)}{(n-k-1)} \text{ (Burham \& Anderson, 2002)(B. 6)}$$

Difference between AIC_c scores:

$$\Delta AIC = AIC_{ci} - AIC_{c\,min} \text{ (B. 7)}$$

TABLES—

ID	Group	DV1 Robs1	DV1 Lobs1	DV1 Robs2	DV1 Lobs2	DV2 Robs1	DV2 Lobs1	DV2 Robs2	DV2 Lobs2	DV3 Robs1	DV3 Lobs1	DV3 Robs2	DV3 Lobs2	DV4 Robs1	DV4 Lobs1	DV4 Robs2	DV4 Lobs2	DV5 Robs1	DV5 Lobs1	DV5 Robs2	DV5 Lobs2	DV6 Robs1	DV6 Lobs1	DV6 Robs2	DV6 Lobs2
AMNH7411	crassituberculatus	.	.	.	.	.	.	.	.	4	4	4	4	6	6	6	6	5	5	5	5	6	6	6	6
AMNH74874b	crassituberculatus	4	4	4	4	5	5	5	5	6	6	6	6	6	6	6	6	6	6	6	6	5	6	5	6
AMNH74878c	crassituberculatus	.	.	.	.	5	5	5	5	6	6	6	6	5	5	5	5	6	6	6	6	4	6	4	6
AMNH74878d	crassituberculatus	2	2	2	2	4	4	4	4	5	5	5	5	5	5	5	5	6	6	6	6	5	5	5	5
AMNH74880	crassituberculatus	3	3	3	3	5	5	5	5	6	6	6	6	6	6	6	6	6	7	6	7	6	6	6	6
AMNH74983	crassituberculatus	4	4	4	4	5	4	5	4	6	6	6	6	6	6	6	6	6	6	6	6	6	6	6	6
BGSU4037a	crassituberculatus	.	.	.	.	.	.	.	.	.	.	.	.	3	4	3	4	4	5	4	5	4	5	4	5
BGSU4038d	crassituberculatus	3	3	3	3	4	4	4	4	5	5	5	5	5	4	5	4	5	5	5	5	5	5	5	5
BGSU4057g	crassituberculatus	4	4	4	4	5	5	5	5	6	6	6	6	5	5	5	5	6	5	6	5	5	6	5	6
PE25589	crassituberculatus	3	3	3	3	5	5	5	5	6	5	6	5	5	5	5	5	6	6	6	6	5	5	5	5
PE25589b	crassituberculatus	4	3	4	3	5	5	5	5	6	5	6	5	5	5	5	5	6	6	6	6	5	5	5	5
PE25592d	crassituberculatus	3	3	3	3	5	5	5	5	6	6	6	6	5	5	5	5	6	6	6	6	6	6	6	6
PE9516a	crassituberculatus	.	.	.	.	4	4	4	4	6	6	6	6	5	5	5	5	6	6	6	6	5	5	5	5
PE9516b	crassituberculatus	3	3	3	3	5	5	5	5	6	6	6	6	5	5	5	5	6	6	6	6	6	6	6	6
PE9516c	crassituberculatus	3	3	3	3	5	4	5	4	6	6	6	6	5	5	5	5	6	6	6	6	6	6	6	6
PE9518	crassituberculatus	4	4	4	4	5	5	5	5	6	6	6	6	5	5	5	5	6	6	6	6	6	6	6	6
AMNH74105a	crassituberculatus	.	.	.	.	4	4	4	4	5	5	5	5	5	5	5	5	6	5	6	5	5	5	5	5
BGSU4049a	crassituberculatus	3	3	3	3	4	5	4	5	6	6	6	6	5	5	5	5	6	6	6	6	6	4	6	4
AMNH74085	milleri	5	5	5	5	6	6	6	6	7	8	7	8	8	8	8	8	9	9	9	9	8	8	8	8
AMNH74874a	milleri	5	4	5	4	6	6	6	6	8	8	8	8	8	8	8	8	8	8	8	8	8	8	8	8
AMNH74874c	milleri	4	4	4	4	5	5	5	5	7	7	7	7	7	7	7	7	8	8	8	8	7	7	7	7
AMNH74874d	milleri	5	5	5	5	6	6	6	6	7	7	7	7	7	7	7	7	7	8	7	8	8	8	8	8
AMNH74875a	milleri	5	5	5	5	5	7	5	7	7	8	7	8	6	7	6	7	7	8	7	8	6	8	6	8
AMNH74875b	milleri	5	5	5	5	7	7	7	7	8	8	8	8	8	8	8	8	8	8	8	8	9	8	9	8
AMNH74876c	milleri	5	5	5	5	6	6	6	6	7	7	7	7	7	7	7	7	8	8	8	8	8	8	8	8
AMNH74964	milleri	5	4	5	4	5	5	5	5	6	6	6	6	6	6	6	6	6	6	6	6	6	6	6	6
AMNH74982	milleri	5	5	5	5	6	6	6	6	7	7	7	7	7	7	7	7	7	8	7	8	8	7	8	7
AMNH75037	milleri	5	5	5	5	5	6	5	6	7	6	7	6	7	7	7	7	7	7	7	7	7	7	7	7
AMNH75054	milleri	5	4	5	4	6	7	6	7	7	7	7	7	7	7	7	7	8	8	8	8	7	8	7	8
AMNH75055	milleri	5	5	5	5	6	7	6	7	7	8	7	8	8	8	8	8	7	8	7	8	7	8	7	8
AMNH75064	milleri	5	5	5	5	6	6	6	6	7	7	7	7	7	7	7	7	8	8	8	8	7	8	7	8
AMNH75147	milleri	4	4	4	4	5	6	5	6	6	6	6	6	6	6	6	6	7	7	7	7	6	6	6	6
BGSU4038b	milleri	4	4	4	4	6	6	6	6	7	7	7	7	7	8	7	8	8	8	8	8	8	8	8	8
BGSU4038c	milleri	5	5	5	5	5	7	5	7	6	8	6	8	7	8	7	8	8	8	8	8	8	8	8	8
BGSU4043b	milleri	4	4	4	4	6	6	6	6	7	7	7	7	7	7	7	7	8	8	8	8	8	8	8	8
BGSU4052	milleri	.	.	.	.	4	4	4	4	6	6	6	6	7	7	7	7	7	7	7	7	7	7	7	7
PE25592b	milleri	5	5	5	5	6	7	6	7	8	8	8	8	8	8	8	8	8	8	8	8	8	8	8	8
PE25592c	milleri	5	5	5	5	7	7	7	7	8	8	8	8	8	8	8	8	8	9	8	9	8	8	8	8
AMNH74081	milleri	5	4	5	4	6	6	6	6	7	7	7	7	7	7	7	7	8	8	8	8	7	8	7	8
AMNH74876b	milleri	4	4	4	4	7	7	7	7	8	8	8	8	8	8	8	8	9	9	9	9	8	8	8	8
AMNH74876d	milleri	.	.	.	.	.	.	.	.	8	8	8	8	7	8	7	8	8	8	8	8	8	8	8	8
AMNH75052	milleri	4	6	4	6	5	7	5	7	7	7	7	7	7	8	7	8	8	8	8	8	8	8	8	8
BGSU4031e	milleri	4	4	4	4	6	7	6	7	6	8	6	8	7	8	7	8	7	9	7	9	7	8	7	8
BGSU4031i	milleri	6	6	6	6	8	8	8	8	9	9	9	9	8	8	8	8	9	9	9	9	9	9	9	9
BGSU4031k	milleri	4	3	4	3	5	5	5	5	7	7	7	7	7	7	7	7	8	8	8	8	7	7	7	7
BGSU4070	milleri	5	5	5	5	6	6	6	6	8	8	8	8	8	7	8	7	8	8	8	8	9	8	9	8

Taable B.1—Left and right eye-lens counts for all specimens of *Eldredgeops.* Data is separated by each dorso-ventral file. Data marked with a (.) represent no data due to matrix obstructing an accurate count or due to the dorso-ventral file not being present.

DV7 Robs1	DV7 Lobs1	DV7 Robs2	DV7 Lobs2	DV8 Robs1	DV8 Lobs1	DV8 Robs2	DV8 Lobs2	DV9 Robs1	DV9 Lobs1	DV9 Robs2	DV9 Lobs2	DV10 Robs1	DV10 Lobs1	DV10 Robs2	DV10 Lobs2	DV11 Robs1	DV11 Lobs1	DV11 Robs2	DV11 Lobs2	DV12 Robs1	DV12 Lobs1	DV12 Robs2	DV12 Lobs2
6	6	6	6	6	6	6	6	5	5	5	5	6	6	6	6	4	5	4	5	5	6	5	6
6	6	6	6	5	5	5	5	6	6	6	6	5	5	5	5	5	5	5	5	5	5	5	5
6	6	6	6	5	6	5	6	6	6	6	6	5	5	5	5	5	5	5	5	5	5	5	5
6	6	6	6	5	5	5	5	6	6	6	6	5	5	5	5	5	5	5	5	4	4	4	4
6	7	6	7	6	6	6	6	6	6	6	6	6	6	6	6	6	6	6	6	5	5	5	5
6	6	6	6	5	5	5	5	6	6	6	6	5	5	5	5	5	6	5	6	5	5	5	5
5	5	5	5	5	5	5	5	5	5	5	5	5	5	5	5	5	5	5	5	4	4	4	4
5	5	5	5	5	5	5	5	5	5	5	5	5	4	5	4	5	5	5	5	4	4	4	4
6	6	6	6	5	5	5	5	6	5	6	5	5	5	5	5	6	5	6	5	5	5	5	5
6	6	6	6	5	5	5	5	6	6	6	6	5	5	5	5	5	5	5	5	4	5	4	5
6	6	6	6	5	5	5	5	6	6	6	6	5	5	5	5	5	5	5	5	4	5	4	5
6	6	6	6	5	5	5	5	6	6	6	6	5	5	5	5	5	5	5	5	5	5	5	5
5	5	5	5	5	5	5	5	6	6	6	6	5	5	5	5	5	5	5	5	5	5	5	5
6	6	6	6	5	5	5	5	6	6	6	6	5	5	5	5	5	5	5	5	5	5	5	5
5	5	5	5	6	5	6	5	5	6	5	6	5	5	5	5	6	6	6	6	5	5	5	5
5	5	5	5	5	5	5	5	5	5	5	5	5	5	5	5	5	5	5	5	5	5	5	5
5	5	5	5	5	6	5	6	6	5	6	5	5	6	5	6	4	5	4	5	5	5	5	5
6	6	6	6	5	5	5	5	5	6	5	6	5	5	5	5	5	5	5	5	5	5	5	5
9	9	9	9	8	9	8	9	7	9	7	9	9	8	9	8	8	8	8	8	7	7	7	7
9	9	9	9	8	8	8	8	8	8	8	8	8	8	8	8	8	8	8	8	7	7	7	7
8	8	8	8	7	7	7	7	7	8	7	8	7	7	7	7	7	7	7	7	6	5	6	5
8	8	8	8	8	8	8	8	8	7	8	7	7	7	7	7	7	7	7	7	7	6	7	6
7	8	7	8	7	8	7	8	7	8	7	8	6	7	6	7	7	8	7	8	6	7	6	7
8	8	8	8	8	7	8	7	8	8	8	8	8	7	8	7	7	7	7	7	7	7	7	7
8	7	8	7	8	7	8	7	8	8	8	8	7	7	7	7	8	8	8	8	7	7	7	7
6	5	6	5	5	6	5	6	6	6	6	6	5	5	5	5	5	6	5	6	5	5	5	5
7	7	7	7	8	8	8	8	8	8	8	8	7	7	7	7	8	8	8	8	7	7	7	7
7	8	7	8	7	7	7	7	7	7	7	7	7	7	7	7	7	7	7	7	6	6	6	6
8	8	8	8	7	8	7	8	7	6	7	6	7	6	7	6	7	7	7	7	7	7	7	7
8	9	8	9	8	8	8	8	7	8	7	8	7	8	7	8	8	8	8	8	7	7	7	7
7	7	7	7	7	7	7	7	8	7	8	7	7	7	7	7	7	6	7	6	7	6	7	6
7	7	7	7	6	6	6	6	7	6	7	6	6	6	6	6	6	6	6	6	5	5	5	5
8	8	8	8	8	8	8	8	8	8	8	8	7	7	7	7	7	8	7	8	6	7	6	7
8	8	8	8	8	8	8	8	8	8	8	8	8	8	8	8	8	7	8	7	7	7	7	7
8	8	8	8	8	8	8	8	8	8	8	8	7	7	7	7	7	7	7	7	6	6	6	6
7	7	7	7	8	8	8	8	7	7	7	7	7	7	7	7	7	7	7	7	6	7	6	7
9	9	9	9	8	8	8	8	8	8	8	8	7	8	7	8	8	8	8	8	7	7	7	7
9	9	9	9	8	8	8	8	8	9	8	9	8	8	8	8	8	8	8	8	7	7	7	7
8	8	8	8	7	7	7	7	8	8	8	8	7	7	7	7	7	6	7	6	6	6	6	6
9	9	9	9	8	8	8	8	9	9	9	9	8	7	8	7	7	8	7	8	7	6	7	6
8	8	8	8	8	8	8	8	8	8	8	8	7	7	7	7	7	8	7	8	7	7	7	7
8	8	8	8	8	8	8	8	8	7	8	7	7	8	7	8	8	7	8	7	7	7	7	7
7	9	7	9	7	7	7	7	8	9	8	9	8	8	8	8	8	8	8	8	8	6	8	6
9	10	9	10	9	9	9	9	9	9	9	9	8	8	8	8	10	9	10	9	8	8	8	8
8	8	8	8	7	7	7	7	8	8	8	8	7	7	7	7	8	7	8	7	6	7	6	7
9	8	9	8	9	8	9	8	9	8	9	8	8	7	8	7	8	8	8	8	7	7	7	7

Taable B.1 (continued)—Left and right eye-lens counts for all specimens of *Eldredgeops.* Data is separated by each dorso-ventral file. Data marked with a (.) represent no data due to matrix obstructing an accurate count or due to the dorso-ventral file not being present.

DV13 Robs1	DV13 Lobs1	DV13 Robs2	DV13 Lobs2	DV14 Robs1	DV14 Lobs1	DV14 Robs2	DV14 Lobs2	DV15 Robs1	DV15 Lobs1	DV15 Robs2	DV15 Lobs2	DV16 Robs1	DV16 Lobs1	DV16 Robs2	DV16 Lobs2	DV17 Robs1	DV17 Lobs1	DV17 Robs2	DV17 Lobs2	DV18 Robs1	DV18 Lobs1	DV18 Robs2	DV18 Lobs2
5	5	5	5	5	5	5	5	4	4	4	4	4	4	4	4	3	3	3	3	2	2	2	2
5	5	5	5	4	4	4	4	4	4	4	4	3	3	3	3	3	3	3	3	2	2	2	2
5	5	5	5	4	4	4	4	4	4	4	4	3	3	3	3	3	3	3	3	2	2	2	2
5	5	5	5	4	4	4	4	4	4	4	4	3	3	3	3	3	3	3	3	2	1	2	1
5	5	5	5	4	4	4	4	4	4	4	4	3	3	3	3	3	3	3	3	2	2	2	2
5	5	5	5	4	4	4	4	4	4	4	4	3	3	3	3	3	3	3	3	2	2	2	2
4	5	4	5	4	4	4	4	4	4	4	4	3	3	3	3	3	3	3	3	2	2	2	2
4	4	4	4	3	3	3	3	3	3	3	3	2	2	2	2	2	2	2	2	1	1	1	1
5	5	5	5	4	3	4	3	4	4	4	4	3	3	3	3	3	3	3	3	2	2	2	2
5	5	5	5	4	4	4	4	4	4	4	4	3	3	3	3	3	3	3	3	2	2	2	2
5	5	5	5	4	4	4	4	4	4	4	4	3	3	3	3	3	2	3	2	2	2	2	2
5	5	5	5	4	4	4	4	4	4	4	4	3	3	3	3	3	3	3	3	2	2	2	2
5	5	5	5	4	4	4	4	4	4	4	4	2	2	2	2	2	2	2	2	1	1	1	1
5	5	5	5	4	4	4	4	4	4	4	4	2	3	2	3	2	3	2	3	2	2	2	2
4	5	4	5	4	4	4	4	3	4	3	4	3	3	3	3	2	3	2	3	2	2	2	2
5	5	5	5	4	4	4	4	4	4	4	4	2	2	2	2	3	3	3	3	2	2	2	2
4	4	4	4	4	4	4	4	4	3	4	3	3	3	3	3	3	3	3	3	2	2	2	2
5	5	5	5	4	4	4	4	4	4	4	4	3	3	3	3	3	3	3	3	1	2	1	2
7	7	7	7	8	6	8	6	5	6	5	6	4	4	4	4	4	4	4	4	3	3	3	3
7	7	7	7	5	6	5	6	4	6	4	6	4	4	4	4	3	4	3	4	3	3	3	3
6	6	6	6	5	5	5	5	5	5	5	5	4	3	4	3	3	3	3	3	2	2	2	2
7	7	7	7	6	5	6	5	6	5	6	5	4	4	4	4	4	3	4	3	3	3	3	3
6	7	6	7	5	5	5	5	4	5	4	5	4	4	4	4	3	4	3	4	2	2	2	2
7	7	7	7	6	6	6	6	6	5	6	5	4	4	4	4	4	4	4	4	3	3	3	3
7	7	7	7	6	6	6	6	5	6	5	6	4	4	4	4	4	4	4	4	2	2	2	2
5	5	5	5	4	4	4	4	3	4	3	4	3	3	3	3	3	3	3	3	2	2	2	2
6	6	6	6	5	5	5	5	5	5	5	5	4	3	4	3	3	3	3	3	2	2	2	2
6	6	6	6	5	5	5	5	5	5	5	5	4	4	4	4	4	4	4	4	3	3	3	3
5	5	5	5	5	5	5	5	4	6	4	6	4	5	4	5	3	4	3	4	2	3	2	3
7	7	7	7	6	6	6	6	5	6	5	6	4	5	4	5	4	4	4	4	3	3	3	3
8	6	8	6	5	5	5	5	5	4	5	4	4	4	4	4	4	3	4	3	2	3	2	3
6	6	6	6	5	5	5	5	5	5	5	5	4	4	4	4	3	3	3	3	3	3	3	3
7	7	7	7	5	6	5	6	5	5	5	5	5	4	5	4	3	3	3	3	2	3	2	3
7	7	7	7	6	6	6	6	4	5	4	5	3	4	3	4	2	3	2	3	1	2	1	2
7	6	7	6	5	5	5	5	5	5	5	5	4	4	4	4	3	3	3	3	2	2	2	2
6	6	6	6	5	6	5	6	5	5	5	5	3	5	3	5	3	4	3	4	2	2	2	2
7	7	7	7	6	6	6	6	5	5	5	5	4	4	4	4	4	4	4	4	3	2	3	2
7	7	7	7	6	6	6	6	5	5	5	5	4	4	4	4	4	4	4	4	3	3	3	3
7	6	7	6	5	5	5	5	5	5	5	5	3	3	3	3	3	3	3	3	2	2	2	2
7	6	7	6	6	5	6	5	6	5	6	5	4	3	4	3	4	4	4	4	3	2	3	2
7	7	7	7	7	6	7	6	6	5	6	5	5	4	5	4	4	4	4	4	3	3	3	3
7	7	7	7	6	6	6	6	6	6	6	6	4	4	4	4	4	4	4	4	3	3	3	3
7	7	7	7	5	6	5	6	5	6	5	6	5	4	5	4	4	4	4	4	3	3	3	3
8	8	8	8	6	7	6	7	7	6	7	6	5	5	5	5	4	5	4	5	2	3	2	3
7	7	7	7	6	5	6	5	5	4	5	4	4	3	4	3	4	3	4	3	2	2	2	2
7	6	7	6	6	5	6	5	4	5	4	5	4	3	4	3	3	4	3	4	2	2	2	2

Taable B.1 (continued)—Left and right eye-lens counts for all specimens of *Eldredgeops.* Data is separated by each dorso-ventral file. Data marked with a (.) represent no data due to matrix obstructing an accurate count or due to the dorso-ventral file not being present.

	DV1	DV2	DV3	DV4	DV5	DV6	DV7	DV8	DV9	DV10	DV11	DV12	DV13	DV14	DV15	DV16	DV17	DV18
Log-Likelihood	-15.3962	-17.8248	-23.9198	-24.3429	-25.1412	-34.451	-18.0411	-16.0797	-10.3415	-15.743	-21.6172	-20.0952	-15.1207	-12.6845	-12.1427	-16.442	-16.6981	-13.6936
Trait Mean (μ)	3.2738	4.5567	5.6061	5.0893	5.7641	5.4113	5.6689	5.4734	5.5169	5.1227	5.112	4.7955	4.6037	3.9513	3.652	2.844	2.5011	1.5252
Symmetric Variation (σGE)	0.5002	0.01253	0.4814	0.5774	0.4317	0.3071	0.4593	0.0136	0.0268	0.3194	0.3277	0.3466	0.13	0.3724	0.105	0.3973	0.0284	0.0189
Fluctuating Asymmetry (σA)	0.0665	0.0627	0.1498	0.1077	0.2198	0.4813	0.0556	0.0205	0.0244	0.1194	0.2191	0.1573	0.1132	0.062	0.1213	0.0509	0.0112	0.0185

Table B.2— Parameter estimates and likelihoods for each dorso-ventral file among all specimens of *Eldredgeops crassituberculatus*.

	DV1	DV2	DV3	DV4	DV5	DV6	DV7	DV8	DV9	DV10	DV11	DV12	DV13	DV14	DV15	DV16	DV17	DV18
Log-Likelihood	-44.2543	-63.6357	-57.4371	-44.4115	-58.834	-56.3529	-61.1251	-51.5934	-60.2505	-52.9997	-58.6085	-55.4461	-51.4193	-56.1532	-60.0893	-48.4321	-44.142	-38.9062
Trait Mean (μ)	4.6697	6.0371	7.2489	7.3046	7.8726	7.6412	7.9809	7.6223	7.664	7.1993	7.4093	6.6048	6.6238	5.5412	5.089	3.9463	3.5773	2.4752
Symmetric Variation (σGE)	0.4296	0.6315	0.5897	0.4958	0.5353	0.5724	0.7529	0.6868	0.5803	0.6233	0.6946	0.5472	0.5484	0.5009	0.319	0.2609	0.365	0.3713
Fluctuating Asymmetry (σA)	0.3366	0.5042	0.3891	0.2131	0.3209	0.3741	0.361	0.2259	0.4318	0.2772	0.3352	0.373	0.3192	0.4159	0.5721	0.4348	0.3033	0.2112

Table B.3— Parameter estimates and likelihoods for each dorso-ventral file among all specimens of *Eldredgeops milleri.*

	DV1	DV2	DV3	DV4	DV5	DV6	DV7	DV8	DV9	DV10	DV11	DV12	DV13	DV14	DV15	DV16	DV17	DV18
Log-Likelihood	-79.8073	-104	-104.9	-103.3	-110	-125	-114.2	-109.5	-118.2	-105.5	-116.6	-107.5	-101	-102.1	-103.1	-90.3094	-75.232	-64.7987
Trait Mean (μ)	4.206	5.247	6.6335	6.4467	7.0538	6.7709	7.089	6.6752	6.9466	6.3846	6.5119	5.9034	5.925	4.9298	4.6223	3.526	3.2717	2.2269
Symmetric Variation (σGE)	0.8047	0.859	0.966	1.1934	1.338	1.1917	1.2909	1.3055	1.379	1.142	1.2597	0.9979	0.9842	0.8788	0.647	0.6257	0.4989	0.4617
Fluctuating Asymmetry (σA)	0.2813	0.4178	0.3346	0.1741	0.2905	0.4229	0.2794	0.1922	0.3605	0.2116	0.2826	0.3121	0.2689	0.3138	0.4395	0.3246	0.2492	0.1726

Table B.4— Parameter estimates and likelihoods for each dorso-ventral file among where data for the two species were combined and treated as a single population.

DV1	df	SS	MS	F-value	P-Value
Side	1	0.1730769	0.1730769	1.000000	0.326891913
Individual	25	14.9423077	0.5976923	3.453333	0.001450882
Interaction	25	0.1730769	4.3269231	NaN	NaN
Error	0	0.00	NaN		
Total	51	19.4423077			

Table B.5—Values corresponding to two-factor mixed-model ANOVA conducted on dorso-ventral file 1 in *Eldredgeops milleri*. "Sides" component represents the level of directional asymmetry in the trait. "Idividual" refers to the measure of symmetric phenotypic variation. Interaction term is a measure of the fluctuating asymmetry (within-individual variation).

DV2	df	SS	MS	F-value	P-Value
Side	1	2.666667	2.6666667	10.947368	2.748245e-03
Individual	26	30.925926	1.1894587	4.883041	6.629722e-05
Interaction	26	6.333333	0.2435897	NaN	NaN
Error	0	0.000000	NaN		
Total	53	39.925926			

Table B.6—Values corresponding to two-factor mixed-model ANOVA conducted on dorso-ventral file 2 in *Eldredgeops milleri* Component measures are as mentioned in Table B.5.

DV3	Df	SS	MS	F-value	P-Value
Side	1	0.6428571	0.6428571	3.240000	0.0830449214
Individual	27	26.5000000	0.9814815	4.946667	0.0000434014
Interaction	27	5.3571429	5.3571429	NaN	NaN
Error	0	0.000000	NaN		
Total	55	32.5000000			

Table B.7—Values corresponding to two-factor mixed-model ANOVA conducted on dorso-ventral file 3 in *Eldredgeops milleri*. Component measures are as mentioned in Table B.5.

DV4	df	SS	MS	F-value	P-Value
Side	1	0.4464286	0.4464286	3.947368	5.717912e-02
Individual	27	18.3392857	0.6792328	6.005848	6.682247e-06
Interaction	27	3.0535714	0.1130952	NaN	NaN
Error	0	0.000000	NaN		
Total	55	21.8392857			

Table B.8—Values corresponding to two-factor mixed-model ANOVA conducted on dorso-ventral file 4 in *Eldredgeops milleri*. Component measures are as mentioned in Table B.5.

DV5	df	SS	MS	F-value	P-Value
Side	1	0.875	0.8750000	6.517241	1.665019e-02
Individual	27	21.625	0.8009259	5.965517	7.145020e-06
Interaction	27	3.625	0.1342593	NaN	NaN
Error	0	0.000000	NaN		
Total	55	26.125			

Table B.9—Values corresponding to two-factor mixed-model ANOVA conducted on dorso-ventral file 5 in *Eldredgeops milleri*. Component measures are as mentioned in Table B.5.

DV6	df	SS	MS	F-value	P-Value
Side	1	0.2857143	0.2857143	1.35	0.2554464948
Individual	27	24.8571429	0.9206349	4.35	0.0001398039
Interaction	27	5.7142857	0.2116402	NaN	NaN
Error	0	0.000000	NaN		
Total	55	30.8571429			

Table B.10—Values corresponding to two-factor mixed-model ANOVA conducted on dorso-ventral file 6 in *Eldredgeops milleri*. Component measures are as mentioned in Table B.5.

DV7	df	SS	MS	F-value	P-Value
Side	1	0.1607143	0.1607143	0.812709	3.752924e-01
Individual	27	24.8571429	0.9206349	4.35	0.0001398039
Interaction	27	5.7142857	0.2116402	NaN	NaN
Error	0	0.000000	NaN		
Total	55	30.8571429			

Table B.11—Values corresponding to two-factor mixed-model ANOVA conducted on dorso-ventral file 7 in *Eldredgeops milleri*. Component measures are as mentioned in Table B.5.

DV8	df	SS	MS	F-value	P-Value
Side	1	0.01785714	0.01785714	0.1384615	7.127199e-01
Individual	27	29.62500000	1.09722222	8.5076923	1.767564e-07
Interaction	27	3.48214286	0.12896825	NaN	NaN
Error	0	0.000000	NaN		
Total	55	33.12500000			

Table B.12—Values corresponding to two-factor mixed-model ANOVA conducted on dorso-ventral file 8 in *Eldredgeops milleri*. Component measures are as mentioned in Table B.5.

DV9	df	SS	MS	F-value	P-Value
Side	1	0.01785714	0.01785714	0.06443914	0.8015356470
Individual	27	26.48214286	0.98082011	3.53937947	0.0008025025
Interaction	27	7.48214286	0.27711640	NaN	NaN
Error	0	0.000000	NaN		
Total	55	33.98214286			

Table B.13—Values corresponding to two-factor mixed-model ANOVA conducted on dorso-ventral file 9 in *Eldredgeops milleri*. Component measures are as mentioned in Table B.5.

DV10	df	SS	MS	F-value	P-Value
Side	1	0.01785714	0.01785714	0.1075697	7.454580e-01
Individual	27	26.33928571	0.97552910	5.8764940	8.292431e-06
Interaction	27	4.48214286	0.16600529	NaN	NaN
Error	0	0.000000	NaN		
Total	55	30.83928571			

Table B.14—Values corresponding to two-factor mixed-model ANOVA conducted on dorso-ventral file 10 in *Eldredgeops milleri*. Component measures are as mentioned in Table B.5.

DV11	df	SS	MS	F-value	P-Value
Side	1	0.01785714	0.01785714	0.08794788	7.690717e-01
Individual	27	32.05357143	1.18716931	5.84690554	8.716237e-06
Interaction	27	5.92857143	0.21957672	NaN	NaN
Error	0	0.000000	NaN		
Total	53	29.35714286			

Table B.15—Values corresponding to two-factor mixed-model ANOVA conducted on dorso-ventral file 11 in *Eldredgeops milleri*. Component measures are as mentioned in Table B.5.

DV12	df	SS	MS	F-value	P-Value
Side	1	0.07142857	0.07142857	0.3253012	0.5731553346
Individual	27	23.35714286	0.86507937	3.9397590	0.0003304142
Interaction	27	5.92857143	0.21957672	NaN	NaN
Error	0	0.000000	NaN		
Total	55	29.35714286			

Table B.16—Values corresponding to two-factor mixed-model ANOVA conducted on dorso-ventral file 12 in *Eldredgeops milleri*. Component measures are as mentioned in Table B.5.

DV13	df	SS	MS	F-value	P-Value
Side	1	0.4464286	0.4464286	2.973568	9.606763e-02
Individual	27	22.6250000	0.8379630	5.581498	1.373871e-05
Interaction	27	4.0535714	0.1501323	NaN	NaN
Error	0	0.000000	NaN		
Total	55	27.1250000			

Table B.17—Values corresponding to two-factor mixed-model ANOVA conducted on dorso-ventral file 13 in *Eldredgeops milleri*. Component measures are as mentioned in Table B.5.

DV14	df	SS	MS	F-value	P-Value
Side	1	0.07142857	0.07142857	0.2783505	0.60209348
Individual	27	20.92857143	0.77513228	3.0206186	0.00273144
Interaction	27	6.92857143	0.25661376	NaN	NaN
Error	0	0.000000	NaN		
Total	55	27.92857143			

Table B.18—Values corresponding to two-factor mixed-model ANOVA conducted on dorso-ventral file 14 in *Eldredgeops milleri*. Component measures are as mentioned in Table B.5.

DV15	df	SS	MS	F-value	P-Value
Side	1	0.4464286	0.4464286	1.090468	0.3056272
Individual	27	17.0535714	0.6316138	1.542811	0.1330958
Interaction	27	11.0535714	0.4093915	NaN	NaN
Error	0	0.000000	NaN		
Total	55	28.5535714			

Table B.19—Values corresponding to two-factor mixed-model ANOVA conducted on dorso-ventral file 15 in *Eldredgeops milleri*. Component measures are as mentioned in Table B.5.

DV16	df	SS	MS	F-value	P-Value
Side	1	0.1607143	0.1607143	0.5912409	0.4486140
Individual	27	11.3392857	0.4199735	1.5450122	0.1323174
Interaction	27	7.3392857	0.2718254	NaN	NaN
Error	0	0.000000	NaN		
Total	55	18.8392857			

Table B.20—Values corresponding to two-factor mixed-model ANOVA conducted on dorso-ventral file 16 in *Eldredgeops milleri*. Component measures are as mentioned in Table B.5.

DV17	df	SS	MS	F-value	P-Value
Side	1	0.2857143	0.2857143	1.636364	0.211709924
Individual	27	12.7142857	0.4708995	2.696970	0.006128033
Interaction	27	4.7142857	0.1746032	NaN	NaN
Error	0	0.000000	NaN		
Total	55	17.7142857			

Table B.21—Values corresponding to two-factor mixed-model ANOVA conducted on dorso-ventral file 17 in *Eldredgeops milleri*. Component measures are as mentioned in Table B.5.

DV#	df	SS	MS	F-value	P-Value
Side	1	0.1607143	0.1607143	1.299465	0.2643228802
Individual	27	12.4821429	0.4623016	3.737968	0.0005136093
Interaction	27	3.3392857	0.1236772	NaN	NaN
Error	0	0.000000	NaN		
Total	55	15.9821429			

Table B.22—Values corresponding to two-factor mixed-model ANOVA conducted on dorso-ventral file 18 in *Eldredgeops milleri*. Component measures are as mentioned in Table B.5.

	milleri	crassituberculatus	sum(m+c)	combined	Likelihood Ratio	p-Value
DV1	44.2543	15.3692	59.6235	79.8073	0.5831	0.5-0.25
DV2	63.6357	17.8248	81.4605	104	0.4885	0.5-0.25
DV3	57.4371	23.9198	81.3569	104.9	0.5083	0.5-0.25
DV4	44.4115	24.3429	68.7544	103.3	0.8142	0.5-0.25
DV5	58.834	25.1412	83.9752	110	0.5399	0.5-0.25
DV6	56.3529	34.2151	90.568	125	0.6444	0.5-0.25
DV7	61.1251	18.0411	79.1662	114.2	0.7328	0.5-0.25
DV8	51.5934	16.0797	67.6731	109.5	0.9625	0.5-0.25
DV9	60.2505	20.6831	80.9336	118.2	0.7575	0.5-0.25
DV10	52.9997	15.743	68.7427	105.5	0.8567	0.5-0.25
DV11	58.6085	21.6172	80.2257	116.6	0.7478	0.5-0.25
DV12	55.4461	20.0952	75.5413	107.5	0.7056	0.5-0.25
DV13	51.4193	15.1207	66.54	101	0.8346	0.5-0.25
DV14	56.1532	12.6845	68.8377	102.1	0.7884	0.5-0.25
DV15	60.0893	12.1427	72.232	103.1	0.7116	0.5-0.25
DV16	48.4321	16.442	64.8741	90.3094	0.6616	0.5-0.25
DV17	44.142	16.6981	60.8401	75.7214	0.4376	0.5-0.25
DV18	38.9062	13.6936	52.5998	64.7987	0.4171	0.75-0.5

Table B.23 Likelihood Ratio Test comparing the likelihood of identifying the two individual populations (sum m+c) as significantly different than if the value recovered were treated as a single population. Values for column 2 are likelihoods from table B.#, and values for column 3 are likelihoods from table B.#. Sum(m+c) (Column 4) is the combined sum of columns 2 and 3. Column 5 are the likelihoods of treating the two species as a single population (Table B.#). The likelihood ratio is calculated from equation B.5, with p-values determined comparing the score to the critical values of a X^2-distribution table with one degree of freedom.

DV File	Model	Parameters	K	N	L	AICc	ΔAIC
1	1	single μ, σGE, σA	3	46	79.8073	-2.1878	0
	2	μ, σGE, σA for each species	6	46	59.6235	5.9777	-8.1655
2	1	single μ, σGE, σA	3	46	104	-2.7173	0
	2	μ, σGE, σA for each species	6	46	81.4605	5.3536	-8.0709
3	1	single μ, σGE, σA	3	46	104.9	-2.7346	0
	2	μ, σGE, σA for each species	6	46	81.3569	5.3562	-8.0908
4	1	single μ, σGE, σA	3	46	103.3	-2.7038	0
	2	μ, σGE, σA for each species	6	46	68.7544	5.6928	-8.3966
5	1	single μ, σGE, σA	3	46	110	-2.895	0
	2	μ, σGE, σA for each species	6	46	83.9752	5.2928	-8.1878
6	1	single μ, σGE, σA	3	46	125	-3.0852	0
	2	μ, σGE, σA for each species	6	46	90.568	5.1416	-8.2268
7	1	single μ, σGE, σA	3	46	114.2	-2.9045	0
	2	μ, σGE, σA for each species	6	46	79.1662	5.4107	-8.3152
8	1	single μ, σGE, σA	3	46	109.5	-2.8204	0
	2	μ, σGE, σA for each species	6	46	67.6731	5.7245	-8.5449
9	1	single μ, σGE, σA	3	46	118.2	-2.9733	0
	2	μ, σGE, σA for each species	6	46	80.9336	5.366	-8.3393
10	1	single μ, σGE, σA	3	46	105.5	-2.746	0
	2	μ, σGE, σA for each species	6	46	68.7427	5.6931	-8.4391
11	1	single μ, σGE, σA	3	46	116.6	-2.9461	0
	2	μ, σGE, σA for each species	6	46	80.2257	5.3842	-8.3303
12	1	single μ, σGE, σA	3	46	107.5	-2.7836	0
	2	μ, σGE, σA for each species	6	46	75.5413	5.5045	-8.2881
13	1	single μ, σGE, σA	3	46	101	-2.6588	0
	2	μ, σGE, σA for each species	6	46	66.54	5.7582	-8.417
14	1	single μ, σGE, σA	3	46	102.1	-2.6805	0
	2	μ, σGE, σA for each species	6	46	68.8377	5.6903	-8.3708
15	1	single μ, σGE, σA	3	46	103.1	-2.7	0
	2	μ, σGE, σA for each species	6	46	72.232	5.5941	-8.2941
16	1	single μ, σGE, σA	3	46	90.3094	-2.4351	0
	2	μ, σGE, σA for each species	6	46	64.8741	5.8089	-8.244
17	1	single μ, σGE, σA	3	46	75.7214	-2.0827	0
	2	μ, σGE, σA for each species	6	46	60.8401	5.9373	-5.9373
18	1	single μ, σGE, σA	3	46	64.7987	-1.7711	0
	2	μ, σGE, σA for each species	6	46	52.5998	6.2284	-7.9995

Table B.24 Results of the multi-model inference tests using Akaike Information Criterion. Data is arranged by file. Test 1 for each file treats both species as belonging to a single population of data. Test 2 treats both species as separate individual populations. Likelihoods (L) are adapted from tables B.2-B.4. AIC_c scores were calculated using equation B.6. ΔAIC scores were determined using equation B.7.

APPENDIX C
SUPPLEMENTAL INFORMATION FOR CHAPTER THREE

TABLES—

--Table C.1 Begins on next page--

ID	Group	DV1 Robs1	DV1 Lobs1	DV1 Robs2	DV1 Lobs2	DV2 Robs1	DV2 Lobs1	DV2 Robs2	DV2 Lobs2	DV3 Robs1	DV3 Lobs1	DV3 Robs2	DV3 Lobs2	DV4 Robs1	DV4 Lobs1	DV4 Robs2	DV4 Lobs2	DV5 Robs1	DV5 Lobs1	DV5 Robs2	DV5 Lobs2	DV6 Robs1	DV6 Lobs1	DV6 Robs2	DV6 Lobs2
AMNH7411	crassituberculatus	.	.	.	.	.	.	.	.	4	4	4	4	6	6	6	6	5	5	5	5	6	6	6	6
AMNH74874b	crassituberculatus	4	4	4	4	5	5	5	5	6	6	6	6	6	6	6	6	6	6	6	6	5	6	5	6
AMNH74878c	crassituberculatus	.	.	.	.	5	5	5	5	6	6	6	6	5	5	5	5	6	6	6	6	4	6	4	6
AMNH74878d	crassituberculatus	2	2	2	2	4	4	4	4	5	5	5	5	5	5	5	5	6	6	6	6	5	5	5	5
AMNH74880	crassituberculatus	3	3	3	3	5	5	5	5	6	6	6	6	6	6	6	6	6	7	6	7	6	6	6	6
AMNH74983	crassituberculatus	4	4	4	4	5	4	5	4	6	6	6	6	6	6	6	6	6	6	6	6	6	6	6	6
BGSU4037a	crassituberculatus	.	.	.	.	.	.	.	.	.	.	.	.	3	4	3	4	4	5	4	5	4	5	4	5
BGSU4038d	crassituberculatus	3	3	3	3	4	4	4	4	5	5	5	5	5	4	5	4	5	5	5	5	5	5	5	5
BGSU4057g	crassituberculatus	4	4	4	4	5	5	5	5	6	6	6	6	5	5	5	5	6	5	6	5	5	6	5	6
PE25589	crassituberculatus	3	3	3	3	5	5	5	5	6	5	6	5	5	5	5	5	6	6	6	6	5	5	5	5
PE25589b	crassituberculatus	4	3	4	3	5	5	5	5	6	5	6	5	5	5	5	5	6	6	6	6	5	5	5	5
PE25592d	crassituberculatus	3	3	3	3	5	5	5	5	6	6	6	6	5	5	5	5	6	6	6	6	6	6	6	6
PE9516a	crassituberculatus	.	.	.	.	4	4	4	4	6	6	6	6	5	5	5	5	6	6	6	6	5	5	5	5
PE9516b	crassituberculatus	3	3	3	3	5	5	5	5	6	6	6	6	5	5	5	5	6	6	6	6	6	6	6	6
PE9516c	crassituberculatus	3	3	3	3	5	4	5	4	6	6	6	6	5	5	5	5	6	6	6	6	6	6	6	6
PE9518	crassituberculatus	4	4	4	4	5	5	5	5	6	6	6	6	5	5	5	5	6	6	6	6	6	6	6	6
AMNH74105a	crassituberculatus	.	.	.	.	4	4	4	4	5	5	5	5	5	5	5	5	6	5	6	5	5	5	5	5
BGSU4049a	crassituberculatus	3	3	3	3	4	5	4	5	6	6	6	6	5	5	5	5	6	6	6	6	6	4	6	4
AMNH74085	milleri	5	5	5	5	6	6	6	6	7	8	7	8	8	8	8	8	9	9	9	9	8	8	8	8
AMNH74874a	milleri	5	4	5	4	6	6	6	6	8	8	8	8	8	8	8	8	8	8	8	8	8	8	8	8
AMNH74874c	milleri	4	4	4	4	5	5	5	5	7	7	7	7	7	7	7	7	8	8	8	8	7	7	7	7
AMNH74874d	milleri	5	5	5	5	6	6	6	6	7	7	7	7	7	7	7	7	7	8	7	8	8	8	8	8
AMNH74875a	milleri	5	5	5	5	5	7	5	7	7	8	7	8	6	7	6	7	7	8	7	8	6	8	6	8
AMNH74875b	milleri	5	5	5	5	7	7	7	7	8	8	8	8	8	8	8	8	8	8	8	8	9	8	9	8
AMNH74876c	milleri	5	5	5	5	6	6	6	6	7	7	7	7	7	7	7	7	8	8	8	8	8	8	8	8
AMNH74964	milleri	5	4	5	4	5	5	5	5	6	6	6	6	6	6	6	6	6	6	6	6	6	6	6	6
AMNH74982	milleri	5	5	5	5	6	6	6	6	7	7	7	7	7	7	7	7	7	8	7	8	8	7	8	7
AMNH75037	milleri	5	5	5	5	5	6	5	6	7	6	7	6	7	7	7	7	7	7	7	7	7	7	7	7
AMNH75054	milleri	5	4	5	4	6	7	6	7	7	7	7	7	7	7	7	7	8	8	8	8	7	8	7	8
AMNH75055	milleri	5	5	5	5	6	7	6	7	7	8	7	8	8	8	8	8	7	8	7	8	7	8	7	8
AMNH75064	milleri	5	5	5	5	6	6	6	6	7	7	7	7	7	7	7	7	8	8	8	8	7	8	7	8
AMNH75147	milleri	4	4	4	4	5	6	5	6	6	6	6	6	6	6	6	6	7	7	7	7	6	6	6	6
BGSU4038b	milleri	4	4	4	4	6	6	6	6	7	7	7	7	7	8	7	8	8	8	8	8	8	8	8	8
BGSU4038c	milleri	5	5	5	5	5	7	5	7	6	8	6	8	7	8	7	8	8	8	8	8	8	8	8	8
BGSU4043b	milleri	4	4	4	4	6	6	6	6	7	7	7	7	7	7	7	7	8	8	8	8	8	8	8	8
BGSU4052	milleri	.	.	.	.	4	4	4	4	6	6	6	6	7	7	7	7	7	7	7	7	7	7	7	7
PE25592b	milleri	5	5	5	5	6	7	6	7	8	8	8	8	8	8	8	8	8	8	8	8	8	8	8	8
PE25592c	milleri	5	5	5	5	7	7	7	7	8	8	8	8	8	8	8	8	8	9	8	9	8	8	8	8
AMNH74081	milleri	5	4	5	4	6	6	6	6	7	7	7	7	7	7	7	7	8	8	8	8	7	8	7	8
AMNH74876b	milleri	4	4	4	4	7	7	7	7	8	8	8	8	8	8	8	8	9	9	9	9	8	8	8	8
AMNH74876d	milleri	.	.	.	.	.	.	.	.	8	8	8	8	7	8	7	8	8	8	8	8	8	8	8	8
AMNH75052	milleri	4	6	4	6	5	7	5	7	7	7	7	7	7	8	7	8	8	8	8	8	8	8	8	8
BGSU4031e	milleri	4	4	4	4	6	7	6	7	6	8	6	8	7	8	7	8	7	9	7	9	7	8	7	8
BGSU4031i	milleri	6	6	6	6	8	8	8	8	9	9	9	9	8	8	8	8	9	9	9	9	9	9	9	9
BGSU4031k	milleri	4	3	4	3	5	5	5	5	7	7	7	7	7	7	7	7	8	8	8	8	7	7	7	7
BGSU4070	milleri	5	5	5	5	6	6	6	6	8	8	8	8	8	7	8	7	8	8	8	8	9	8	9	8

Taable C.1—Left and right eye-lens counts for all specimens of *Eldredgeops.* Data is separated by each dorso-ventral file. Data marked with a (.) represent no data due to matrix obstructing an accurate count or due to the dorso-ventral file not being present.

DV7 Robs1	DV7 Lobs1	DV7 Robs2	DV7 Lobs2	DV8 Robs1	DV8 Lobs1	DV8 Robs2	DV8 Lobs2	DV9 Robs1	DV9 Lobs1	DV9 Robs2	DV9 Lobs2	DV10 Robs1	DV10 Lobs1	DV10 Robs2	DV10 Lobs2	DV11 Robs1	DV11 Lobs1	DV11 Robs2	DV11 Lobs2	DV12 Robs1	DV12 Lobs1	DV12 Robs2	DV12 Lobs2
6	6	6	6	6	6	6	6	5	5	5	5	6	6	6	6	4	5	4	5	5	6	5	6
6	6	6	6	5	5	5	5	6	6	6	6	5	5	5	5	5	5	5	5	5	5	5	5
6	6	6	6	5	6	5	6	6	6	6	6	5	5	5	5	5	5	5	5	5	5	5	5
6	6	6	6	5	5	5	5	6	6	6	6	5	5	5	5	5	5	5	5	4	4	4	4
6	7	6	7	6	6	6	6	6	6	6	6	6	6	6	6	6	6	6	6	5	5	5	5
6	6	6	6	5	5	5	5	6	6	6	6	5	5	5	5	5	6	5	6	5	5	5	5
5	5	5	5	5	5	5	5	5	5	5	5	5	5	5	5	5	5	5	5	4	4	4	4
5	5	5	5	5	5	5	5	5	5	5	5	5	4	5	4	5	5	5	5	4	4	4	4
6	6	6	6	5	5	5	5	6	5	6	5	5	5	5	5	6	5	6	5	5	5	5	5
6	6	6	6	5	5	5	5	6	6	6	6	5	5	5	5	5	5	5	5	4	5	4	5
6	6	6	6	5	5	5	5	6	6	6	6	5	5	5	5	5	5	5	5	4	5	4	5
6	6	6	6	5	5	5	5	6	6	6	6	5	5	5	5	5	5	5	5	5	5	5	5
5	5	5	5	5	5	5	5	6	6	6	6	5	5	5	5	5	5	5	5	5	5	5	5
6	6	6	6	5	5	5	5	6	6	6	6	5	5	5	5	5	5	5	5	5	5	5	5
5	5	5	5	6	5	6	5	5	6	5	6	5	5	5	5	6	6	6	6	5	5	5	5
5	5	5	5	5	5	5	5	5	5	5	5	5	5	5	5	5	5	5	5	5	5	5	5
5	5	5	5	5	6	5	6	6	5	6	5	5	6	5	6	4	5	4	5	5	5	5	5
6	6	6	6	5	5	5	5	5	6	5	6	5	5	5	5	5	5	5	5	5	5	5	5
9	9	9	9	8	9	8	9	7	9	7	9	9	8	9	8	8	8	8	8	7	7	7	7
9	9	9	9	8	8	8	8	8	8	8	8	8	8	8	8	8	8	8	8	7	7	7	7
8	8	8	8	7	7	7	7	7	8	7	8	7	7	7	7	7	7	7	7	6	5	6	5
8	8	8	8	8	8	8	8	8	7	8	7	7	7	7	7	7	7	7	7	7	6	7	6
7	8	7	8	7	8	7	8	7	8	7	8	6	7	6	7	7	8	7	8	6	7	6	7
8	8	8	8	8	7	8	7	8	8	8	8	8	7	8	7	7	7	7	7	7	7	7	7
8	7	8	7	8	7	8	7	8	8	8	8	7	7	7	7	8	8	8	8	7	7	7	7
6	5	6	5	5	6	5	6	6	6	6	6	5	5	5	5	5	6	5	6	5	5	5	5
7	7	7	7	8	8	8	8	8	8	8	8	7	7	7	7	8	8	8	8	7	7	7	7
7	8	7	8	7	7	7	7	7	7	7	7	7	7	7	7	7	7	7	7	6	6	6	6
8	8	8	8	7	8	7	8	7	6	7	6	7	6	7	6	7	7	7	7	7	7	7	7
8	9	8	9	8	8	8	8	7	8	7	8	7	8	7	8	8	8	8	8	7	7	7	7
7	7	7	7	7	7	7	7	8	7	8	7	7	7	7	7	7	6	7	6	7	6	7	6
7	7	7	7	6	6	6	6	7	6	7	6	6	6	6	6	6	6	6	6	5	5	5	5
8	8	8	8	8	8	8	8	8	8	8	8	7	7	7	7	7	8	7	8	6	7	6	7
8	8	8	8	8	8	8	8	8	8	8	8	8	8	8	8	8	7	8	7	7	7	7	7
8	8	8	8	8	8	8	8	8	8	8	8	7	7	7	7	7	7	7	7	6	6	6	6
7	7	7	7	8	8	8	8	7	7	7	7	7	7	7	7	7	7	7	7	6	7	6	7
9	9	9	9	8	8	8	8	8	8	8	8	7	8	7	8	8	8	8	8	7	7	7	7
9	9	9	9	8	8	8	8	8	9	8	9	8	8	8	8	8	8	8	8	7	7	7	7
8	8	8	8	7	7	7	7	8	8	8	8	7	7	7	7	7	6	7	6	6	6	6	6
9	9	9	9	8	8	8	8	9	9	9	9	8	7	8	7	7	8	7	8	7	6	7	6
8	8	8	8	8	8	8	8	8	8	8	8	7	7	7	7	7	8	7	8	7	7	7	7
8	8	8	8	8	8	8	8	8	7	8	7	7	8	7	8	8	7	8	7	7	7	7	7
7	9	7	9	7	7	7	7	8	9	8	9	8	8	8	8	8	8	8	8	8	6	8	6
9	10	9	10	9	9	9	9	9	9	9	9	8	8	8	8	10	9	10	9	8	8	8	8
8	8	8	8	7	7	7	7	8	8	8	8	7	7	7	7	8	7	8	7	6	7	6	7
9	8	9	8	9	8	9	8	9	8	9	8	8	7	8	7	8	8	8	8	7	7	7	7

Taable C.1 (continued)—Left and right eye-lens counts for all specimens of *Eldredgeops.* Data is separated by each dorso-ventral file. Data marked with a (.) represent no data due to matrix obstructing an accurate count or due to the dorso-ventral file not being present.

DV13 Robs1	DV13 Lobs1	DV13 Robs2	DV13 Lobs2	DV14 Robs1	DV14 Lobs1	DV14 Robs2	DV14 Lobs2	DV15 Robs1	DV15 Lobs1	DV15 Robs2	DV15 Lobs2	DV16 Robs1	DV16 Lobs1	DV16 Robs2	DV16 Lobs2	DV17 Robs1	DV17 Lobs1	DV17 Robs2	DV17 Lobs2	DV18 Robs1	DV18 Lobs1	DV18 Robs2	DV18 Lobs2
5	5	5	5	5	5	5	5	4	4	4	4	4	4	4	4	3	3	3	3	2	2	2	2
5	5	5	5	4	4	4	4	4	4	4	4	3	3	3	3	3	3	3	3	2	2	2	2
5	5	5	5	4	4	4	4	4	4	4	4	3	3	3	3	3	3	3	3	2	2	2	2
5	5	5	5	4	4	4	4	4	4	4	4	3	3	3	3	3	3	3	3	2	1	2	1
5	5	5	5	4	4	4	4	4	4	4	4	3	3	3	3	3	3	3	3	2	2	2	2
5	5	5	5	4	4	4	4	4	4	4	4	3	3	3	3	3	3	3	3	2	2	2	2
4	5	4	5	4	4	4	4	4	4	4	4	3	3	3	3	3	3	3	3	2	2	2	2
4	4	4	4	3	3	3	3	3	3	3	3	2	2	2	2	2	2	2	2	1	1	1	1
5	5	5	5	4	3	4	3	4	4	4	4	3	3	3	3	3	3	3	3	2	2	2	2
5	5	5	5	4	4	4	4	4	4	4	4	3	3	3	3	3	3	3	3	2	2	2	2
5	5	5	5	4	4	4	4	4	4	4	4	3	3	3	3	3	2	3	2	2	2	2	2
5	5	5	5	4	4	4	4	4	4	4	4	3	3	3	3	3	3	3	3	2	2	2	2
5	5	5	5	4	4	4	4	4	4	4	4	2	2	2	2	2	2	2	2	1	1	1	1
5	5	5	5	4	4	4	4	4	4	4	4	2	3	2	3	2	3	2	3	2	2	2	2
4	5	4	5	4	4	4	4	3	4	3	4	3	3	3	3	2	3	2	3	2	2	2	2
5	5	5	5	4	4	4	4	4	4	4	4	2	2	2	2	3	3	3	3	2	2	2	2
4	4	4	4	4	4	4	4	4	3	4	3	3	3	3	3	3	3	3	3	2	2	2	2
5	5	5	5	4	4	4	4	4	4	4	4	3	3	3	3	3	3	3	3	1	2	1	2
7	7	7	7	8	6	8	6	5	6	5	6	4	4	4	4	4	4	4	4	3	3	3	3
7	7	7	7	5	6	5	6	4	6	4	6	4	4	4	4	3	4	3	4	3	3	3	3
6	6	6	6	5	5	5	5	5	5	5	5	4	3	4	3	3	3	3	3	2	2	2	2
7	7	7	7	6	5	6	5	6	5	6	5	4	4	4	4	4	3	4	3	3	3	3	3
6	7	6	7	5	5	5	5	4	5	4	5	4	4	4	4	3	4	3	4	2	2	2	2
7	7	7	7	6	6	6	6	6	5	6	5	4	4	4	4	4	4	4	4	3	3	3	3
7	7	7	7	6	6	6	6	5	6	5	6	4	4	4	4	4	4	4	4	2	2	2	2
5	5	5	5	4	4	4	4	3	4	3	4	3	3	3	3	3	3	3	3	2	2	2	2
6	6	6	6	5	5	5	5	5	5	5	5	4	3	4	3	3	3	3	3	2	2	2	2
6	6	6	6	5	5	5	5	5	5	5	5	4	4	4	4	4	4	4	4	3	3	3	3
5	5	5	5	5	5	5	5	4	6	4	6	4	5	4	5	3	4	3	4	2	3	2	3
7	7	7	7	6	6	6	6	5	6	5	6	4	5	4	5	4	4	4	4	3	3	3	3
8	6	8	6	5	5	5	5	5	4	5	4	4	4	4	4	4	3	4	3	2	3	2	3
6	6	6	6	5	5	5	5	5	5	5	5	4	4	4	4	3	3	3	3	3	3	3	3
7	7	7	7	5	6	5	6	5	5	5	5	5	4	5	4	3	3	3	3	2	3	2	3
7	7	7	7	6	6	6	6	4	5	4	5	3	4	3	4	2	3	2	3	1	2	1	2
7	6	7	6	5	5	5	5	5	5	5	5	4	4	4	4	3	3	3	3	2	2	2	2
6	6	6	6	5	6	5	6	5	5	5	5	3	5	3	5	3	4	3	4	2	2	2	2
7	7	7	7	6	6	6	6	5	5	5	5	4	4	4	4	4	4	4	4	3	2	3	2
7	7	7	7	6	6	6	6	5	5	5	5	4	4	4	4	4	4	4	4	3	3	3	3
7	6	7	6	5	5	5	5	5	5	5	5	3	3	3	3	3	3	3	3	2	2	2	2
7	6	7	6	6	5	6	5	6	5	6	5	4	3	4	3	4	4	4	4	3	2	3	2
7	7	7	7	7	6	7	6	6	5	6	5	5	4	5	4	4	4	4	4	3	3	3	3
7	7	7	7	6	6	6	6	6	6	6	6	4	4	4	4	4	4	4	4	3	3	3	3
7	7	7	7	5	6	5	6	5	6	5	6	5	4	5	4	4	4	4	4	3	3	3	3
8	8	8	8	6	7	6	7	7	6	7	6	5	5	5	5	4	5	4	5	2	3	2	3
7	7	7	7	6	5	6	5	5	4	5	4	4	3	4	3	4	3	4	3	2	2	2	2
7	6	7	6	6	5	6	5	4	5	4	5	4	3	4	3	3	4	3	4	2	2	2	2

Taable C.1 (continued)—Left and right eye-lens counts for all specimens of *Eldredgeops*. Data is separated by each dorso-ventral file. Data marked with a (.) represent no data due to matrix obstructing an accurate count or due to the dorso-ventral file not being present.

LITERATURE CITED

Abe, F. R., & Lieberman, B. S. (2012). Quantifying morphological change during an evolutionary radiation of Devonian trilobites. *Paleobiology*, *38*(2), 292-307.

Adrain, J.M., (2011). Class Trilobita Walch, 1771. In: Zhang, Z.Q.(Ed.) Animal biodiversity: An outline of higher-level classification and survey of taxonomic richness. *Zootaxa*, *3148*(1), pp.104-109.

Akaike, H., (1973). Maximum likelihood identification of Gaussian autoregressive moving average models. *Biometrika*, *60*(2), pp.255-265.

Akaike, H., (1974). A new look at the statistical model identification. *IEEE transactions on automatic control*, *19*(6), pp.716-723.

Alberti, G.B.K. (1966). Über einige neue Trilobiten aus dem Silurium und Devon, besonders von Marokko. *Senckenbergiana lethaea*, *47*(2), 111-121.

AIberti, G.B.K. (1969). Trilobiten des jüngeren Silurs sowie de Unter- und Mittel-Devons I. Mit Beiträgen zur Silur-Devon Stratigraphie einiger Gebiete Marokkos und Oberfrankens. *Abhandlugen der Senckenbergischen Naturforschenden Gesellschaft*, 520: 1-692.

AIberti, G.B.K. (1970a). Trilobiten des jüngeren Silurs sowie de Unter- und Mittel-Devons II. *Abhandlugen der Senckenbergischen Naturforschenden Gesellschaft*, 525: 1-233.

Alberti, G.K., (1970b). Zur Augenreduktion bei devonischen Trilobiten. *Paläontologische Zeitschrift*, *44*(3), pp.145-160.

AIberti, G.B.K. (1981). Trilobiten des jüngeren Silurs sowie de Unter- und Mittel-Devons III. Mit Beiträgen zur Devon-Biostratigraphie(insbesondere nach Nowakiidae) in N-Afrika, Sardinien Oberfranken und im Harz. *Senckenbergiana lethaea*, 62(1):1-75.

AIberti, G.B.K. (1983). Trilobiten des jüngeren Silurs sowie de Unter- und Mittel-Devons IV. *Senckenbergiana lethaea*, 64(1):1-87.

Babcock, L. E. (1992). Lectotype of Phacops rana milleri Stewart, 1927 (Trilobita, Devonian of Ohio). *Journal of Paleontology*, *66*(4), 692-693.

Bapst, D. W., & Hopkins, M. J. (2017). Comparing cal3 and other a posteriori time-scaling approaches in a case study with the pterocephaliid trilobites. *Paleobiology*, *43*(1), 49-67.

Barrande, J. (1846). *Notice préliminaire sur le systême Silurien et les Trilobites de Bohême*. CL Hirschfeld.

Barrande, J. (1872). *Systême Silurien du centre de la Bohême: Ière. Partie: Recherches Paléontologiques. Supplément au Vol. I. Trilobites, Crustacés divers et Poissons*(Vol. 1). Chez l'auteur et éditeur.

Barrande, J., Počta, F., Perner, J., Waagen, W. H., & Jahn, J. (1852). *Systême silurien du centre de la Bohême* (Vol. 1). l'auteur.

Basse, M. (2006). *Eifel-Trilobiten. 4. Proetida (3), Phacopida (3)*. Goldschneck-Verlag.

Basse, M. (2012). Fossilium Catalogus I: Animalia. Pars 150. Trilobites Africae: Catalogus typorum. 311 pp.

Beecher, C.E., (1895). The larval stages of trilobites. *The American Geologist*, *16*(5), pp.166-196.

Bergsten, J. (2005). A review of long-branch attraction. *Cladistics*, *21*(2), 163-193.

Billings, E. (1860). *Description of some new species of fossils from Lower and Middle Silurian rocks of Canada*.

Brett, C.E., (1999). Ch. 15 Middle Devonian Arkona Shale of Ontario, Canada, and Silica Shale of Ohio, USA. In Hess, H., Ausich, W.I., Brett, C.E. and Simms, M.J. *Fossil crinoids*. Cambridge University Press.

Bouckaert, R., Heled, J., Kühnert, D., Vaughan, T., Wu, C-H., Xie, D., Suchard, MA., Rambaut, A., & Drummond, A. J. (2014). BEAST 2: A Software Platform for Bayesian Evolutionary Analysis. PLoS Computational Biology, 10(4), e1003537. doi:10.1371/journal.pcbi.1003537

Bronn, H. (1825). Über zwei neue Trilobiten-Arten zum Calymene-Geschlechte gehörig. *Zeitschrift für Mineralogie, Taschenbuch*, *1*, 317-21.

Bruton, D., & Haas, W. (1999). The anatomy and functional morphology of Phacops (Trilobita) from the Hunsrück Slate (Devonian). *Palaeontographica Abteilung A*, 29-75.

Bruton, D.L. and Haas, W., (2003). The puzzling eye of Phacops. *Special Papers in Palaeontology*, *70*, pp.349-362.

Buschbeck, E.K., (2005). The compound lens eye of Strepsiptera: morphological development of larvae and pupae. *Arthropod Structure & Development*, *34*(3), pp.315-326.

Burton, C. J., & CJ, B. (1974). Two new subspecies of Phacops rana (Trilobita) from the Middle Devonian of North-West Africa.

Campbell, K. S. W. (1967). *Trilobites of the Henryhouse Formation (Silurian) in Oklahoma*. University of Oklahoma.

Campbell, K.S.W., 1977. Trilobites of the Haragan, Bois d'Arc and Frisco Formations (Early Devonian) Arbuckle Mountains Region, Oklahoma. *Bulletin of the Oklahoma Geologic Survey*, 123 pp. 233.

Canon, W.B., (1932). The wisdom of the body. *London: Kegan Paul*.

Cau, A. (2017). Specimen-level phylogenetics in paleontology using the Fossilized Birth-Death model with sampled ancestors. *PeerJ*, *5*, e3055.

Chatterton, B.D.E., Johnson, B.D., and Campbell, K.S. (1979). Silicified Lower Devonian trilobites from New South Wales. Palaeontology 22: 799-837.

Chatterton, B. D., & Ludvigsen, R. (2004). *Early Silurian trilobites of Anticosti Island, Québec, Canada*. Canadian Society of Petroleum Geologist.

Chatterton, B., Fortey, R. A., & Brett, K. (2006). Trilobites from the upper Lower to Middle Devonian Timrhanrhart Formation, Jbel Gara el Zguilma, southern Morocco.

Chippindale, A.K. and Palmer, A.R., 1994. Persistence of subtle departures from symmetry over multiple molts in individual brachyuran crabs: relevance to developmental stability. In *Developmental Instability: Its Origins and Evolutionary Implications* (pp. 187-201). Springer, Dordrecht.

Chlupáč, I. (1971). New phacopid trilobites from the Devonian of Czechoslovakia. *Časopis pro mineralogii a geologii*, *16*(3), 255-261.

Chulpáč, I., 1972, New Silurian and Lower Devonian phacopid trilobites from the Barrandian area (Czechloslovakia): Časopis pro mineralogii a geologi, v.17, p.365–401

Chlupáč, I. (1975). The distribution of phacopid trilobites in space and time. *Fossils and Strata*, *4*, 399-408.

Chlupáč, I. (1977). The phacopid trilobites of the Silurian and Devonian of Czechoslovakia. Praha : Vydal ústřední ústav geologický : Academii, nakladatelství Československé akademie věd. 172 p.

Chlupáč, I., & Lukeš, P. (1999). Pragian/Zlíchovian and Zlíchovian/Dalejan boundary sections in the Lower Devonian of the Barrandian area, Czech Republic. *Newsletters on Stratigraphy*, 75-100.

Clarke, G.M., (1997). The genetic and molecular basis of developmental stability: the Lucilia story. *Trends in ecology & evolution*, *12*(3), pp.89-91.

Clarke, G.M., (1998). The genetic basis of developmental stability. IV. Individual and population asymmetry parameters. *Heredity*, *80*(5), pp.553-561.

Clarkson, E.N., (1966). Schizochroal eyes and vision of some Silurian acastid trilobites. *Palaeontology*, *9*(1), pp.1-29.

Clarkson, E.N.K., (1967). Fine structure of the eye in two species of Phacops (Trilobita). *Palaeontology*, *10*(4), pp.603-616.

Clarkson, E.N., (1969). VIII.—On the Schizochroal Eyes of Three Species of Reedops (Trilobita: Phacopidae) from the Lower Devonian of Bohemia. *Earth and Environmental Science Transactions of The Royal Society of Edinburgh*, *68*(8), pp.183-205.

Clarkson, E.N., (1975). The evolution of the eye in trilobites. *Fossils and strata*, *4*(7) pp.7-31.

Clarkson, E.N. and Levi-Setti, R., (1975). Trilobite eyes and the optics of Des Cartes and Huygens. *Nature*, *254*(5502), pp.663-667.

Clarkson, E.N.K., Eldredge, N., and Henry, J.L. (1977). Some Phacopina (Trilobita) from the Silurian of Scotland. *Palaeontology,* 20(1), p. 119-142

Clarkson, E.N.K. and Tripp, R.P., (1982). The Ordovician trilobite Calyptaulax brongniartii (Portlock). *Earth and Environmental Science Transactions of The Royal Society of Edinburgh*, *72*(4), pp.287-294.

Clarkson, E., Levi-Setti, R. and Horváth, G., (2006). The eyes of trilobites: the oldest preserved visual system. *Arthropod Structure & Development*, *35*(4), pp.247-259.

Crônier, C., & Feist, R. (1997). Morphologie et évolution ontogénétique de Trimerocephalus lelievrei nov. sp., premier trilobite phacopidé aveugle du Famennien nord-africain. *Geobios*, *30*, 161-170.

Crônier, C. and Feist, R., (2000). Evolution et systématique du groupe Cryphops (Phacopinae, Trilobita) du Dévonien supérieur. *Senckenbergiana lethaea*, *79*(2), pp.501-515.

Crônier, C. and Clarkson, E.N., (2001). Variation of eye-lens distribution in a new late Devonian phacopid trilobite. *TRANSACTIONS-ROYAL SOCIETY OF EDINBURGH*, *92*(2), pp.103-113.

Crônier, C., Feist, R., & Auffray, J. C. (2004). Variation in the eye of Acuticryphops (Phacopina, Trilobita) and its evolutionary significance: a biometric and morphometric approach. *Paleobiology*, *30*(3), 471-481.

Crônier, C., Bignon, A. and François, A., (2011). Morphological and ontogenetic criteria for defining a trilobite species: the example of Siluro-Devonian Phacopidae. *Comptes Rendus Palevol*, *10*(2-3), pp.143-153.

Crônier, C., Budil, P., Fatka, O., & Laibl, L. (2015). Intraspecific bimodal variability in eye lenses of two Devonian trilobites. *Paleobiology*, *41*(4), 554-569.

Darwin, C., (1859). *On the origin of species by means of natural selection, or, the preservation of favoured races in the struggle for life*. J. Murray.

Debat, V., Alibert, P., David, P., Paradis, E. and Auffray, J.C., (2000). Independence between developmental stability and canalization in the skull of the house mouse. *Proceedings of the Royal Society of London. Series B: Biological Sciences*, *267*(1442), pp.423-430.

Delo, D. M. (1935). A revision of the phacopid trilobites. *Journal of Paleontology*, 402-420.

Delo, D. M. (1940). *Phacopid trilobites of North America* (No. 29). The Society.

Didier, G., Royer-Carenzi, M., & Laurin, M. (2012). The reconstructed evolutionary process with the fossil record. *Journal of Theoretical Biology*, *315*, 26-37.

Drummond, A. J. and A. Rambaut. 2007. BEAST: Bayesian evolutionary analysis by sampling trees. BMC Evolutionary Biology 7:214.

Eldredge, N. (1971). The allopatric model and phylogeny in Paleozoic invertebrates. *Evolution*, 156-167.

Eldredge, N. (1972). Systematics and evolution of Phacops rana (Green, 1832) and Phacops iowensis Delo, 1935 (Trilobita) from the Middle Devonian of North America. Bulletin of the AMNH; v. 147, article 2.

Eldredge, N. (1973). Systematics of Lower and Lower Middle Devonian species of the trilobite Phacops Emmrich in North America. Bulletin of the AMNH; v. 151, article 4.

Eldredge, N. (2001). The nature and origin of supraspecific taxa revisited—with special reference to Trilobita. In *Fossils, Phylogeny, and Form* (pp. 341-375). Springer, Boston, MA.

Eldredge, N. (2015). *Eternal ephemera: Adaptation and the origin of species from the nineteenth century through punctuated equilibria and beyond*. Columbia University Press.

Eldredge, N. & Gould, S. J. (1972). Punctuated equilibria: an alternative to phyletic gradualism. *Essential readings in evolutionary biology*, 82-115.

Emmrich, H. F. (1839). *De Trilobitis: Dissertatio petrefactologica quam consensu & auctoritate amplissimi philosophorum ordinis in Alma litterarum Universitate Frederica Guildma pro summis in philosophia honoribus*.

Falconer, D.S., (1981). *Introduction to quantitative genetics*. Pearson Education India.

Feist, R. and Clarkson, E.N., (1989). Environmentally controlled phyletic evolution, blindness and extinction in Late Devonian tropidocoryphine trilobites. *Lethaia*, *22*(4), pp.359-373.

Feist, R., (2019). Post-Kellwasser event recovery and diversification of phacopid trilobites in the early Famennian (Late Devonian). *Bulletin of Geosciences*, *94*(1), pp.1-22.

Feist, R., McNamara, K.J., Cronier, C. and Lerosey-Aubril, R., (2009. Patterns of extinction and recovery of phacopid trilobites during the Frasnian–Famennian (Late Devonian) mass extinction event, Canning Basin, Western Australia. *Geological Magazine*, *146*(1), pp.12-33.

Flick, H., & Struve, W. (1984). Chotecops sollei and Chotecops ferdinandi aus devonischen Schiefern des Rheinischen Schiefergebirges. Beiträge zur Kenntnis des Phacopina (Trilobita), 11. *Senckenbergiana lethaea*, *65*(1-3), 137-163.

Foote, M. and Cowie, R.H., (1988). Developmental Buffereing as a Mechanism for Stasis: Evidence from the Pulmonate Theba pisana. *Evolution*, *42*(2), pp.396-399.

Fortey, R.A. and Morris, S.F., (1977). Variation in lens packing of Phacops (Trilobita). *Geological Magazine*, *114*(1), pp.25-32.

Gál, J., Horváth, G. and Clarkson, E.N., 2000. Reconstruction of the shape and optics of the lenses in the abathochroal-eyed trilobite Neocobboldia chinlinica. *Historical Biology*, *14*(4), pp.193-204.

Gavryushkina, A., Welch, D., Stadler, T., & Drummond, A. J. (2014). Bayesian inference of sampled ancestor trees for epidemiology and fossil calibration. *PLoS computational biology*, *10*(12).

Gavryushkina, A., Heath, T. A., Ksepka, D. T., Stadler, T., Welch, D., & Drummond, A. J. (2017). Bayesian total-evidence dating reveals the recent crown radiation of penguins. *Systematic biology*, *66*(1), 57-73.

Goloboff, P. A., Torres, A., & Arias, J. S. (2018). Weighted parsimony outperforms other methods of phylogenetic inference under models appropriate for morphology. *Cladistics*, *34*(4), 407-437.

Gonzalez, P.N., Pavlicev, M., Mitteroecker, P., Pardo-Manuel de Villena, F., Spritz, R.A., Marcucio, R.S. and Hallgrímsson, B., (2016). Genetic structure of phenotypic robustness in the collaborative cross mouse diallel panel. *Journal of evolutionary biology*, *29*(9), pp.1737-1751.

Gould, S.J. and Eldredge, N., (1977). Punctuated equilibria: the tempo and mode of evolution reconsidered. *Paleobiology*, pp.115-151.

Gould, S.J. and Eldredge, N., (1986). Punctuated equilibrium at the third stage. *Systematic Zoology*, *35*(1), pp.143-148.

Gould, S.J. and Eldredge, N., (1993). Punctuated equilibrium comes of age. *Nature*, *366*(6452), pp.223-227.

Gradstein, F. M., Ogg, J. G., Schmitz, M., & Ogg, G. (Eds.). (2012). *The geologic time scale 2012*. Elsevier.

Graham, J.H., Raz, S., Hel-Or, H. and Nevo, E., (2010). Fluctuating asymmetry: methods, theory, and applications. *Symmetry*, *2*(2), pp.466-540.

Graham, J.H. and Özener, B., (2016). Fluctuating asymmetry of human populations: a review. *Symmetry*, *8*(12), p.154.

Green, J. (1832). *A monograph of the trilobites of North America: with coloured models of the species...* J. Brano.

Haas, W. (1998). Remarks on the phylogeny of some Phacopinae (Trilobita). *Senckenbergiana lethaea*, *77*(1-2), 43-45.

Hall, J. (1859). Description and figures of the organic remains of the lower Helderberg Group and the Oriskany Sandstone. Nat Hist New York; Paleontology, Geol Surv, Albany. *NY*, *3*, 544.

Hallgrímsson, B., Willmore, K. and Hall, B.K., (2002). Canalization, developmental stability, and morphological integration in primate limbs. *American Journal of Physical Anthropology: The Official Publication of the American Association of Physical Anthropologists*, *119*(S35), pp.131-158.

Hansen, T.F. and Houle, D., (2004). Evolvability, stabilizing selection, and the problem of stasis. *Phenotypic integration: Studying the ecology and evolution of complex phenotypes*, pp.130-150.

Harzsch, S. and Hafner, G., (2006). Evolution of eye development in arthropods: phylogenetic aspects. *Arthropod Structure & Development*, *35*(4), pp.319-340.

Harzsch, S., Vilpoux, K., Blackburn, D.C., Platchetzki, D., Brown, N.L., Melzer, R., Kempler, K.E. and Battelle, B.A., (2006). Evolution of arthropod visual systems: development of the eyes and central visual pathways in the horseshoe crab Limulus polyphemus Linnaeus, 1758 (Chelicerata, Xiphosura). *Developmental Dynamics*, *235*(10), pp.2641-2655.

Hawle, I., & Corda, A. J. (1847). *Prodrom einer Monographie der böhmischen Trilobiten*. JG Calve.

Heath, T. A. (2015). Divergence time estimation using BEAST v2. 2.0. In *Source URL: http://treethinkers. org/tutorials/divergence-time-estimation-using-beast/: Tutorial written for workshop on applied phylogenetics and molecular evolution, Bodega Bay California* (pp. 1-44).

Heath, T. A., Huelsenbeck, J. P., & Stadler, T. (2014). The fossilized birth–death process for coherent calibration of divergence-time estimates. *Proceedings of the National Academy of Sciences*, *111*(29), E2957-E2966.

Henry, J.L. (1980). Trilobites ordovicien du Massif Armoricain. *Mém. Soc. Geol. Min. Bretagne* 22: 1-250.

Henry, J. L. (1984). Analyse cladistique et Trilobites: un point de vue. *Lethaia*, *17*(1), 61-66.

Holloway, D. J. (2005). The trilobite genera *Eocryphops* and *Plagiolaria* (Phacopidae). *Paläontologische Zeitschrift*, *79*(2), 227-239.

Horváth, G., (1989). Geometric optics of trilobite eyes: a theoretical study of the shape of the aspherical interface in the cornea of schizochroal eyes of phacopid trilobites. *Mathematical biosciences*, *96*(1), pp.79-94.

Horvath, G. and Clarkson, E.K., (1993). Computational reconstruction of the probable change of form of the corneal lens and maturation of optics in the post-ecdysial development of the schizochroal eye of the Devonian trilobite Phacops rana milleri Stewart 1927. *Journal of theoretical biology*, *160*(3), pp.343-373.

Horváth, G., Clarkson, E. N., & Pix, W. (1997). Survey of modern counterparts of schizochroal trilobite eyes: structural and functional similarities and differences. *Historical Biology*, *12*(3-4), 229-263.

Howells, Y., (1982). Scottish Silurian trilobites. *Monograph of the Palaeontographical Society* 135(561), pp.1-76.

Hughes, N. C., Adrain, J. M., Holmes, J. D., Hong, P. S., Hopkins, M. J., Hou, J.-B., Minelli, A., Park, T.-Y. S., Paterson, J. R., Peng, J., Webster, M., Zhang, X.-G., Zhang, X.-L., and Fusco. G. (2021). Articulated trilobite ontogeny: suggestions for a methodological standard. Journal of Paleontology 95 (2): 298-304.

Hurvich, C.M. and Tsai, C.L., (1989). Regression and time series model selection in small samples. *Biometrika*, *76*(2), pp.297-307.

Jell, P.A., (1975). The abathochroal eye of Pagetia, a new type of trilobite eye. *Fossils and Strata*, *4*, pp.33-43.

Jell, P. A., & Adrain, J. M. (2002). Available generic names for trilobites. *MEMOIRS-QUEENSLAND MUSEUM*, *48*(2), 331-552.

Kass, R. E., and Raftery, A. E. (1995). Bayes factors. *Journal of the American Statistical Association, 90*(430), 773-795.

Kaufmann, B. (2006). Calibrating the Devonian Time Scale: a synthesis of U–Pb ID–TIMS ages and conodont stratigraphy. *Earth-Science Reviews*, *76*(3-4), 175-190.

Kayser, E., (1889). *Ueber einige neue oder wenig gekannte Versteinerungen des rheinischen Devon*.

Kegel, W. (1952). Umbennennung von Plagiops Kiegel, 1931 (Tril.) in Plagiolaria. *Senckenbergiana*, *33*, 4-6.

Kesling, R.V. and Chilman R.B., (1975). Strata and megafossils of the Middle Devonian Silica Formation. Published by the "Friends of the University of Michigan Museum of Paleontology," pp. 407.

Khaldi, A. Y., Cronier, C., Hainaut, G., Abbache, A., & Mehadji, A. O. (2016). A trilobite faunule from the Lower Devonian of the Saoura Valley, Algeria: biodiversity, morphological variability and palaeobiogeographical affinities. *Geological Magazine*, *153*(3), 357-387.

Kielan, Z. (1954). *Les trilobites mésodévoniens des Monts de Sainte-Croix*. Państwowe Wydawn. Naukowe.

Klingenberg, C.P., (2015). Analyzing fluctuating asymmetry with geometric morphometrics: concepts, methods, and applications. *Symmetry*, *7*(2), pp.843-934.

Klingenberg, C.P., (2019). Phenotypic plasticity, developmental instability, and robustness: The concepts and how they are connected. *Frontiers in Ecology and Evolution*, *7*, p.56.

Klingenberg, C.P., Badyaev, A.V., Sowry, S.M. and Beckwith, N.J., (2001). Inferring developmental modularity from morphological integration: analysis of individual variation and asymmetry in bumblebee wings. *The American Naturalist*, *157*(1), pp.11-23.

Klingenberg, C.P., Mebus, K. and Auffray, J.C., (2003). Developmental integration in a complex morphological structure: how distinct are the modules in the mouse mandible?. *Evolution & development*, *5*(5), pp.522-531.

Klingenberg, C.P. and Zaklan, S.D., (2000). Morphological integration between developmental compartments in the Drosophila wing. *Evolution*, *54*(4), pp.1273-1285.

Koch II, W.F. (1990). The distribution of *Phacops rana* in Eastern North America – a Paleobiogeographic Vuew. In *Evolutionary Paleobiology of Behavior and Coevolution* (pp. 589-594). Elsevier, New York, NY.

Laland, K.N., Uller, T., Feldman, M.W., Sterelny, K., Müller, G.B., Moczek, A., Jablonka, E. and Odling-Smee, J., (2015). The extended evolutionary synthesis: its structure, assumptions and predictions. *Proceedings of the Royal Society B: Biological Sciences*, *282*(1813), p.20151019.

Lane, P. D. (1988). Silurian trilobites from Peary Land, central North Greenland. *Grønlands Geologiske Undersøgelse*, 137, p.93-117.

Lazić, M.M., Carretero, M.A., Crnobrnja-Isailović, J. and Kaliontzopoulou, A., (2015). Effects of environmental disturbance on phenotypic variation: an integrated assessment of canalization, developmental stability, modularity, and allometry in lizard head shape. *The American Naturalist*, *185*(1), pp.44-58.

Leamy, L., (1984). Morphometric studies in inbred and hybrid house mice. V. Directional and fluctuating asymmetry. *The American Naturalist*, *123*(5), pp.579-593.

Leamy, L.J. and Klingenberg, C.P., (2005). The genetics and evolution of fluctuating asymmetry. *Annu. Rev. Ecol. Evol. Syst.*, *36*, pp.1-21.

Lee, M.R., Torney, C. and Owen, A.W., (2007). Magnesium-rich intralensar structures in schizochroal trilobite eyes. *Palaeontology*, *50*(5), pp.1031-1037.

Lee, M. S., & Palci, A. (2015). Morphological phylogenetics in the genomic age. *Current Biology*, *25*(19), R922-R929.

Legendre, P. and Oksanen, M.J., (2018). Package 'lmodel2'. *See https://CRAN. R-project. org/package= lmodel2*.

Lespérance, P.J., (1987). Trilobites et Brachiopodes ashgilliens (Ordovicien supérieur). *Bulletin de l'Institut Royal des Sciences Naturelles de Belgique, Sciences de la Terre*, *57*, pp.91-123.

Lesperance, P.J., (1991). Vincular furrows in some early Silurian and Devonian Phacopidae (Trilobita), predominantly from North America. *Journal of Paleontology*, pp.276-294.

Lespérance, P. J., & Letendre, J. (1982). Some early Silurian Phacopidae (Trilobita). In *Proceedings of the Third North American Paleontological Convention, Montreal* (pp. 329-336).

Levi-Setti, R. (2014). *The Trilobite Book: A Visual Journey*. University of Chicago Press.

Lewis, P. O. (2001). A likelihood approach to estimating phylogeny from discrete morphological character data. *Systematic biology*, *50*(6), 913-925.

Lindström, G., (1901). *Researches on the visual organs of the trilobites* (Vol. 34). PA Norstedt & Söner.

Lindgren, J., Nilsson, D.E., Sjövall, P., Jarenmark, M., Ito, S., Wakamatsu, K., Kear, B.P., Schultz, B.P., Sylvestersen, R.L., Madsen, H. and LaFountain, J.R., (2019). Fossil insect eyes shed light on trilobite optics and the arthropod pigment screen. *Nature*, *573*(7772), pp.122-125.

Li, W. L. S., & Drummond, A. J. (2012). Model averaging and Bayes factor calculation of relaxed molecular clocks in Bayesian phylogenetics. *Molecular biology and evolution*, *29*(2), 751-761.

Ludvigsen, R., (1979). *Fossils of Ontario: The Trilobites*. Royal Ontario Museum.

Ludvigsen, R., & Chatterton, B. D. (1982). Ordovician Pterygometopidae (Trilobita) of North America. *Canadian Journal of Earth Sciences*, *19*(11), 2179-2206.

Maksimova (Maximova), Z.A., 1971, Importance of trilobites to the resolution of the Siluro-Devonian boundary of central Kazakstan. In *the Siluro-Devonian Boundary and Silurian Biostratigraphy.* Proceedings of the Third International Symposium, vol. 1, p. 144-149.

Maksimova (Maximova), Z.A., 1972, New Devonian Trilobites of the Phacopidea: Paleontology Journal, v.6, p.78–83.

Marshall, C. R. (2017). Five palaeobiological laws needed to understand the evolution of the living biota. *Nature Ecology & Evolution*, *1*(6), 1-6.

Mau, B., Newton, M. A., & Larget, B. (1999). Bayesian phylogenetic inference via Markov chain Monte Carlo methods. *Biometrics*, *55*(1), 1-12.

McKellar, R. C., & Chatterton, B. D. (2009). *Early and Middle Devonian Phacopidae (Trilobita) of southern Morocco*. Canadian Soc. of Petroleum Geologists.

McCormick, Timothy (1995) *Patterns and implications of stasis in trilobites.* PhD thesis, University of Glasgow.

McNamara, K.J. and Feist, R., 2016. The effect of environmental changes on the evolution and extinction of Late Devonian trilobites from the northern Canning Basin, Western Australia. *Geological Society, London, Special Publications*, *423*(1), pp.251-271.

Miller, J. and Clarkson, E.N.K., (1980). The post-ecdysial development of the cuticle and the eye of the Devonian trilobite Phacops rana milleri Stewart 1927. *Philosophical Transactions of the Royal Society of London. B, Biological Sciences*, *288*(1030), pp.461-480.

Møller, A.P. and Pomiankowski, A., (1993). Punctuated equilibria or gradual evolution: fluctuating asymmetry and variation in the rate of evolution. *Journal of Theoretical Biology*, *161*(3), pp.359-367.Møller, A.P. and Swaddle, J.P., 1997. *Asymmetry, developmental stability and evolution*. Oxford University Press, UK.

Møller, A.P. and Swaddle, J.P., (1997). *Asymmetry, developmental stability and evolution*. Oxford University Press, UK.

Moore, R. C. (Ed.). (1959). *Treatise on Invertebrate Paleontology: Arthropoda 1: Arthropoda-General Features, Protarthropoda, Euarthropoda-General Features, Trilobitomorpha; by HJ Harrington. Pt. O*. Geological Society of America.

Muñoz-Muñoz, F., Sans-Fuentes, M.A., López-Fuster, M.J. and Ventura, J., (2006). Variation in fluctuating asymmetry levels across a Robertsonian polymorphic zone of the house mouse. *Journal of Zoological Systematics and Evolutionary Research*, *44*(3), pp.236-250.

Nijhout, H.F. and Davidowitz, G., (2003). Developmental perspectives on phenotypic variation, canalization, and fluctuating asymmetry. *Developmental instability: causes and consequences*, pp.3-13.

Nylander, J. A., Ronquist, F., Huelsenbeck, J. P., & Nieves-Aldrey, J. (2004). Bayesian phylogenetic analysis of combined data. *Systematic biology*, *53*(1), 47-67.

O'Reilly, J. E., Puttick, M. N., Parry, L., Tanner, A. R., Tarver, J. E., Fleming, J., Pisani D., & Donoghue, P. C. (2016). Bayesian methods outperform parsimony but at the expense of precision in the estimation of phylogeny from discrete morphological data. *Biology letters*, *12*(4), 20160081.

Oudot, M., Crônier, C., Neige, P., & Holloway, D. (2019). Phylogeny of some Devonian trilobites and consequences for the systematics of Austerops (Phacopidae). *Journal of Systematic Palaeontology*, *17*(9), 775-790.

Owen, A.W., (1985). Trilobite abnormalities. *Earth and Environmental Science Transactions of the Royal Society of Edinburgh*, *76*(2-3), pp.255-272.

Packard Jr, A.S., (1880). The structure of the eye of trilobites. *The American Naturalist*, *14*(7), pp.503-508.

Palmer, A.R., (1994). Fluctuating asymmetry analyses: a primer. In *Developmental instability: its origins and evolutionary implications* (pp. 335-364). Springer, Dordrecht.

Palmer, A.R. and Strobeck, C., (1986). Fluctuating asymmetry: measurement, analysis, patterns. *Annual review of Ecology and Systematics*, pp.391-421.

Palmer, A.R. and Strobeck, C., (2003). CH 17. Fluctuating asymmetry analyses revisited. *Developmental Instability: Causes and Consequences, Oxford University Press, Oxford*, pp.279-319.

Paterson, J. R., Edgecombe, G. D., & Lee, M. S. (2019). Trilobite evolutionary rates constrain the duration of the Cambrian explosion. *Proceedings of the National Academy of Sciences*, *116*(10), 4394-4399.

Patzkowsky, M.E. and Holland, S.M., (2012). *Stratigraphic paleobiology: understanding the distribution of fossil taxa in time and space*. University of Chicago Press.

Polak, M. ed., (2003). *Developmental instability: causes and consequences*. Oxford University Press on Demand.

Pribyl, A., & Erben, H. K. (1952). Uber einige neue oder wenig bekannte Acanthopyginae (Tril.) des böhmischen und des deutschen Devons. *Paläontologische Zeitschrift*, *26*, 141-174.

Puttick, M. N., Morris, J. L., Williams, T. A., Cox, C. J., Edwards, D., Kenrick, P., ... & Donoghue, P. C. (2018). The interrelationships of land plants and the nature of the ancestral embryophyte. *Current Biology*, *28*(5), 733-745.

Pyron, R. A. (2011). Divergence time estimation using fossils as terminal taxa and the origins of Lissamphibia. *Systematic biology*, *60*(4), 466-481.

Rambaut A, Drummond AJ, Xie D, Baele G and Suchard MA (2018) Posterior summarisation in Bayesian phylogenetics using Tracer 1.7. *Systematic Biology*. **syy032**. doi:10.1093/sysbio/syy032

Ramsköld, L. (1988). Heterochrony in Silurian phacopid trilobites as suggested by the ontogeny of Acernaspis. *Lethaia*, *21*(4), 307-318.

Ramsköld, L., & Werdelin, L. (1991). The phylogeny and evolution of some phacopid trilobites. *Cladistics*, *7*(1), 29-74.

Raup, D. M. (1985). Mathematical models of cladogenesis. *Paleobiology*, *11*(1), 42-52.

Raup, D. M., Gould, S. J., Schopf, T. J., & Simberloff, D. S. (1973). Stochastic models of phylogeny and the evolution of diversity. *The Journal of Geology*, *81*(5), 525-542.

Réale, D. and Roff, D.A., (2003). Inbreeding, developmental stability, and canalization in the sand cricket Gryllus firmus. *Evolution*, *57*(3), pp.597-605.

Reed, F. C. (1905). VI.—The Classification of the Phacopidæ. *Geological Magazine*, *2*(4), 172-178.

Richter, R. and Richter, E., 1925. Unterlagen zum Fossilium Catalogus. Trilobita II: Senckenbergiana, v.7, 126p.

Richter, R. and Richter, E. 1931. Unterlagen zum Fossilium Catalogus. Trilobitae, 5: Senckenbergiana, v. 13, p. 140-146.

Richter, R. and Richter, E., 1933. Die letzten Phacopidae. *Bulletin du Musée royal d'Histoire naturelle de Belgique,* 9(21): 1-19.

Richter, R. and Richter, E., 1939. Sur quelque trilobites du Dévonien marocain. *Service des Mines du Maroc*, Rabat.

Richter, R. and Richter, E., 1943. Studien im Paläozoikum der Mittelmeer-Länder. 4a. Trilobiten aus dem Devon von Marokko mit einem Anhang über Arten des Rheinlands. *Senkenbergiana,* 26(1): 116-199.

Roemer, F. A. (1852). *Beiträge zur geologischen Kenntniss des nordwestlichen Harzgebirges* (Vol. 1). Theodor Fischer.

Ronquist, F., Klopfstein, S., Vilhelmsen, L., Schulmeister, S., Murray, D. L., & Rasnitsyn, A. P. (2012). A total-evidence approach to dating with fossils, applied to the early radiation of the Hymenoptera. *Systematic Biology*, *61*(6), 973-999.

Rosa, D., (1899). *La Riduzione progressiva della variabilità ei suoi rapporti coll'estinzione e coll'origine delle specie*. Clausen.

Rutherford, S.L., (2000). From genotype to phenotype: buffering mechanisms and the storage of genetic information. *Bioessays*, *22*(12), pp.1095-1105.

Rutherford, S.L. and Lindquist, S., (1998). Hsp90 as a capacitor for morphological evolution. *Nature*, *396*(6709), pp.336-342.

Salter, J. W. (1864-1883). A Monograph of the British Trilobites from the Cambrian, Silurian, and Devonian Formations. *Monographs of the Palaeontographical Society*, 1 1864, pp. 1-80; 2, 1865pp.81-128; 3, 1866, pp. 129-176; 4, 1867, pp. 177-214; 5, 1883, pp. 215-224.

Sanderson, M. J., Wojciechowski, M. F., Hu, J. M., Khan, T. S., & Brady, S. G. (2000). Error, bias, and long-branch attraction in data for two chloroplast photosystem genes in seed plants. *Molecular Biology and Evolution*, *17*(5), 782-797.

Scheiner, S.M., (1993). Genetics and evolution of phenotypic plasticity. *Annual review of ecology and systematics*, *24*(1), pp.35-68.

Schoenemann, B., (2021). An overview on trilobite eyes and their functioning. *Arthropod Structure & Development*, *61*, p.101032.

Schoenemann, B., Clarkson, E.N. and Franz, A., (2008). Sublensar capsules in phacopid eyes. *Advances in Trilobite Research*, p.355.

Schoenemann, B. and Clarkson, E.N.K., (2011). Light guide lenses in trilobites?. *Earth and Environmental Science Transactions of the Royal Society of Edinburgh*, *102*(1), pp.17-23.

Schoenemann, B. and Clarkson, E.N., (2015). Vision in fossilised eyes. *Earth and Environmental Science Transactions of the Royal Society of Edinburgh*, *106*(4), pp.209-220.

Schoenemann, B., Pärnaste, H. and Clarkson, E.N., (2017). Structure and function of a compound eye, more than half a billion years old. *Proceedings of the National Academy of Sciences*, *114*(51), pp.13489-13494.

Schoenemann, B., Poschmann, M. and Clarkson, E.N., (2019). Insights into the 400 million-year-old eyes of giant sea scorpions (Eurypterida) suggest the structure of Palaeozoic compound eyes. *Scientific reports*, *9*(1), pp.1-10.

Schraut, G., (2000a). Trilobiten aus dem Unter-Devon des südöstlichen Anti-Atlas, Süd-Marokko. *Senckenbergiana lethaea*, *79*(2), pp.361-433.

Schraut, G. (2000b). Eine neue Unterart vonPhacops (Phacops) sparsinodosus Struve 1970 aus dem Mittel-Devon von Marokko. *Senckenbergiana lethaea*, *80*(2), 525-535.

Schuchert, C. and Cooper, G.A., (1930). Upper Ordovician and Lower Devonian stratigraphy and paleontology of Perce, Quebec; Part II (cont.). *American Journal of Science*, *5*(119), pp.365-392.

Sokal, R.R. and Rohlf, F.J., (1995). Biometry: the principles and practice of statistics in biological research.

Stadler, T. (2010). Sampling-through-time in birth–death trees. *Journal of theoretical biology*, *267*(3), 396-404.

Stearns, S.C., (1993). The evolutionary links between fixed and variable traits. *Acta Palaeontologica Polonica*, *38*(3-4), pp.215-232.

Stewart, G. A. (1927). *Fauna of the Silica shale of Lucas County*. Ohio. Division of Geological Survey.

Strausfeld, N.J., Ma, X., Edgecombe, G.D., Fortey, R.A., Land, M.F., Liu, Y., Cong, P. and Hou, X., (2016). Arthropod eyes: the early Cambrian fossil record and divergent evolution of visual systems. *Arthropod structure & development*, *45*(2), pp.152-172.

Stumm, E. C. (1953). Trilobites of the Devonian Traverse group of Michigan. *Contributions from the Museum of Paleontology, University of Michigan*, 10(6), p.101-157.

Stumm, E. C. (1954). Lower Middle Devonian Phacopid Trilobites from Michigan, Southwestern Ontario, and the Ohio Valley. *Contributions from the Museum of Paleontology, University of Michigan*, 11(11), p.201-221.

Struve, W. (1970). Beiträge zur Kenntnis der Phacopina (Trilobita), 7: Phacops-Arten aus dem Rheinischen Devon. 1. *Senckenbergiana lethaea*, *51*(2/3), 133-189.

Struve, W. (1972). Phacops-Arten aus dem Rheinischen Devon. 2. Untergattungs-Zuweisung. *Senckenbergiana lethaea*, *53*(5), 383-403.

Struve, W. (1982). Beiträge zur Kenntnis der Phacopina (Trilobita), 10: Neue Untersuchungen über Geesops (Phacopinae; Unter-und Mittel-Devon). *Senckenbergiana lethaea*, *63*(5-6), 473-495.

Struve, W. (1989). Rabienops evae aus dem späten Ober-Devon des Rheinischen Gebirges. *Bulletin de la Société belge de Géologie*, *98*(3-4), 335-342.

Struve, W. (1990). Paläozoologie III (1986-1990). *Courier Forschungsinstitut Senckenberg*, *127*, 251-279.

Struve, W. (1992). Neues zur Stratigraphie und Fauna des rhenotypen Mittel-devon. *Senckenbergiana lethaea*, *71*, 503-624.

Struve, W. (1995). Die Riesen-Phacopiden aus dem Maieder, SE-marokkanische Prae-Sahara. *Senckenbergiana lethaea*, *75*, 77-130.

Swaddle, J.P. and Witter, M.S., (1997). The effects of molt on the flight performance, body mass, and behavior of European starlings (Sturnus vulgaris): an experimental approach. *Canadian Journal of Zoology*, *75*(7), pp.1135-1146.

Swafford, D. L. (2002). PAUP*. Phylogenetic analysis using parsimony (* and other models). Version 4.0 b10 for Macintosh. *Sunderland, Mass: Sinauer Associates Inc*.

Swain, D.P., (1987). A problem with the use of meristic characters to estimate developmental stability. *The American Naturalist*, *129*(5), pp.761-768.

Thomas, A.T., (1998). Variation in the eyes of the Silurain trilobites Eophacops and Acaste and its significance. *Palaeontology*, *41*(5), pp.897-912.

Thomas, A.T., (2005). Developmental palaeobiology of trilobite eyes and its evolutionary significance. *Earth-Science Reviews*, *71*(1-2), pp.77-93.

Tomkins, J.L., (1999). The ontogeny of asymmetry in earwig forceps. *Evolution*, *53*(1), pp.157-163.

Torney, C., Lee, M.R. and Owen, A.W., (2008). An electron backscatter diffraction study of Geesops: a broader view of trilobite vision. *Adv. Trilobite Res*, *389*.

Torney, C., Lee, M.R. and Owen, A.W., (2014). Microstructure and growth of the lenses of schizochroal trilobite eyes. *Palaeontology*, *57*(4), pp.783-799.

Van Dongen, S., (2006). Fluctuating asymmetry and developmental instability in evolutionary biology: past, present and future. *Journal of evolutionary biology*, *19*(6), pp.1727-1743.

Van Valen, L., (1962). A study of fluctuating asymmetry. *Evolution*, pp.125-142.

van Viersen, A. P. (2007). Preliminary report of trilobites from the Hanonet Formation (Eifelian–Givetian transition), southern border of Dinant Synclinorium, Belgium. *Bulletin de l'Institut royal des Sciences naturelles de Belgique, Sciences de la Terre*, *77*, 15-29.

van Viersen, A., Holland, D., & Koppka, J. (2017). The phacopine trilobite genera *Morocops* Basse, 2006 and *Adrisiops* gen. nov. from the Devonian of Morocco. *Bulletin of Geosciences*, *92*(1).

Vogdes, A. W. (1890). *A bibliography of Paleozoic Crustacea from 1698 to 1889, including a list of North American species and a systematic arrangement of genera* (No. 62-65). US Government Printing Office.

Waddington, C.H., (1940). The genetic control of wing development in Drosophila. *Journal of Genetics*, *41*(1), pp.75-113.

Waddington, C.H., (1957). The strategy of the genes. A discussion of some aspects of theoretical biology. With an appendix by H. Kacser. *The strategy of the genes. A discussion of some aspects of theoretical biology. With an appendix by H. Kacser.*

Wagner, P.J., (2000). Exhaustion of morphologic character states among fossil taxa. *Evolution*, *54*(2), pp.365-386.

Walch, J.E.I. (1771). *Die Naturgeschichte der Versteinerungen zur Erläuterung der Knorrischen Sammlung von Merkwürdigkeiten der Natur*. Nürnberg: Felßecker.

Wagner, G.P., (1988). The influence of variation and of developmental constraints on the rate of multivariate phenotypic evolution. *Journal of Evolutionary Biology*, *1*(1), pp.45-66.

Webster, M. (2019). Morphological homeostasis in the fossil record. *Seminars in cell & developmental biology*, 88, 91-104.

Williamson, P.G. and Foote, M.J., (1984). Global selection patterns in the prosobranch Melanoides tuberculata: Implications for stasis and speciation. In *Geol. Soc. Amer. Abstr. Prog* (Vol. 16, pp. 695-696).

Willmore, K.E., Klingenberg, C.P. and HallgrÍmsson, B., (2005). The relationship between fluctuating asymmetry and environmental variance in rhesus macaque skulls. *Evolution*, *59*(4), pp.898-909.

Wright, A. M., & Hillis, D. M. (2014). Bayesian analysis using a simple likelihood model outperforms parsimony for estimation of phylogeny from discrete morphological data. *PLoS One*, *9*(10).

Wright, D. F. (2017). Bayesian estimation of fossil phylogenies and the evolution of early to middle Paleozoic crinoids (Echinodermata). *Journal of Paleontology*, *91*(4), 799-814.

Young, J.R., (2007). Removing bias for fluctuating asymmetry in meristic characters. *Journal of agricultural, biological, and environmental statistics*, *12*(4), pp.485-497.

Zhang, X., Clarkson EK., (1990). The eyes of Lower Cambrian eodiscid trilobites. Palaeontology: 33(4):911-32.